2001

Molecular Anatomy of a Living Nerve Terminal: Actin and Synapsin in the Synaptic Vesicle Cycle

Ona E. Bloom

Molecular Anatomy of a Living Nerve Terminal:

Actin and Synapsin in the Synaptic Vesicle Cycle

A thesis presented to the faculty of

The Rockefeller University

in partial fulfillment of the requirements for

the degree of Doctor of Philosophy

by

Ona E. Bloom
2001

Dedicated to my family

ACKNOWLEDGEMENTS

First of all, I wish to thank my thesis supervisor, Paul Greengard, for his support, patience, encouragement, and of course, wonderful sense of humor. Paul has an inspiring and voracious appetite for science. It has been a privilege to participate in his investigations of the basic biology of the nerve terminal.

I thank Lennart Brodin, Oleg Shupliakov and their research group for a wonderful scientific collaboration. Their ultrastructural studies of the presynaptic terminal have raised the standard for the field and I am grateful to have received such rigorous technical training from them.

I thank all members of the Greengard Laboratory, who have contributed much to my scientific education. In particular, I wish to thank Angus Nairn as well as the past and present members of the Synapsin Group, including Andy Czernik, HT Kao and Barbara Porton. I am grateful for the advice, friendship, and shared experiences of fellow students Jasmina Jovanovic, a recent graduate, and the talented Ms. Ping Chi, a soon-to-be graduate. The graphics presented in this thesis bear the mark of perfectionism due to the tireless efforts of Elisabeth Griggs.

I would like to thank my thesis committee members, RU faculty Bruce McEwen, Jim Hudspeth, and Sandy Simon, as well as Tim Ryan of The Weill Medical College of Cornell University. All of my committee members have contributed much to my scientific education. I feel privileged to have had the opportunity to discuss this and other scientific work with them over the years.

I gratefully acknowledge support from the Rockefeller Dean's Office. Marta Delgado and Kristen Cullen miraculously appear to have a personal commitment to every student on this campus and I have been no exception.

Tony Cerami introduced me to this campus when I was a summer student in his laboratory 10 years ago. That experience and his encouragement have had a profound impact on my scientific training. Tony has supported me at every stage of my education and has been an invaluable advisor and friend.

After college, I joined the laboratory of Kevin J. Tracey at North Shore University Hospital. During my three years there, I received outstanding scientific training from Kevin. Quite simply, Kevin taught me how to be a scientist, inspired me to become one, and has been a wonderful mentor.

Many friends have helped me over the years and I wish to thank them all (but not here!) To name a few who have contributed to my scientific as well as extracurricular life, thanks to Ellen Lumpkin for her earnest answers to my unending questions, Haleh Razani for providing a home away from home, and Kambiz Shekdar for his unabashed sincerity and spiritedness.

Above all, I could not have reached my academic achievements without the support of my family. Till Christian, tack for alla mitzvot. I thank my father Barry for his appreciation of the beauty in nature. My sisters Beryl and Rachel are my closest friends. My late grandmother Rose is missed especially today. Last but certainly not least, my mother Jane is the most supportive, generous, gracious, and kind person that I know. Together, they are all the colors and all the numbers.

TABLE OF CONTENTS

LIST OF FIGURES

LIST OF TABLES

Abbreviations

ADP	**adenosine diphosphate**
ATP	**adenosine 5'triphosphate**
BSA	**bovine serum albumin**
BWSV	**Black Widow Spider Venom**
cAMP	**adenosine 3':5'-cyclic monophosphate**
CaM	**calmodulin**
CaMK	**Ca2+/calmodulin-dependent protein kinase (I, II, & IV)**
CDK	**cyclin-dependent kinase (1, 2, 5)**
CNS	**central nervous system**
COOH	**carboxy**
F-actin	**filamentous actin**
G-actin	**globular actin**
GST	**glutathione S-transferase**
HEPES	**N-2-hydroxyethylpiperazine-N'-2-ethanesulfonic acid**
HRP	**horseradish peroxidase**
kDa	**kilodaltons**
LTP	**long term potentiation**
LTX	**latrotoxin**
MAPK	**mitogen-activated protein kinase**
NEM-S1	**N-ethylmaleimide-modified myosin subfragment 1**
NH_2	**amino**
NMJ	**neuromuscular junction**
PI3K	**phosphatidylinnositol-3 kinase**
PKA	**cAMP-dependent protein kinase**
PKC	**Ca2+/phospholipid-dependent protein kinase**
PLCγ	**phospholipase Cγ**
PP2B	**protein phosphatase 2B (calcineurin)**
PRD	**proline-rich domain**
QF-DE	**quick-freeze deep etch**

SDS-PAGE	**sodium dodecyl sulfate polyacrylamide gel eletrophoresis**
ser/thr	**serine and threonine**
SH2 and SH3	**src-homology domain 2 and src-homology domain 3**
SV	**synaptic vesicle**
SV2	**synaptic vesicle protein 2**
Tris	**tris (hydroxymethyl) aminoethane**

ABSTRACT

Neurotransmission is based on a series of events termed the synaptic vesicle cycle. Several molecular components contributing to the synaptic vesicle cycle are known, including the cytoskeletal protein actin and the synaptic vesicle-associated phosphoprotein synapsin. The studies presented in this thesis were designed to investigate the role of the interaction between synapsin and actin in an intact model of synaptic transmission, the lamprey reticulospinal synapse.

To establish the role of actin in the presynaptic terminal, several actin-directed compounds were injected into reticulospinal axons. Axons were maintained at rest or stimulated under various conditions, fixed, and the ultrastructure of the terminal was studied by electron microscopy. Unexpectedly, an actin-based network was revealed that appears to participate in the translocation of synaptic vesicles from endocytic regions of the plasma membrane back to the vesicle cluster.

The prevailing hypothesis of synapsin function states that it interacts with actin to maintain organization of the vesicle cluster. In the present experiments, actin-modifying compounds did not visibly affect the vesicle cluster organization. Therefore, to investigate the potential relevance of the interaction between synapsin and actin to the novel actin-based translocation of vesicles, the localization of synapsin was determined in synapses fixed after several conditions of activity, using post-embedding techniques.

In active synapses, synapsin was found on synaptic vesicles throughout the vesicle cluster, supporting a role for synapsin in mediating the dynamics of synaptic vesicle distal and proximal to the active zone. Synapsin was also present on several elements of the actin-based translocation network, including: the plasma membrane area where filaments are localized, the actin matrix itself and vesicles enmeshed in the matrix. Consistent with all data obtained, a novel hypothesis is presented, namely that the interaction of synapsin and actin plays an important role in the translocation of locally recycled synaptic vesicles in the presynaptic nerve terminal, facilitating the continuous supply of vesicles necessary to

sustain neurotransmitter release. This hypothesis provides that synapsin serves as a direct functional link between the endocytic and exocytic pathways, as suggested by its binding partners that are known to participate in signal transduction, the endocytic pathway and the regulation of actin dynamics.

I. INTRODUCTION

The proper function of the nervous system depends on the transfer of information at specific sites within neurons. In 1894, Santiago Ramon y Cajal formally presented his "neuron doctrine" which proposed that the nervous system is made up of discrete cellular entities (Ramon y Cajal, 1894). He proposed that "because there is no continuity, currents must be transmitted from one cell to another by way of contiguity or contact, as in the splicing of two telegraph wires. This contact takes place between the terminal arborizations and collaterals of axons on one side, and the cell bodies and dendritic arborizations on the other." In 1897, these sites of contact were named "synapses", by Charles Sherrington, a term derived from the Greek verb *synaptein* meaning to fasten together (Tansey, 1997).

In an effort to understand how information transfer in the nervous system is achieved, the development, anatomy, physiology, and molecular components of synapses have been studied extensively. These investigations have led to our current understanding that neurotransmitter, the chemical signaling entity transmitted from one cell to another, is stored in synaptic vesicles, which are clustered together at release sites known as active zones. Following activation of a neuron, the presynaptic nerve terminal is depolarized and Ca^{2+} flows into the terminal through membrane channels, triggering the fusion of synaptic vesicles with the active zone, and the subsequent release of neurotransmitter into the synaptic cleft, the space between the pre- and post-synaptic neurons. Synaptic vesicles then reform locally, are refilled with neurotransmitter, and rejoin the synaptic vesicle cluster. These events are collectively termed the synaptic vesicle cycle.

In the middle of the 20^{th} century, the morphological events constituting the synaptic vesicle cycle were elucidated using ultrastructural techniques. During the past three decades, biochemical, genetic, and molecular approaches have led to the identification of several molecular components of the synaptic vesicle cycle. Among the best established are the cytoskeletal protein actin and the synaptic vesicle phosphoprotein synapsin. While both actin and synapsin have also been proposed to play major roles in the growth of neurons

and synaptogenesis, only studies relevant to the mature synaptic terminal are discussed below.

Origins of the vesicle hypothesis of neurotransmitter release

In the mid-1940s, scientists at The Rockefeller University introduced techniques for the morphological analysis of subcellular components and published the first images of cultured cells using an electron microscope (Porter et al., 1944). In the early 1950s, Porter, Claude, Palade and colleagues introduced several significant technical advances in processing specimens for electron microscopy such as buffered osmium fixation, sectioning by an improved ultramicrotome, plastic resin embedding, and staining with heavy metals such as lead and uranium. These innovations facilitated a series of definitive studies of intracellular morphology in a wide variety of cell types, including neurons.

Using these innovations, studies of central and peripheral nervous system synapses described several common anatomical features. In joint abstracts presented to the American Association of Anatomists on April 9, 1954, Palade and Palay described their electron microscopic studies of mammalian central synapses of the brain and spinal cord, as well as of neuromuscular junctions (Palade, 1954; Palay, 1954). Within the presynaptic terminal, they observed populations of mitochondria, groups of small vesicles 30-50 nm in diameter, and a filamentous axoplasm. They noted that the axon and dendrite were bounded by their respective plasma membranes, and that an electron-dense specialization marked their closest association (Palay and Palade, 1955). At the same meeting, Robertson presented similar findings in crayfish giant axons (Robertson, 1954), published in expanded form in (Robertson, 1955).

A week later, Robertson, as well deRobertis and Bennett, presented comparable findings to the American Physiological Society. In their abstract, deRobertis and Bennett described the presynaptic mitochondria, filamentous axoplasm and named the small, rounded lipid profiles "synaptic vesicles." They noted that synaptic vesicles appeared to be organized in clusters close to the presynaptic membrane, and in some cases were observed

"...to perforate the presynaptic membrane" (De Robertis and Bennett, 1954; De Robertis and Bennett, 1955). The discontinuous space between the pre-and postsynaptic neurons was named the "synaptic cleft" (Palay, 1956). As these investigators observed, the visualization of the synaptic cleft was of particular importance, as it provided the "final confirmation of the neuron doctrine" as proposed by Ramon y Cajal (De Robertis, 1958b; De Robertis and Bennett, 1955; Palay, 1956; Palay, 1958). Independent studies of different types of synapses in numerous species confirmed the commonality of the structural elements of synaptic terminals and characterized the variations among them (Birks et al., 1960; Couteaux, 1955; Couteaux, 1958; Couteaux and Pecot-Dechavassine, 1970; De Robertis, 1958a; De Robertis, 1958b; Palay, 1956; Palay, 1958; Sjostrand, 1953a; Sjostrand, 1953b).

In his discussion of ultrastructural data, Palay pointed out that the synapse was "partly a morphological and partly a physiological concept" (Palay, 1956). Contemporary studies characterized the physiological behavior of synapses, mainly the frog neuromuscular junction (NMJ), and laid the foundations for determining the quantal mechanism of neurotransmitter release (Katz, 1971). In 1954, del Castillo and Katz proposed that synaptic transmission in the NMJ occurred in "all-or-none 'quanta' whose sizes are indicated by the spontaneously occurring miniature discharges" (del Castillo and Katz, 1954). It was suggested that the machinery for neurotransmitter release at the NMJ consists of many independent subunits (Fatt, 1954). Influenced by contemporary observations of vesicular systems in non-neuronal cells, anatomists drew an important link towards identifying such a unit: "vesicles may move to the presynaptic membrane, perforate it, and discharge their contents into the space immediately adjacent to the postsynaptic membrane" (De Robertis and Bennett, 1955), see also (Palade, 1954; Palay, 1956; Palay, 1958).

In a synthesis of morphological and electrophysiological observations, del Castillo and Katz then hypothesized that if the neurotransmitter acetylcholine was released at the

NMJ in discrete quanta, then perhaps the size of the quanta was determined by the storage capacity of the organelle carrying the neurotransmitter (del Castillo and Katz, 1956). They proposed that the "presynaptic corpuscles" or "granules" observed by electron microscopy corresponded to such an organelle. del Castillo and Katz successfully predicted that the release of neurotransmitter could be achieved by a "critical collision" between an intracellular "carrier particle" filled with neurotransmitter and the presynaptic membrane, whereby the two membranes would open simultaneously, thus discharging the contents of the vesicle. Subsequent studies combining electrophysiology and electron microscopy would extend these observations to suggest the mechanisms by which the supply of synaptic vesicles is maintained.

Ultrastructural studies describe the synaptic vesicle cycle

During the early 1960s, further technical advances in electron microscopy were essential for the acceptance of the vesicle hypothesis of neurotransmitter release and its logical extension, the synaptic vesicle cycle (reviewed in (Ceccarelli and Hurlbut, 1980b). In particular, Sabatini, Bensch, and Barrnett systematically presented the effects of different chemical fixations on a variety of tissues and cell types. They showed that fixation of biological specimens in buffered aldehyde solutions followed by post-fixation in osmium tetroxide substantially improved both cellular ultrastructure and histochemistry, as compared to the heavy metal fixation methods then in use (Sabatini et al., 1963). As discussed in the Methods section below, this paper is the basis of all current chemical fixation protocols. This and other technical advances fostered years of intense observations of neuronal and non-neuronal vesicle populations and theories of their dynamic biogenesis and trafficking (Palade and Bruns, 1968) reviewed in (Mellman, 1996). In 1970, Pecot-Dechavassine and Couteaux synthesized the prevailing theory of the vesicle hypothesis of quantal release, in designating the specialized, electron densities where synaptic vesicles accumulate "les zones actives" (Couteaux and Pecot-Dechavassine, 1970).

Jointly relying on the techniques of electrophysiology and electron microscopy to study the frog NMJ, a correlation between the fusion of synaptic vesicles, the release of neurotransmitter and the subsequent local recycling of synaptic vesicles was demonstrated (Ceccarelli et al., 1972; Heuser and Reese, 1972). Specifically, it was observed that neurotransmission and the number of synaptic vesicles were sustained for only a few hours of stimulation; very prolonged stimulation (6-8 hours) led to an exhaustion of both neurotransmitter release and synaptic vesicles. Using black widow spider venom (BWSV) to force the exocytosis of all synaptic vesicles in resting NMJs, the total basal amount of neurotransmitter was estimated. The amount of neurotransmitter released over a period of time was shown to be several-fold higher than the starting concentration, implying that neurotransmitter was being re-supplied during synaptic transmission. This was confirmed in additional studies (Ceccarelli et al., 1979b; Gorio and Mauro, 1979; Longenecker et al., 1970) reviewed in (Schiavo et al., 2000). Based on the relationship between neurotransmitter release and synaptic vesicle number, Ceccarelli and his colleagues postulated that under normal conditions, the synaptic vesicle supply must be maintained locally in the nerve terminal. In stimulated terminals, approximately half of all synaptic vesicles were labeled by bath-applied horseradish peroxidase (HRP). As HRP was known to be membrane-impermeable, labeled vesicles were considered to represent either original vesicles that had opened transiently to the synaptic cleft during neurotransmitter release, or vesicles that had fused with and recycled from the presynaptic axolemma. They proposed that vesicle replenishment was consistent with three separate mechanisms, operating exclusively or in combination: transport of vesicles from the axon, production of vesicles within the terminal via intermediates, or via direct recycling of the presynaptic plasma membrane.

Ceccarelli and his colleagues followed this paper with an extensive analysis of the recycling of synaptic vesicles at the frog NMJ, again using the combined techniques of electron microscopy and electrophysiology (Ceccarelli and Hurlbut, 1980a; Ceccarelli et

al., 1973; Hurlbut and Ceccarelli, 1974). They compared the amount of neurotransmitter released, the number of synaptic vesicles in terminals fixed at rest and during stimulation, and the number of HRP-labeled vesicles in terminals fixed at rest and after various stimulation paradigms. While they did not cite a mechanism, the authors again concluded that synaptic vesicles fuse transiently or permanently with and are recycled from the presynaptic plasma membrane, and are capable of undergoing subsequent rounds of fusion and neurotransmitter release.

In the same volume of the Journal of Cell Biology, using methods similar to Ceccarelli *et al.*, Heuser and Reese provided independent observations supporting the local recycling of synaptic vesicles as well as additional evidence to propose a mechanism of clathrin-mediated endocytosis for retrieval of vesicle components (Heuser and Reese, 1973). This pathway was first described in non-neuronal cells (Roth and Porter, 1964) and the structure of clathrin was soon well characterized by electron microscopy (Kanseki and Kadota, 1969). Based on morphological observations, Heuser and Reese proposed that vesicles were recycled via this mechanism directly from the presynaptic membrane or from intermediate cisternae. In agreement with Ceccarelli *et al.*, approximately 50% of vesicles in a given stimulated terminal were labeled by HRP. Furthermore, recycled vesicles labeled by HRP could be lost during subsequent stimulation and wash-out of HRP, indicating that recycled vesicles were capable of performing additional rounds of release. Although the protein clathrin was not yet identified,(Pearse, 1976), the authors noted the activity-dependent accumulation of intermediates, vesicles and cisternae coated with basket-like structures, connected to the presynaptic membrane. Some of these coated intermediates were also labeled by HRP, thus demonstrating that they too were derived from the presynaptic axolemma that was accessible to HRP. Heuser and Reese postulated that these intermediates were precursors to the observed HRP-labeled uncoated synaptic vesicles. Endocytosis typically occurred lateral to the active zone, in the area of contact with the Schwann cell. At the conclusion of this landmark study, Heuser and Reese

presented a cartoon of the events underlying the synaptic vesicle cycle (Figure 1). Characterizing the molecular events underlying the stages depicted in this cartoon has been the subject of many subsequent investigations, including that of this thesis.

Throughout their studies of the synaptic vesicle cycle, Ceccarelli and colleagues were careful to point out that in relying upon static images such as electron micrographs, it was difficult to formally distinguish between the clathrin-mediated pathway of vesicle recycling and a more direct pathway whereby vesicles that fused with the active zone reformed at the site of fusion, now referred to as the "kiss and run" mechanism of neurotransmitter release. They reasoned that the number of coated intermediates observed by electron microscopy could never be sufficient to sustain synaptic transmission unless, "...coats were associated with vesicles for only a small fraction of the time required for endocytosis" [Ceccarelli, 1979 #932]; see also (Heuser, 1989).

Similar studies performed in isolated nerve terminals (synaptosomes) and in other systems such as torpedo electric organ supported the hypothesis of a local synaptic vesicle cycle (Fried and Blaustein, 1976; Zimmerman and Denston, 1977). Several groups, beginning with both Ceccarelli *et al.* and Heuser and Reese noted that vesicle cycling could occur under conditions in which neurotransmitter synthesis was blocked, uncoupling these two events (Ceccarelli and Hurlbut, 1975; Cousin and Nicholls, 1997; Heuser and Reese, 1973; Hurlbut and Ceccarelli, 1974).

In his own ultrastructural investigations of the synapse, Katz recognized that by conventional methods, "...even if it were possible to fix the specimen at the peak of synaptic activity, the chances of finding a 'discharging vesicle' are very small, and it would be a hopeless task to identify it" (Birks et al., 1960). The development of another microscopy technique, freeze fraction replication, addressed this challenge (Akert et al., 1972). Freeze fracturing reveals the opposing membrane faces of the plasma membrane, and vesicles can be viewed as concave or convex interruptions of the plasma membrane surface (described in (Bozzola and Russell, 1992). Evidence of the fusion of synaptic

Figure 1. The Synaptic Vesicle Cycle

This figure presented the first schematic framework of the local synaptic vesicle cycle. It provoked decades of research aimed at understanding each step, at the morphological, molecular, and functional levels.

This figure is reproduced from The Journal of Cell Biology, 57:315-44, Heuser, J. E., Reese, T. S. *Evidence for recycling of synaptic vesicle membrane during transmitter release at the frog neuromuscular junction*, by copyright permission of The Rockefeller University Press.

Original Figure Legend:

"Diagrammatic summary of the path of synaptic vesicle membrane recycling proposed in this study: synaptic vesicles discharge their content of transmitter by coalescing with the plasma membrane at specific regions adjacent to the muscle; then equal amounts of membrane are retrieved by coated vesicles arising from regions of the plasma membrane adjacent to the Schwann sheath; and then, the coated vesicles lose their coats and coalesce to form cisternae which accumulate in regions of vesicle depletion and slowly divide to form new synaptic vesicles."

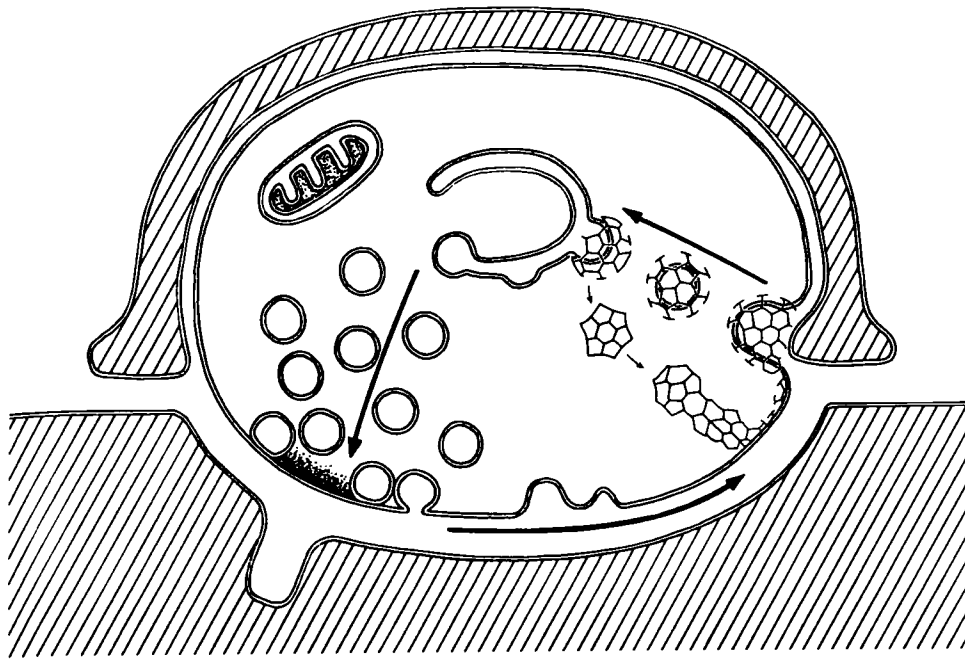

J. E. Heuser and T. S. Reese, *Recycling of Synaptic Vesicle Membrane*, The Journal of Cell Biology, Volume 57, 1973, pp. 315-344

vesicles with the active zone was obtained using this technique to study the lamprey spinal cord, where structures representing synaptic vesicle fusion seemingly accumulated at active zones with Ca^{2+}-dependent stimulation (Pfenninger and Rovainen, 1974). The authors postulated that the discharge of transmitter from synaptic vesicles was represented morphologically by the appearance of temporary crater-like openings in the site of vesicle attachment.

The Ca^{2+}-dependent fusion of synaptic vesicles at active zones and the appearance of slightly larger vesicle intermediates in areas outside of the active zone were further documented by several freeze-fracture studies of frog NMJs under varying conditions of stimulation (Ceccarelli et al., 1988; Ceccarelli et al., 1979a; Ceccarelli et al., 1979b; Ceccarelli and Hurlbut, 1980b; Fesce et al., 1980; Heuser and Kirschner, 1980; Heuser et al., 1979; Heuser et al., 1974; Heuser et al., 1976).

Several techniques developed more recently can provide real-time measurements of the synaptic vesicle cycle. For example, the exocytosis and endocytosis of individual synaptic vesicles can be monitored via the changes in membrane capacitance arising from the addition and removal of synaptic vesicle membrane during the synaptic vesicle cycle (von Gersdorff and Matthews, 1999). Furthermore, fluorescent compounds such as FMI-43 have facilitated the demonstration of quantal release and re-uptake in real time by light microscopy (reviewed in (Cousin and Robinson, 1999; Neher, 1998; Ryan et al., 1996b). As the dye is membrane-impermeable, FMI-43 traces synaptic vesicle cycling in a manner analogous to that of HRP, so that the fluorescence of a vesicle indicates that it has been exposed to the extracellular space and therefore has fused with the presynaptic membrane, albeit transiently. Using this reagent, the time course of endocytosis has been determined in neuronal cultures (Ryan et al., 1993). In agreement with ultrastructural studies (Gad et al., 1998; Miller and Heuser, 1984), the maximum rate of endocytosis was determined to occur 30-45 seconds after depolarization. The amount of time between endocytosis and subsequent exocytosis of

a newly recycled vesicle, "repriming," was placed at an upper limit of 30 seconds, bringing the total recycling time to something on the order of 90 seconds. Thus, it appears that clathrin-mediated endocytosis occurs at a rate commensurate with most synaptic requirements for sustaining neurotransmitter release and the short "life-span" of coated intermediates as required by Ceccarelli and colleagues to sustain recycling has been addressed. However, the fundamental reservation of using static images to describe dynamic processes is still a relevant caution and the real-time imaging experiments thus provide important insights into issues related to the kinetics of synaptic vesicle cycling.

The role of Ca^{2+} in the synaptic vesicle cycle has been investigated intensely and a comprehensive review of such studies is not intended here (for review, see (Neher, 1998). Briefly, upon nerve terminal depolarization, Ca^{2+} flows into the terminal through channels located in the area of the active zone, possibly in those structures referred to as dense projections, and accumulates in microdomains (Heuser et al., 1974; Llinas et al., 1992; Pumplin et al., 1981; Simon and Llinas, 1985). The microdomains of Ca^{2+} in the terminal are estimated to surround Ca^{2+} channels within a range of 20-200 nm (Neher, 1998). Intracellular concentrations of calcium sufficient to induce neurotransmitter release have been measured in different synapses and are in the low micromolar range (Beutner et al., 2001; Schneggenburger and Neher, 2000). The exocytosis of synaptic vesicles triggered by Ca^{2+} is possibly sensed by an isoform of the synaptic vesicle integral membrane protein synaptotagmin (Sugita et al., 2001).

Endocytosis is also sensitive to internal Ca^{2+} levels (Gad et al., 1998). This sensitivity has also been linked to a synaptotagmin isoform (Jorgensen et al., 1995; Zhang et al., 1994). In the NMJ, the most active areas of endocytosis correspond to the areas in contact with Schwann cell processes (Miller and Heuser, 1984). In the lamprey spinal cord, endocytosis occurs within a range of 0.5 μm from the edges of the active zone, in the area apposing glial cell processes (Gad et al., 1998). While the Ca^{2+}

levels present in the areas of endocytosis have not been determined, the presence of internal Ca^{2+} is required (Ceccarelli and Hurlbut, 1990; Gad et al., 1998). Low micromolar ranges of intracellular Ca^{2+} are thought to be sufficient for clathrin-mediated endocytosis to occur (Gad et al., 1998; Ryan et al., 1993).

Actin in the presynaptic nerve terminal

As studies of synaptic ultrastructure and physiology firmly established the local recycling of synaptic vesicles, investigators used the principles of subcellular fractionation techniques developed by Claude, de Duve, and Palade to isolate and study the biochemical components from a variety of tissues, including the brain. Using biochemical techniques, actin and myosin were first identified in brain and synaptosomal homogenates (Berl et al., 1973; Fine et al., 1973; Fine and Bray, 1971; Kuczmarksi and Rosenblum, 1979; Kuczmarkski and Rosenbaum, 1979; Puszkin and Berl, 1970; Puszkin and Berl, 1972; Puszkin et al., 1968; Puszkin et al., 1972; Tashiro and Stadler, 1978; Walker et al., 1985). Informed by the knowledge of muscle contraction and ultrastructural studies of synaptic vesicle cycling, the earliest models of actin function in the nerve terminal suggested an actomyosin-based mechanism to drive the fusion event itself, with a synaptic vesicle-bound myosin and presynaptic plasma membrane-bound actin interacting to pull the membranes together (a concept not unlike the current SNARE hypothesis (Berl et al., 1973; Puszkin and Kochwa, 1974).

Using anti-actin antibodies, the presence of actin in nerve terminals was confirmed by light level cytochemistry (Toh et al., 1976). In an ultrastructural study, the presence of actin in synaptosomes was demonstrated histochemically by heavy meromyosin binding (Inestrosa et al., 1976). Intracellularly, actin can be found cycling between two forms, individual monomers (globular, G) or polymerized filaments (filamentous, F). Many actin-binding proteins preferentially bind to one or the other of these forms and can influence the cycling of actin between these two forms. Early biochemical studies of clathrin co-purified both globular and filamentous actin,

providing additional links with the synaptic vesicle cycle (Puszkin et al., 1982; Schook et al., 1979). The presence of actin in extruded axoplasm of the squid giant axon was confirmed by biochemical and ultrastructural analyses (Fath and Lasek, 1988; Morris and Lasek, 1984).

Once the presence of actin was demonstrated in the presynaptic nerve terminal, its participation in the synaptic vesicle cycle was tested using actin-modifying compounds, often yielding contradictory results. Cytochalasins are drugs that cause the depolymerization of actin (Brown and Spudich, 1981) reviewed in (Cooper, 1987). Application of cytochalasins in a variety of experimental systems was shown to affect synaptic transmission (Delgado et al., 2000; Nicklas and Berl, 1974; Rubin et al., 1976; Thoa et al., 1972; Wang et al., 1996). For example, in cultured chicken NMJs, spontaneous and evoked end-plate potentials were inhibited reversibly in the presence of cytochalasin B (Rubin et al., 1976). Due to the effect on spontaneous miniature end-plate potentials, the authors concluded that the defect must be related to the release mechanism itself.

Additional studies tested the functional role of actin in the synaptic vesicle cycle using a bicyclic hexapeptide toxin derived from the *Amanita phalloides* mushroom, phalloidin, which binds to and stabilizes actin filaments (Cooper, 1987; Lengsfeld et al., 1974; Wulf et al., 1979). This toxin has been shown to shift the equilibrium between F- and G-actin, and lowers the critical concentration for polymerization. The net effect of applying phalloidin is an accumulation and preservation of filamentous actin. Since phalloidin retains its activity when labeled by fluorophores, it is a valuable tool in light and electron microscopy. Phalloidin-bound F-actin can still participate in some of actin's normal molecular interactions such as those with the molecular motor myosin (Lengsfeld et al., 1974). Using phalloidin to disrupt actin cycling, a series of studies on neurotransmitter release from whole brain synaptosomes were performed by Bernstein and Bamburg. These authors found that stimulation of nerve terminals

induces a decrease in F-actin and an increase in G- actin (Bernstein and Bamburg, 1985). This perturbation in cytoskeletal actin dynamics is transient (Bernstein and Bamburg, 1987) and depolymerization of actin was proposed to be a necessary condition for release (Bernstein and Bamburg, 1989). Recently, these observations were confirmed in intact neurons (Bernstein et al., 1998). Studies with other toxins such as the *Clostridium botulinum* C2 toxin, which causes a net depolymerization of actin, (see Figure 9), also supported a role for actin in regulating synaptic vesicle traffic (Matter et al., 1989).

Many additional studies support the presence of actin in the presynaptic terminal, some of which are described briefly here. Fifkova and Delay identified actin filaments in the presynaptic terminals of the mouse hippocampus (Fifkova and Delay, 1982). Using phalloidin, Drenckhahn and Kaiser also showed evidence for actin in rat synaptosomes and axons, directly beneath the axonal membrane (Drenckhahn and Kaiser, 1983). In axoplasm extruded from squid giant axons, it was demonstrated that synaptic vesicles could move on an endogenous actin filament network (Kuznetsov et al., 1992). Movement of synaptic vesicles along actin filaments required the presence of energy in the form of ATP. In target-deprived frog motor nerve terminals, labeling of actin and synaptic vesicle markers determined that actin was excluded from release sites but positioned in domains interdigitating clusters of synaptic vesicles (Dunaevsky and Connor, 2000).

More recent investigations of the functional role of actin in the synaptic vesicle cycle have used a variety of real-time optical methods to correlate changes in actin dynamics and synaptic vesicle recycling in neurons. In synaptic terminals of retinal bipolar cells, application of cytochalasin D did not affect the cycling of synaptic vesicles, as visualized at the light microscopic level by FMI-43 (Job and Lagnado, 1998). By contrast, high frequency neurotransmission in the fly NMJ was shown to be inhibited by cytochalasin D, and the reserve pool appeared to be affected by

cytochalasin D under conditions in which endocytosis was also blocked (Kuromi and Kidokoro, 1998).

Studies aimed at disrupting normal actomyosin dynamics provide indirect support for a role for actin in the nerve terminal. In cultured neurons, electrophysiological studies demonstrated that inhibitors of myosin light chain kinase (MLCK) inhibited release in a dose-dependent manner (Mochida, 1995; Mochida et al., 1994). Furthermore, Ryan used FMI-43 in cultured hippocampal synapses to demonstrate that inhibitors of MLCK blocked the mobilization of the reserve and not the releasable pool of synaptic vesicles (Ryan, 1999). While endocytosis was not affected, the degree of MLCK inhibition was dependent on the level of synaptic activity, implicating a role for MLCK at a stage in the synaptic vesicle cycle after endocytosis.

A role for actin in vesicle mobilization was supported in a recent study of snake motor terminals. In this study, disruption of actin by the marine toxin latrunculin A, which inhibits actin polymerization, impaired the destaining of FMI-43 within synaptic vesicles, indicating an effect on neurotransmitter release (Cole et al., 2000). This event was followed by a marked decrease in end-plate potentials (EPPs) elicited at high frequency and prolonged recovery from post-tetanic depression. The authors concluded that the most likely mode of action for actin was in the mobilization of vesicles from the reserve pool to the release sites. In a puzzling contemporary study, Morales *et al.* found that treatment of autapsing hippocampal neurons with latrunculin A enhanced evoked neurotransmitter release and caused the elongation of presynaptic actin linked to green fluorescent protein (GFP)(Morales et al., 2000).

The synapsins

With the mechanism of quantal release and experimental models of synaptic transmission firmly established, investigators began to search for intracellular molecules that influenced or were influenced by synaptic transmission. In the late 1960s, the discovery of cyclic (c) AMP-dependent protein kinase in muscle provided

the opportunity to link phosphorylation with physiological actions of adrenaline (reviewed in (Nestler and Greengard, 1984). Subsequently, cAMP-dependent protein kinase was discovered in other tissues, and in particular it was found to be present at high levels in the brain and enriched in synapses (Maeno et al., 1971; Miyamoto et al., 1969). These observations led to the hypothesis that cAMP-dependent protein kinase modulated some of the molecular events underlying synaptic transmission (Greengard, 1976; Greengard et al., 1971). With the subsequent purification and study of other protein kinases, this hypothesis was elaborated to state that many classes of physiological responses, including synaptic transmission, were regulated by specific protein kinases (Greengard, 1978). In 1979, Greengard and colleagues began to purify substrates of cAMP-dependent protein kinase from brain. Among the first substrates purified from cerebral cortex were synapsins Ia and Ib (Ueda et al., 1979).

The synapsin domain model

Since the discovery of synapsin by biochemical purification, three distinct synapsin genes, synapsin I, II, and III, have been cloned from a wide variety of species (reviewed in (Hilfiker et al., 1999). These genes give rise to several isoforms, via alternative splicing, that range in molecular weight from 55-86 kDa. While distinct functions of the synapsin gene products are not known, the dominant isoforms in the mature nerve terminal are synapsins Ia, Ib, IIa, and IIb (Sudhof et al., 1989). Synapsin III appears to function most prominently during development and is therefore outside of the scope of this discussion (Ferreira et al., 2000; Kao et al., 1998; Kao et al., 1999).

The synapsins conform to a domain structure that is shared across species and among isoforms (see Figure 2, adapted from (Kao et al., 1999). Vertebrate synapsins contain a highly conserved primary sequence in their amino terminal, designated as domains A-C, while the carboxy terminal of the protein is more varied and comprises domains D-J. Among these molecules in vertebrates, the most highly conserved

Figure 2. The domain structure of the synapsin family

Synapsins cloned from some vertebrate and invertebrate species are represented schematically here. The number of amino acids is indicated by the scale at the top (AA). The vertebrate isoforms shown are rat synapsin Ia and Ib (r-synIa, r-synIb), rat synapsin IIa and IIb, (r-synIIa, r-synIIb) and human synapsin IIIa (h-synIIa). The invertebrate synapsins shown are drosophila (d-syn-short) and squid (s-syn short, s-syn-long). Domains A, C, and E are the most highly conserved among isoforms and across species. Domains D, H, I, and J share an overall similarity of high proline content.

This figure was slightly modified and reproduced by permission of the authors from Kao *et al.,* Molecular Evolution of the Synapsin Gene Family, 1999, Journal of Experimental Zoology, 285:360-377.

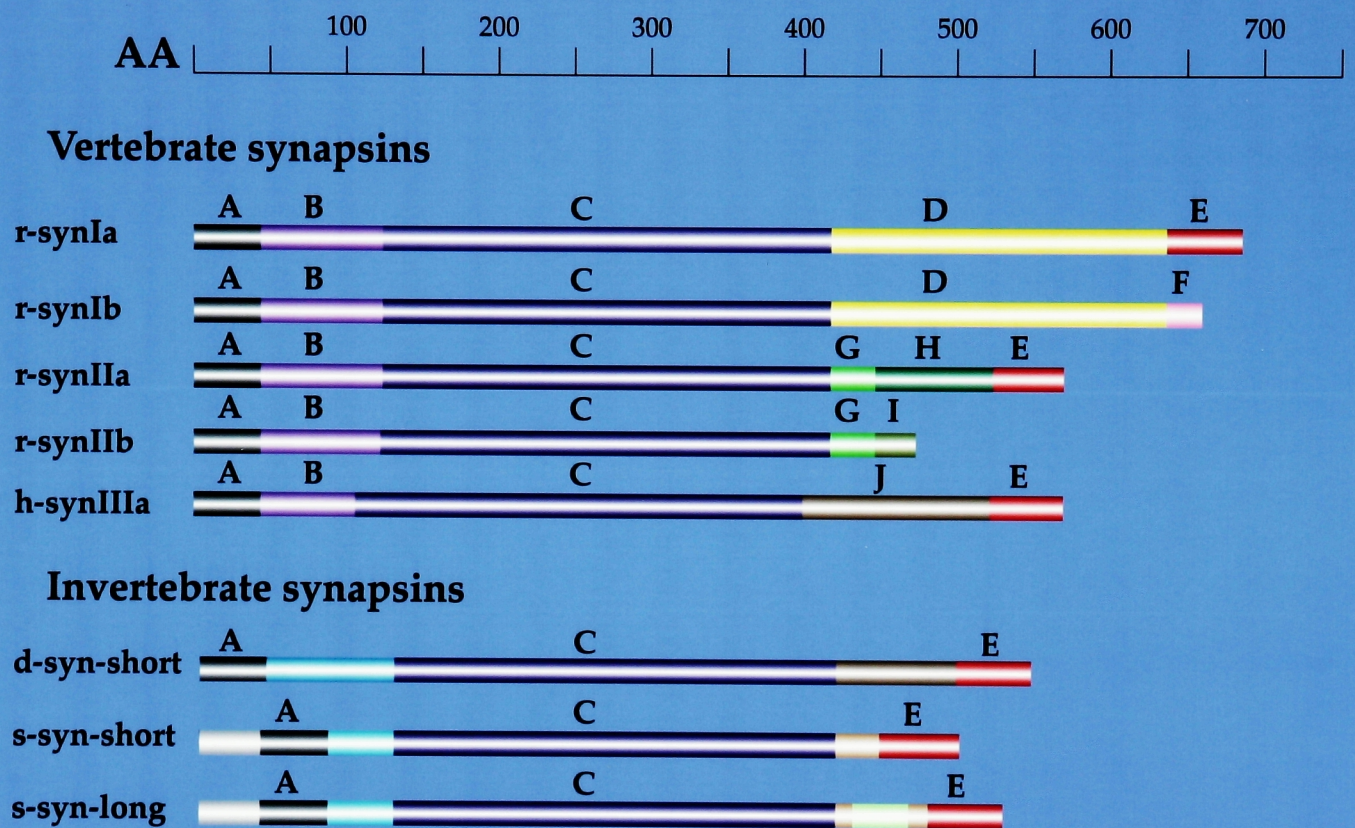
AA
100
200
300
400
500
600
700
Vertebrate synapsins
r-synIa
A
B
C
D
E
r-synIb
A
B
C
D
F
r-synIIa
A
B
C
G
H
E
r-synIIb
A
B
C
G
I
h-synIIIa
A
B
C
J
E
Invertebrate synapsins
d-syn-short
A
C
E
s-syn-short
A
C
E
s-syn-long
A
C
E

domain is the A domain. This is linked by a somewhat more variable B domain to the extensively conserved core of the molecule, designated as the C domain, which binds to synaptic vesicle phospholipids via several sites (Cheetham et al., 2001). Among the "I" isoforms, the amino acid proline is enriched in the D domain. Among the "a" isoforms, the carboxy terminal E domain is also strikingly conserved.

Previous localization studies of synapsin

In an effort to understand how synaptic vesicles cluster at active zones and move through the axoplasm during recycling, Landis *et al.* investigated the organization of the presynaptic axoplasm, using conventional and quick freeze deep etch (QF-DE) electron microscopy (Landis et al., 1988). Using different fixation techniques, the authors described the presence of a filamentous material surrounding vesicles clustered at active zones. They observed several populations of filaments with various dimensions in contact with and enmeshing synaptic vesicles. Landis *et al.* concluded that few, if any, actin-like filaments were present in the area immediately adjacent to the active zone, and proposed that other large diameter filaments extending from the active zone corresponded to spectrin. (These filaments may also include some of the proteins recently discovered to be specific to the active zone, reviewed in (Dresbach et al., 2001). In the same study, Landis *et al.* suggest that short lollipop-shaped filaments in contact with synaptic vesicles throughout the cluster resemble the shape of purified synapsin I, as visualized by rotary-shadowing. Based on these observations, they postulated that synapsin may not only help cluster vesicles at active zones, but also modulate their availability for release. In a subsequent investigation of the cytoskeleton in neurons, Hirokawa *et al.* used QF-DE to study the presynaptic terminal (Hirokawa et al., 1989). These *in vitro* studies agreed well with Landis *et al.* and concluded that purified synapsin had a lollipop-like appearance using this technique. In electric organs of electric rays, randomly organized actin filaments were identified by decoration with myosin S1 heads. In cerebellar nerve terminals and in neuromuscular junctions, actin

filaments were observed close to the plasma membrane and to contact synaptic vesicles via short linking strands, that the authors hypothesized to be synapsin. Based on these studies, it was concluded that synapsin could bind to itself and simultaneously, to actin and synaptic vesicles.

Immunocytochemical studies of synapsins at the light and electron microscopic levels demonstrated that they are present on synaptic vesicles in virtually all neurons of the peripheral and central nervous system, suggesting an important role in the regulation of vesicle dynamics (Bloom et al., 1979; De Camiili et al., 1979; De Camilli et al., 1983a; De Camilli et al., 1983b). Interestingly, the only presynaptic terminals that have been shown to lack synapsins are ribbon synapses such as those in retinal bipolar cells and dense-body synapses of hair cells, sensory synapses that maintain high numbers of synaptic vesicles and high tonic firing rates (von Gersdorff and Matthews, 1994). Synapsin I was found to be associated specifically with small clear synaptic vesicles rather than with large dense-core vesicles (Navone et al., 1984). At the frog NMJ, synapsin was shown to be present on synaptic vesicles throughout the nerve terminal (Valtorta et al., 1988).

The relationship between the localization of the synapsins and synaptic activity has been studied extensively. Specifically, this was investigated in the frog NMJ in the presence of the vesicle fusion promoting component of black widow spider venom (BWSV, latrotoxin (Torri-Tarelli et al., 1990). As determined previously in resting preparations, synapsin was present on synaptic vesicles throughout the frog NMJ. In terminals where vesicle fusion was promoted by the presence of latrotoxin (LTX) but vesicle recycling was blocked by the absence of Ca^{2+}, synapsin was found to be redistributed in clusters along the presynaptic membrane, indicating that synapsin dissociation is not a requirement for vesicle fusion under these conditions. In terminals where LTX was applied in the presence of Ca^{2+}, thereby allowing synaptic vesicle cycling, synapsin was present on synaptic vesicles in a manner similar to that of resting

terminals. These data indicate that the reassociation of synapsin with vesicles occurs rapidly during the recycling process.

The localization of synapsin I was subsequently investigated in the frog NMJ under more physiological conditions (Torri-Tarelli et al., 1992). After high frequency stimulation, when the rate of exocytosis exceeds that of endocytosis, less synapsin was associated with synaptic vesicles over time as compared with unstimulated preparations. However, in stimulated preparations, the proportion of total synapsin labeling was still greatest on synaptic vesicles and least on the axolemma, again indicating that synapsin reassociates with synaptic vesicles following endocytosis. This material was preserved by cryofixation, which does not reliably preserve the axoplasm, and thus the distribution of synapsin on occasional filamentous structures was only tentatively noted.

The localization of synapsin in resting synaptic terminals was recently investigated in lamprey reticulospinal synapses (Pieribone et al., 1995). Using antisera raised against the E domain (G304) of synapsin to detect synapsin using the post-embedding immunogold method, synapsin was found to be present throughout the vesicle clusters of resting synapses. At a distance of 0-100 nm and 100-200 nm from the active zone, approximately 0.7 and 2.1 gold particles per 100 nm^2 were detected. This result was well correlated with the disruption of the synaptic vesicle cluster induced by axonal microinjection of the same antibody (see below).

Regulation of synapsin by phosphorylation

As mentioned previously, synapsin was first identified as a substrate for brain protein kinases (Ueda et al., 1979). In biochemical studies, it was subsequently discovered that the association between synaptic vesicles and synapsin was regulated by phosphorylation by both Ca^{2+}/calmodulin-dependent protein kinases (CaMKs) and cAMP-dependent protein kinase (Huttner et al., 1981; Huttner and Greengard, 1979; Kennedy and Greengard, 1981; Kennedy et al., 1983). In synaptic vesicles purified

from rat cerebral cortex, synapsin dissociated from synaptic vesicles under high ionic strength conditions, indicating that it is tightly associated with, but not integral to the synaptic vesicle membrane (Huttner et al., 1983). Synapsin was found to account for 9% of (De Camilli et al., 1990; Huttner et al., 1983; Sudhof et al., 1989). The vesicle fraction contained a Ca^{2+}-dependent protein kinase activity that phosphorylated synapsin in its COOH-terminal region and promoted its dissociation from synaptic vesicles. This kinase was determined to be Ca^{2+}/calmodulin-dependent protein kinase II (CaMKII) (McGuinness et al., 1983).

To date, several serine/threonine (ser/thr) kinases have been found to phosphorylate synapsin I. There are seven confirmed phosphorylation sites and several of these sites are conserved within synapsin I across species, offering potentially important modes of regulation (see Discussion, Figures 3 and 37). As most biochemical studies have been performed on rat synapsin Ia, the amino acid numbering refers to that sequence, unless otherwise specified (Figure 3). Ser^{9}, historically referred to as site 1, is phosphorylated by cAMP-dependent protein kinase (PKA), CaMKI and CaMKIV (Czernik et al., 1987). This site has been claimed to be an important factor for synapsin's association with synaptic vesicles (Hosaka et al., 1999). Ser^{566} and Ser^{603}, referred to as sites 2 and 3, are phosphorylated by CaMKII and CaMKIV (Czernik et al., 1987). Ser^{62} and Ser^{67} are phosphorylated by the proline-directed mitogen activated kinase (MAPK) and referred to as sites 4-5 (Jovanovic et al., 1996), (Matsubara et al., 1996). Ser^{551}, (site 6), also within a proline-rich region of the protein, can be phosphorylated by MAPK, (Jovanovic et al., 1996; Matsubara et al., 1996), cyclin-dependent kinase (cdk1) (Hall et al., 1990), cdk2 and cdk5 (Matsubara et al., 1996). Ser^{553}, (site 7), can be phosphorylated by cdk5 (Matsubara et al., 1996). The regulation of some of these sites by specific phosphatases has also been determined (see Discussion). In addition to regulation by ser/thr phosphorylation, there are several potential tyrosine phosphorylation sites within the highly conserved domain Cof synapsin. Moreover,

Figure 3. Phosphorylation sites of rat synapsin Ia

There are currently seven known serine residues that are phosphorylation sites (P-sites) within rat synapsin I (a and b differ only in the very carboxy terminus). Many of these sites are conserved across species and isoforms (see Figure 37). The number of the serine (Ser) residue in the polypeptide (out of total 704 amino acids) is shown in black and the appropriate kinase for that site is indicated above in color. The sites are clustered located in domains A, B, and D. The sites are referred to as sites 1-7 (below synapsin schematic).

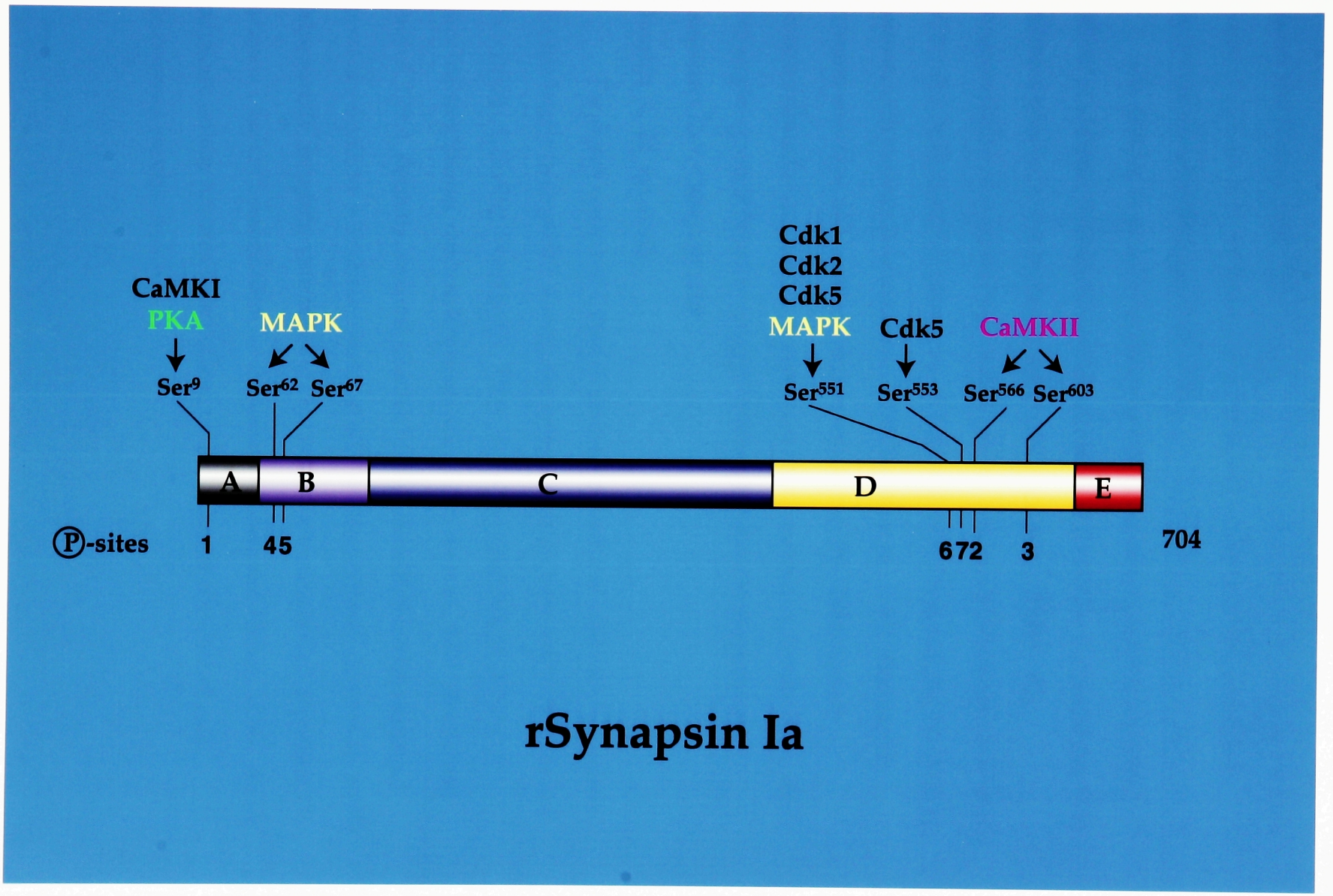

rSynapsin Ia

synapsin I is known to interact with a vesicle form of the tyrosine kinase c-Src (Foster-Barber and Bishop, 1998; Onofri et al., 1997). Phosphorylation of synapsin has been linked to changes in its physiological activities in a variety of *in vitro* and *in vivo* studies (reviewed in (Hilfiker et al., 1999).

In addition to its ability to phosphorylate the protein, CaMKII is a binding partner of synapsin on synaptic vesicles (Benfenati et al., 1992a) at sites distinct from its interactions with vesicle phospholipids (Benfenati et al., 1989a). The phosphorylation of synapsin I by CaMKII induces conformational changes in synapsin which alter its biochemical interactions with synaptic vesicles as well as other binding partners such as actin (Benfenati et al., 1990; Stefani et al., 1997). Dephospho-synapsin associates with purified synaptic vesicles rapidly, while synapsin phosphorylated by CaMKII has an attenuated rate of association (Stefani et al., 1997). Dephospho-synapsin bound to synaptic vesicles dissociates in the presence of exogenous Ca^{2+}, CaM, and ATP.

Domain C of synapsin

The highly conserved C domain mediates a number of important interactions. Via this largely hydrophobic domain, the synapsins exhibit intra- and inter-molecular associations, including dimerization. These interactions may help to stabilize or associate neighboring vesicles (Benfenati et al., 1993; Ho et al., 1991; Hosaka and Sudhof, 1999). Recently, a crystal structure of the C domain of bovine synapsin I revealed a similarity with certain classes of ATP-utilizing enzymes (Esser et al., 1998). Subsequently, synapsins were found to bind ATP; this binding is Ca^{2+}-dependent for synapsin I and Ca^{2+}-independent for synapsin II (Hosaka and Sudhof, 1998). As no enzymatic activity has been demonstrated, the physiological relevance of such observations remains elusive.

Biochemical interaction of synapsins with actin

A phosphorylation-dependent interaction of synapsin I with actin has been demonstrated *in vitro* (Bahler and Greengard, 1987). It was suggested that this interaction might "be important in the regulation of vesicle movement and/or neurotransmitter release." It was subsequently shown that synapsin can bind to synaptic vesicles and actin simultaneously (Benfenati et al., 1989b). These interactions have been shown *in vitro* to be rapid (Ceccaldi et al., 1993) and mediated by domain C (Bahler et al., 1989). Dephospho-synapsin I can promote the initial phases of G-actin nucleation (Benfenati et al., 1992a), so that more nuclei elongate into filaments (Fesce et al., 1992). Synapsin can also stabilize and bundle F-actin in a phosphorylation-dependent manner (Bahler et al., 1989). *In vitro*, synaptic vesicles with endogenous synapsin are able to promote G-actin nucleation and F-actin polymerization while synaptic vesicles stripped of synapsin are unable to do so (reviewed in (Greengard et al., 1994).

Thus, the following widely-cited hypothesis of synapsin function has been proposed: Desphospho-synapsin is able to bind to synaptic vesicles and actin. Upon depolarization, CaMKII phosphorylates synapsin, changing its conformation and forcing its dissociation from synaptic vesicles and from actin, thereby diminishing the ability of vesicles to interact with the actin cytoskeleton (Figures 4, 6 and (Chieregatti et al., 1996). Biochemical studies have demonstrated that synapsin binds to itself, synaptic vesicles, and several cytoskeletal elements, including microtubules (Aubert-Foucher and Font, 1990; Baines and Bennett, 1986; Bennett and Baines, 1992; Bennett et al., 1991; Bennett et al., 1985; McGuinness et al., 1989), and spectrin (Baines and Bennett, 1985), reviewed in(Goodman et al., 1988). Synapsin also interacts with several signal transduction molecules, vesicle phospholipids (Benfenati et al., 1989b; Benfenati et al., 1993; Cheetham et al., 2001), and presynaptic proteins, as described in the Discussion.

Figure 4. Schematic model of possible mechanisms of interaction between synaptic vesicles and actin

Top: Synaptic vesicle (SV) bound to dephospho-synapsin I (square) binds to pre-formed actin filaments (F-actin).

Middle: Synapsin bound to synaptic vesicle binds actin monomers, (G-actin), thus forming a pseudo-nucleus that then further elongates to form actin filaments.

Lower: When Ca^{2+} flows into the nerve terminal, various kinases such as Ca^{2+}/calmodulin-dependent protein kinase II (CaMKII) are activated and phosphorylate synapsin (P-sites and square). The result is a lowered affinity of synapsin for both synaptic vesicles and actin and the dissociation of this ternary complex.

Modified from and reprinted by permission of the authors from Greengard *et al.*, Synapsin I, an actin-binding protein regulating synaptic vesicle traffic in the nerve terminal. Molecular and Cellular Mechanisms of Neurotransmitter Release, 1994:31-45.

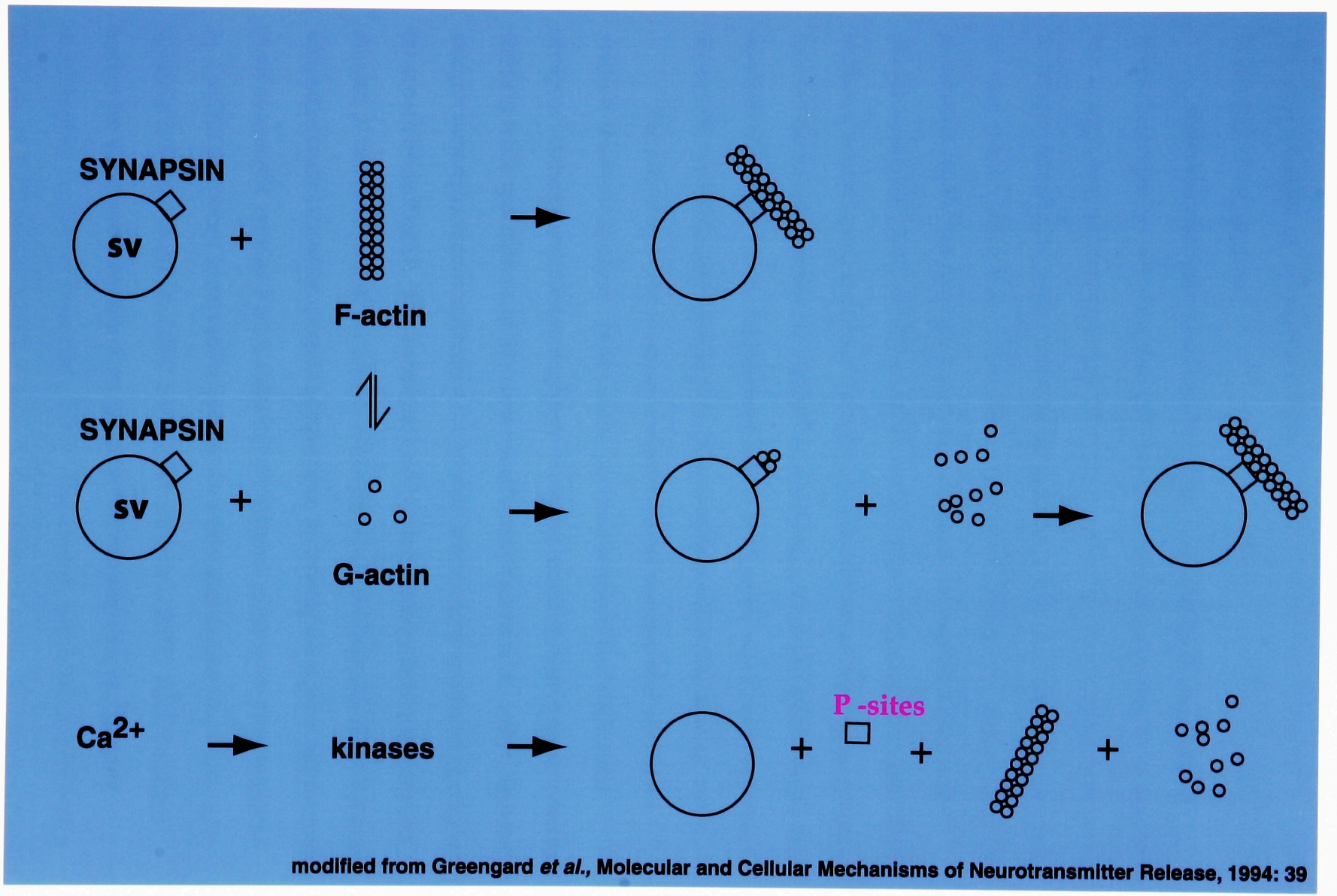

modified from Greengard *et al.*, Molecular and Cellular Mechanisms of Neurotransmitter Release, 1994: 39

In vivo studies of synapsin function

Microinjection studies

Several studies have microinjected synapsin in a variety of vertebrate and invertebrate species. All of these studies demonstrated that synapsins play an important role in regulating neurotransmission. In 1985, biochemical and immunocytochemical techniques revealed the presence of a synapsin I-like protein and CaMKII in the squid nervous system (Llinas et al., 1985). Microinjection of dephospho-synapsin I into the preterminal digit of the squid giant axon decreased neurotransmitter release while phospho-synapsin I (on CaMKII sites) was without effect. Injection of CaMKII itself increased neurotransmitter release. Furthermore, introduction of dephospho-synapsin reduced the rate of spontaneous synaptic vesicle release, while phospho-synapsin had no effect (Lin et al., 1990). Inhibition of release by synapsin was shown to be dose-dependent, reversible, and specific to its phosphorylation state (Llinas et al., 1991).

The role of synapsin in neurotransmitter release was also examined in the goldfish Mauthner synapse. In this study, presynaptic injection of dephospho-synapsin I caused a reduction in amplitude of evoked excitatory post-synaptic potentials (EPSPs) while spontaneous EPSPs were not affected (Hackett et al., 1990). Quantal analysis indicated synapsin influenced the number of transmitter quanta being released (n) at each evoked EPSP. This parameter could be decreased by having a decreased number of vesicles available for release, either physically or biochemically, consistent with other studies showing synapsin's importance in defining the reserve and releasable pools of synaptic vesicles. Recent microinjection studies of synapsin phosphorylated by CaMKII performed in the snail supported the model that the presence of phospho-synapsin increases neurotransmitter release (Fiumara et al., 2001). Antisera raised against the conserved E domain of rat synapsin was microinjected into lamprey reticulospinal axons (Pieribone et al., 1995). The antisera, which was labeled with a fluorophore, Cy5, accumulated into spots on the surface of axons, which corresponded

to synaptic vesicle clusters (reviewed in (Shupliakov and Brodin, 2000). In the absence of stimulation, the result of synapsin antibody injection was variable, ranging from subtle to profound disruptions in the morphology of vesicle clusters. In axons injected with anti-synapsin antibodies, stimulated at 1Hz for 12 minutes, and then maintained at rest for 1.5 hours, the distal portion of synaptic vesicle clusters was completely disrupted (Figure 5). These effects were specific for synapsin antibodies, as rabbit anti-mouse IgG had no effect. In synapses of axons injected with anti-synaptotagmin antibodies, the most striking morphological change was extensive infoldings of the plasma membrane, suggesting a primary effect on endocytosis. Electrophysiological recordings showed that in the presence of synapsin antisera, neurotransmission was maintained at low (0.2 Hz) frequency. High (18 Hz) frequency stimulation could not be sustained, in accordance with a loss of the distal portion of the synaptic vesicle cluster.

Recent studies in the squid giant synapse also support a role for the E domain of synapsin I in mediating vesicle dynamics (Hilfiker et al., 1998). In stimulated axons, presynaptic injection of a peptide contained within the E domain caused the reduction of vesicles away from the active zone, and synaptic depression, in agreement with the lamprey study. Interestingly, the presynaptic injection of the E domain peptide also slowed the kinetics of neurotransmitter release, a rare electrophysiological effect. A role of synapsin at multiple steps of the synaptic vesicle cycle, including fusion or repriming of vesicles, was further supported by a recent study in which synapsin antisera was injected into cholinergic synapses of Aplysia (Humeau et al., 2001).

Genetic studies of synapsin depletion

Studies of mice rendered genetically deficient in synapsins have further supported a role for synapsin in sustaining neurotransmission. Mice lacking synapsin I, II or I/II have been raised independently by the Greengard, Sudhof and Hirokawa laboratories. Structural alterations in nerve terminals of synapsin-deficient mice were reported (Li et al., 1995; Takei et al., 1995b). In synapsin I-deficient mice, the total

number of synaptic vesicles was reduced and vesicles away from the active zone were found to be more dispersed. Studies of synapsin II and I/II-deficient mice indicate similar ultrastructural defects (Greengard and McEwen Laboratories, manuscript in preparation). In another study, an overall decrease in the number of synaptic vesicles was observed, correlating with the number of deficient alleles (Rosahl et al., 1995). The decrease described in this study was not limited to vesicles distal to the active zone. Ultrastructural changes in mature nerve terminals of synapsin III knockout mice are not apparent (Feng et al., 2001), in contrast to mice deficient in synapsins I, II, and III, which appear to have nerve terminals severely depleted of synaptic vesicles (Greengard laboratory, unpublished observations).

As expected from such morphological changes, synapsin deficiency also resulted in functional changes. In a study of hippocampal synapses from mice lacking synapsin I, electrophysiological parameters of short-term plasticity were altered (Rosahl et al., 1993). Subsequently, it was found that mice lacking synapsins I, II, or I/II develop seizures with a frequency correlating with deletion of synapsin genes (Li et al., 1995; Rosahl et al., 1995). Investigations performed on synapsin I-deficient mice found that glutamate release from synaptosomes was markedly decreased and recovery of synaptic transmission was delayed after high-frequency stimulation of hippocampal slices from these animals (Li et al., 1995). Knockout mice in this study also displayed an increased propensity towards seizures. Independently, a study of synapsin I, II and I/II deficient mice also found several changes in electrophysiological responses of CA1 pyramidal cells in hippocampal slices (Rosahl et al., 1995).

Recent studies of synaptic vesicle cycling in synapsin knockout mice

Synaptic vesicle recycling in hippocampal cultures prepared from synapsin I-deficient mice has been studied in real time using FMI-43 (Ryan et al., 1996a). In cultures from knockout mice, the amount of FMI-43 released was reduced by 30-40%, as compared to wild type cultures, and the number of vesicles released during a train of

50 action potentials was significantly reduced. While the kinetics of dye-uptake was normal, the steady state amount of dye uptake was markedly reduced in synapsin I-deficient mice, indicating a reduction in the total synaptic vesicle pool size. The time of "repriming", meaning the time between endocytosis and availability for subsequent rounds of release also appeared to be unaltered in the absence of synapsin I. The data support the hypothesis that an equilibrium exists between the reserve and releasable pools of synaptic vesicles. The decreased pool of synaptic vesicles distal to the active zone in synapsin I-deficient mice, as evidenced by morphological studies and the physiologically correlated decrease in the reserve pool of synaptic vesicles shown by physiological studies, would lead to a diminished pool of vesicles functionally available for release. A similar range of functional analyses is underway for mice deficient in synapsin II, III and in all three synapsin genes (Chi, Ryan, and Greengard, personal communication).

All of the studies discussed above measured the role of synapsins in excitatory synapses. Subsequently, the role of synapsin I in inhibitory synapses was investigated using synapsin I-deficient mice (Terada et al., 1999). In hippocampal cultures from synapsin I-deficient mice, synaptic vesicles in inhibitory nerve terminals stimulated by hypertonic solution did not recycle properly and as a result, these synapses could not sustain subsequent rounds of transmitter release. The mechanism of this defect in recycling was not identified. Oddly, the vesicle replenishing time was judged to be accelerated in inhibitory synapses lacking synapsin I. The authors concluded from this data that synapsin plays an important role in anchoring synaptic vesicles in inhibitory synapses.

The synapsin hypothesis investigated in living synapses

As evidenced by these studies, synapsin plays an important role in regulating the dynamics of events in the presynaptic terminal. Actin has been hypothesized to serve as a scaffold to support the distinct pools of synaptic vesicles, due to its localization to

Figure 5. Activity-dependent disruption of synaptic vesicle clusters in living synapses by synapsin antibody injection

This figure shows the effects of injection of synapsin antibodies into lamprey reticulospinal axons. Axons were then stimulated at 1 Hz for 12 minutes, maintained at rest for 1.5 hours, and fixed for analysis by electron microscopy. The dramatic effect of synapsin antibodies on the distal portion of the cluster supports synapsin's importance in maintaining neurotransmitter release.

This figure was reproduced by permission of the authors from Pieribone *et al.*, Distinct pools of neurotransmitter release, 1995, Nature, Vol. 375:493-497. Only the upper two panels of the original figure are shown here.

Relevant portion of the original figure legend:
Axons were injected with A, no antibodies; B, synapsin antibodies (G304)...All electron micrographs correspond to the center section from serially sectioned synapses located within 100 μm of the injection site.

Scale bar, 0.5μm.

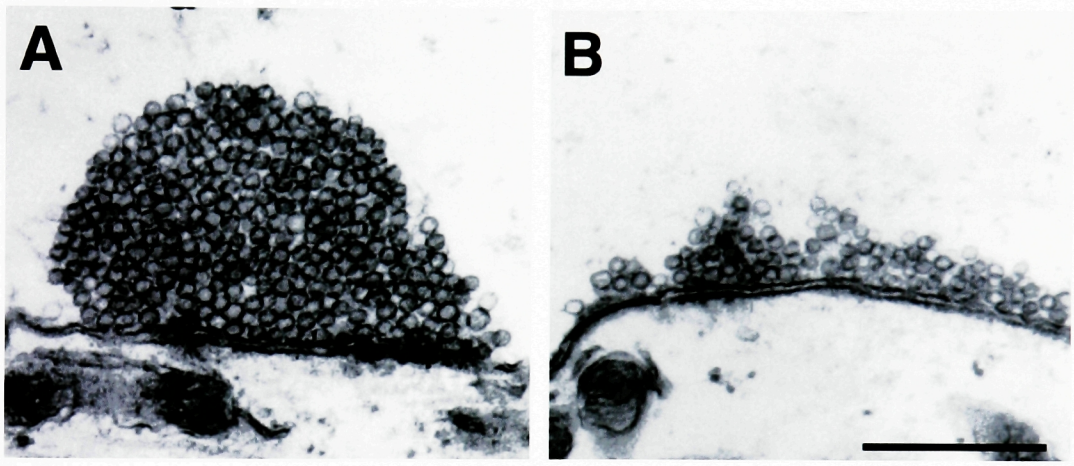
A
B

presynaptic terminals, its interaction with synapsin, and the modulation of this interaction by phosphorylation. Consistent with the data, it has been proposed in resting nerve terminals, dephospho-synapsin is associated with synaptic vesicles primarily within the distal pool of synaptic vesicles, where it links vesicles to an underlying cytoskeletal cage. Upon depolarization of the nerve terminal and the influx of Ca^{2+}, phosphorylation of synapsin by CaMKII causes a conformational change in synapsin, leading to a dramatic reduction in its affinity for actin and synaptic vesicles. The dissociation of phospho-synapsin from synaptic vesicles releases a reserve pool of synaptic vesicles from the cytoskeletal cage. Vesicles can then proceed through the subsequent stages in the synaptic vesicle cycle, sustaining neurotransmission (Figure 6, reviewed in (Greengard et al., 1993).

The studies presented in this thesis were designed to use light and electron microscopy to investigate this hypothesis in a living model of synaptic transmission. A series of experiments were performed to:

a) localize the actin cytoskeleton in the presynaptic terminal

b) observe the effects of cytoskeletal disruption on nerve terminal morphology

c) localize synapsin in relation to the actin cytoskeleton under varying conditions of neurotransmitter release.

Figure 6. The synaptic vesicle cycle and the local interaction of synapsin with actin

The currently accepted stages of the synaptic vesicle cycle and the hypothetical roles of synapsin and actin are depicted in this cartoon. The presynaptic axon is shown here as an unbranched tube, modeled on the architecture of the lamprey reticulospinal axon. Synaptic vesicles (gray spheres) are clustered at active zones both proximal and distal to the active zone (black line). Synaptic vesicles proximal to the active zone are referred to as "docked," based on their apposition to the active zone. The synaptic vesicles distal to the active zone contain dephospho-synapsin (black lollipops) on their cytoplasmic surface. Synapsin is proposed to tether clustered synaptic vesicles to an underlying actin cytoskeleton (blue lines). In an active nerve terminal, Ca^{2+} (greenish yellow) enters through channels localized to the active zone, promoting fusion of a docked synaptic vesicle and neurotransmitter release (small blue dots). An additional consequence of raised intraterminal Ca^{2+} levels is the phosphorylation of synapsin by CaMKII at specific sites (red "P"s).

Synaptic vesicles are then recycled locally via clathrin-mediated endocytosis. This process is further divided into several steps, including initiation of the clathrin (short black bars) on the periactive zone membrane, invagination of the coated pit, constriction of the coated pit, and fission of the coated pit by a dynamin-dependent mechanism (green line). A coated synaptic vesicle is rapidly uncoated and refilled with neurotransmitter. Previous investigations have hypothesized the presence of an endosomal intermediate that may also give rise to clathrin-coated vesicles.

This cartoon is adapted from many currently published reviews, in particular: TINS 1999 Vol. 22:459-464 and Annu. Rev. Biochem. 2000 Vol. 69:699-727.

Synaptic Vesicle Cycle 2000

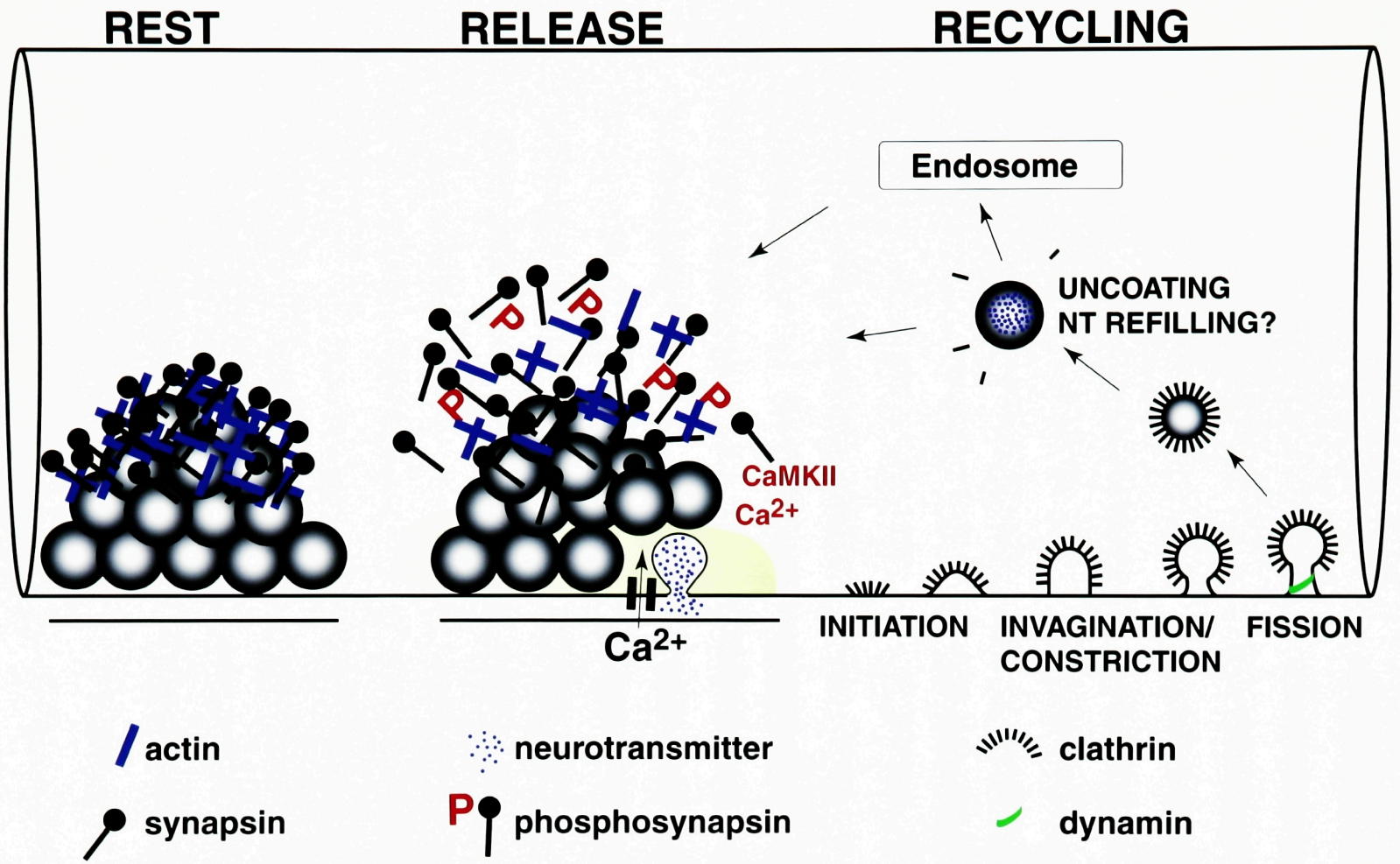

adapted from TINS 1999 Vol. 22:459-464, Annu. Rev Biochem. 2000 Vol. 69: 699-727

II. Methods

The lamprey: a model of vertebrate neurotransmission

In the 1970s, seminal morphological studies of the synaptic vesicle cycle were performed using the frog NMJ as a model of vertebrate neurotransmission (reviewed in (Ceccarelli and Hurlbut, 1980b). Since that time, insights into the mechanisms of neurotransmission have been gained from studies performed in a wide variety of species. Due to the unique features described below, the interaction between synapsin and actin has been investigated *in vivo* using the lamprey spinal cord preparation.

Lampreys belong to the most ancient class of living vertebrates and were separated from the main vertebrate line some 500 million years ago (reviewed in (Rovainen, 1979; Shupliakov and Brodin, 2000). Along with the hagfish, the multiple species of lamprey are the only living members of the jawless vertebrates (cyclostomes). For most of their life, lampreys exist as ammocoetes, a larval form, filter feeding in the mud of freshwater streams. They remain in this form for 3-15 years, after which they undergo several months of metamorphosis and become adult lampreys. Non-parasitic species then spawn and die. By contrast, adult lampreys of parasitic species living in rivers, lakes, or seas, survive by using their sucker mouths to attach onto fish, boring a hole through their prey with their rasping tongue and sucking out their tissue. This parasitic stage lasts for a period of approximately a year (although in some species this stage can last a few years), during which time they grow substantially in size. At the end of this period, lampreys lose their digestive tract, spawn, and die. Studies of neurotransmission are performed on lamprey in the post-parasitic stage.

Preliminary experiments investigating the interaction between synapsin and actin *in vivo* were performed using adult lamprey of the species *Petromyzon marinus,* supplied by the Great Lakes Fish and Wildlife Commission. However, as a lamprey central nervous system (CNS) cDNA library was prepared from *Lampetra fluviatilis* in

the Greengard laboratory (Kao et al., 1999) and used to clone synapsins, as well as a number of other presynaptic proteins (Gad et al., 2000; Ringstad et al., 1999), the present studies were performed in adult *Lampetra fluviatilis*. These animals, (20-30 cm long), were supplied by local fisherman to the Nobel Institute for Neurophysiology, Department of Neuroscience, Karolinska Institutet, Stockholm, Sweden. The lampreys were maintained in aerated fresh water tanks at 6-8 °C, according to institutional guidelines.

The lamprey spinal cord has been used as an experimental system to study various aspects of central nervous system function since the late 19th century (reviewed in Rovainen, 1979) and by the early 20th century, many researchers characterized the anatomical organization of the lamprey CNS. In the mid-20th century, Carl Rovainen at the University of Washington began to develop the lamprey CNS as an *in vitro* preparation for studying neurotransmission (Rovainen, 1967).

All lamprey species have a common CNS organization. The lamprey CNS, although reduced in cell number, shares a similar basic organization with higher vertebrates (in the spinal cord of *Petromyzon marinus*, ~10^5 (Rovainen, 1979). In a typical adult lamprey, the spinal cord is ribbon-like in shape and 1mm in width, 150-300 μm in thickness, and 10-15 cm long. Two features uncommon to higher vertebrates enhance the lamprey spinal cord as an *in vitro* preparation: it lacks both myelin and intrinsic blood vessels. The ability of the lamprey spinal cord to regenerate after complete transection has been attributed by some to its lack of myelin (see (Rovainen, 1976).

To achieve "fast" conductance without myelination, the reticulospinal axons in the lamprey CNS have a large diameter (50-80 μm). These large axons allow accessibility for intracellular physiological recordings via sharp microelectrodes. Furthermore, the lack of myelin affords excellent visibility at the light microscopic level. This enhanced visibility permits reliable multiple impalements of the same axon

in the intact spinal cord. The second attribute of the lamprey nervous system that makes it particularly amenable to studies of presynaptic function is its lack of a blood supply. Instead, the spinal cord receives all of its nutrients and oxygen through the cerebrospinal fluid. Therefore, the entire spinal cord can be removed from the animal and maintained *in vitro* for 2-3 days in cold, oxygenated Ringer's solution without a significant decline in physiological or functional parameters (reviewed in (Rovainen, 1979; Shupliakov and Brodin, 2000). The preferred living temperature of the animal is 7-13°C, which further slows the decay of the preparation *in vitro*. Taken together, these properties present an excellent opportunity to study aspects of an intact nervous system in an experimental setting.

The lamprey reticulospinal synapse

For this thesis, the relevant feature of this experimental model is the synapse made by the large, unbranched reticulospinal axons of the nine pairs of Müller and Mauthner cells. This fiber system is an integral part of the escape and turning reflex in the lamprey. Reticulospinal axons are similarly positioned in all lamprey species. They run straight down the length of the spinal cord, and form *en passant* synapses with spinal motoneurons and interneurons. As reticulospinal axons are located only 50 μm from the ventral surface of the spinal cord, they are readily visualized by light microscopy, as are the synapses that form along the entire length of the axon.

By all physiological, anatomical and neurochemical parameters, the lamprey reticulospinal synapse closely resembles fast excitatory synapses found in mammals (reviewed in (Shupliakov and Brodin, 2000). For example, these synapses are glutamatergic and have small clear synaptic vesicles. Once released, glutamate acts on mixed AMPA/NMDA receptors located on the dendrites of spinal neurons. Many reticulospinal synapses also have gap junctions that produce small but stable electrotonic potentials accompanying the chemically produced potentials in post-synaptic neurons. During experimentation, these electrical potentials provide an internal

control for consistent synaptic depolarization, as their size appears to depend exclusively on the size of the presynaptic action potential.

Under normal conditions, reticulospinal synapses have a characteristic morphology. The sizes of the active zone and vesicle cluster are correlated linearly and can vary in diameter between 1-3 μm (Shupliakov and Brodin, 2000). Synaptic vesicles (1000-3000), accumulate at individual active zones in single, densely packed, dome-shaped clusters (see Figure 5). Synapses are separated from each other by varying distances of axoplasm and thus it is usually possible to attribute recycling intermediates to a particular synapse. Because of this unique architecture, a complete synapse can be collected on serial ultrathin sections (~20-45). Due to its characteristic shape, the middle section of each reticulospinal synapse reveals the longest area of active zone and the largest number of synaptic vesicles, which is proportional to the dimensions of the complete cluster (Shupliakov and Brodin, 2000).

Clathrin-mediated endocytosis is the predominant method of recycling at the reticulospinal synapse, and takes place in the area of the plasma membrane surrounding the vesicle cluster (Shupliakov et al., 1997). Therefore, sections at the edges of the synapse typically show the greatest proportion of endocytic intermediates. As these synapses are phasic and only fire when needed, it is possible for a presynaptic terminal to undergo a complete depletion of vesicles after extended periods of tonic stimulation at high frequency, such as 30 minutes of 20 Hz stimulation (this thesis and (Wickelgren et al., 1985). Previous studies have demonstrated that it is possible to inject active compounds into reticulospinal axons and examine the effects of such compounds on the presynaptic machinery (Pieribone et al., 1995). Although the precise intraaxonal concentrations are difficult to determine, the effects of a substance can be analyzed in a dose-dependent fashion, since microinjected compounds spread by diffusion from the injection site down the unbranched cylindrical length of the reticulospinal axon (Figure 7).

Figure 7. Fluorescently labeled compounds spread along the unbranched reticulospinal axon

The lamprey spinal cord contains unbranched reticulospinal axons that are 50-80μm in diameter. Since these axons are localized close to the surface of the spinal cord, they can be visualized by light microscopy. This figure shows a time course of microinjection of rhodamine-phalloidin. Each panel was captured at successive one-minute intervals. The top panel shows the pipette prior to injection (white). The spots of fluorescence indicate accumulation of rhodamine-phalloidin in presynaptic terminals. The image was converted into pseudo-color.

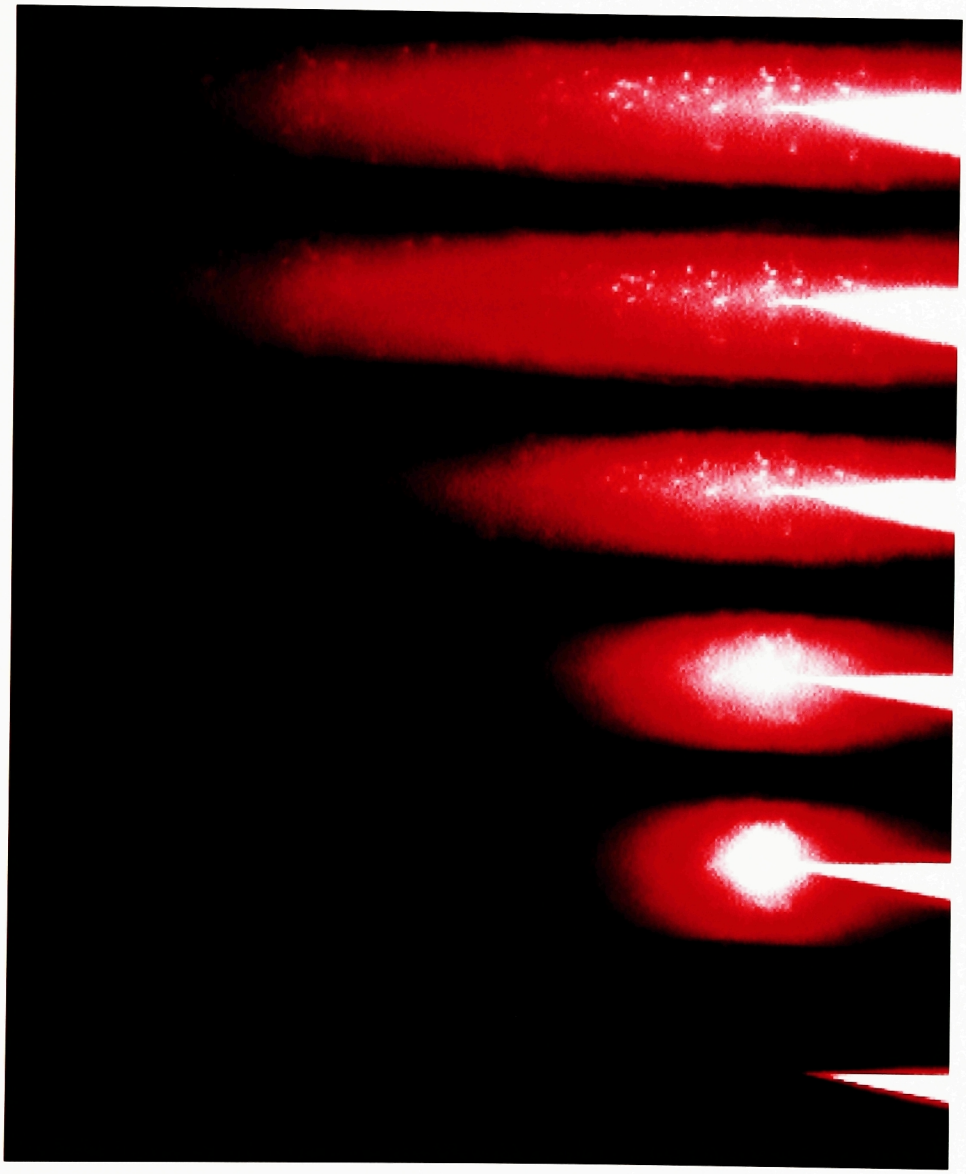

Experimental Procedures

Spinal cord preparation

All procedures were performed essentially as described in (Pieribone et al., 1995; Shupliakov et al., 1997). A fresh physiological Ringer's solution was prepared on the day of each experiment, containing (in mM): NaCl 109, KCl 2.1, $CaCl_2$ 2.6, $MgCl_2$ 1.8, glucose 4, glutamine 0.5 and HEPES 2 (pH 7.4, bubbled with 100% O_2). For experiments in which ultrastructural analysis was performed, fresh fixative was prepared a few hours prior to the experiment (see below). The animal was removed from the tank and anaesthetized by immersion in 0.1% tricaine methanesulfphonate (MS-222) for a few minutes. The animal was then decapitated in the caudal part of the gill region and the spinal cord dissected out, as described previously (Shupliakov et al., 1997).

Briefly, the spinal cord was dissected out in a chamber lined with Sylgard containing Ringer's solution. A piece of the spinal cord was cut, approximately 7 cm long, and mounted with the ventral side up in a Sylgard-lined experimental chamber with Ringer's solution maintained at 7-9°C. At the beginning of all experiments, an artificial "landmark" was created by inserting a small metal insect pin in the lateral cell column of the spinal cord, outside the area of reticulospinal axons, in a position parallel to the site of injection. The pin remained in place throughout the fixation of the tissue for ultrastructural analysis. When the pin was subsequently removed, a round hole of regular shape and fixed diameter remained. For microinjection, all reagents were dissolved in injection buffer, and injected with pressure pulses (5-15 psi, 200 ms duration) through thin-walled glass microelectrodes (resistance of 50 -70 MΩ) into giant reticulospinal axons with resting membrane potentials of at least -60 mV. The fluorescence of injected axons was monitored with a charge-coupled device (CCD) detector cooled to –50°C (Princeton Instruments). Stimulation was applied through an

extracellular suction electrode placed at the caudal end of the spinal cord (Shupliakov and Brodin, 2000); Figure 8). The efficiency of the stimulation was verified in each axon immediately after the injection, and then the injection microelectrode was removed. The extracellular spike volley was monitored throughout the stimulation period with a second extracellular electrode placed at the rostral end of the spinal cord. In specimens maintained at rest or designated as "low Ca^{2+}" the Ca^{2+} level was reduced in Ringer's solution to 0.1 mM and the Mg^{2+} level increased to 4 mM (Shupliakov et al., 1997). In specimens designated as "High K^{+}" the K^{+} level was increased to 30 mM and the Na^{+} level reduced to 81.1 mM, after (Wickelgren et al., 1985). For ultrastructural specimen preparation, see the section titled "Electron Microscopy."

Reagents

For these studies, all reagents were solubilized or diluted in a standard injection buffer (250 mM potassium acetate, 10 mM HEPES, pH 7.4). All reagents, (except for NEM-S1, which was prepared freshly), were aliquotted, flash frozen in liquid N_2 and stored at -80°C. On the day of the microinjection experiment, the appropriate reagent was thawed on ice and spun through an eppendorf 0.2 μm filter (Millipore) at 10,000 rpm at 4 °C for 5 minutes to remove any particulate matter that might clog sharp electrodes.

Actin-Directed Compounds

Rhodamine- and Oregon green-labeled phalloidin were obtained from Molecular Probes, Inc (Eugene, OR). The sulfhydryl reagent N-ethylmaleimide (NEM) was used to modify myosin subfragment 1 (S1). It has been demonstrated that incubation of S1 with the alkylating agent NEM modifies two cysteine sulfhydryls that are located in the ATPase sites of myosin, thus abrogating its ATPase activity (Meeusen and Cande, 1979). Since the actin binding site is distinct from the ATPase site, treatment with NEM results in S1 heads that can bind to actin but cannot complete the ATP-dependent cycle

Figure 8. A schematic diagram of the experimental system

The spinal cord from adult lampreys was dissected out and placed in an experimental recording chamber with the ventral side up. Reticulospinal axons form *en passant* glutamatergic synapses with dendrites of spinal moto-and interneurons. Synapses typically contain 1000-3000 synaptic vesicles (50 nm) accumulated in dense dome-shaped clusters at active zones that are distinctly separated by axoplasm. Action potential stimulation was applied via an extracellular electrode and their conductance in reticulospinal axons were recorded either with an extracellular suction electrode or with sharp intracellular electrodes. Fluorescently labeled compounds such as antibodies were microinjected into reticulospinal axons with a glass electrode and the increase in fluorescence was monitored with a CCD unit connected to a computer. The pink spots in the axon represent labeled synapses on the surface of the axon, as shown in Figure 7. The preparations were fixed and embedded for analysis by electron microscopy. The ultrastructure of uninjected or injected axons at various distances from the injection site was examined in serial ultrathin sections.

This figure was slightly modified and reprinted by permission of the author from Gad,H *Synaptic vesicle endocytosis studied in a living synapse,* Doctoral Dissertation, 2000, The Karolinska Institute, Stockholm, Sweden.

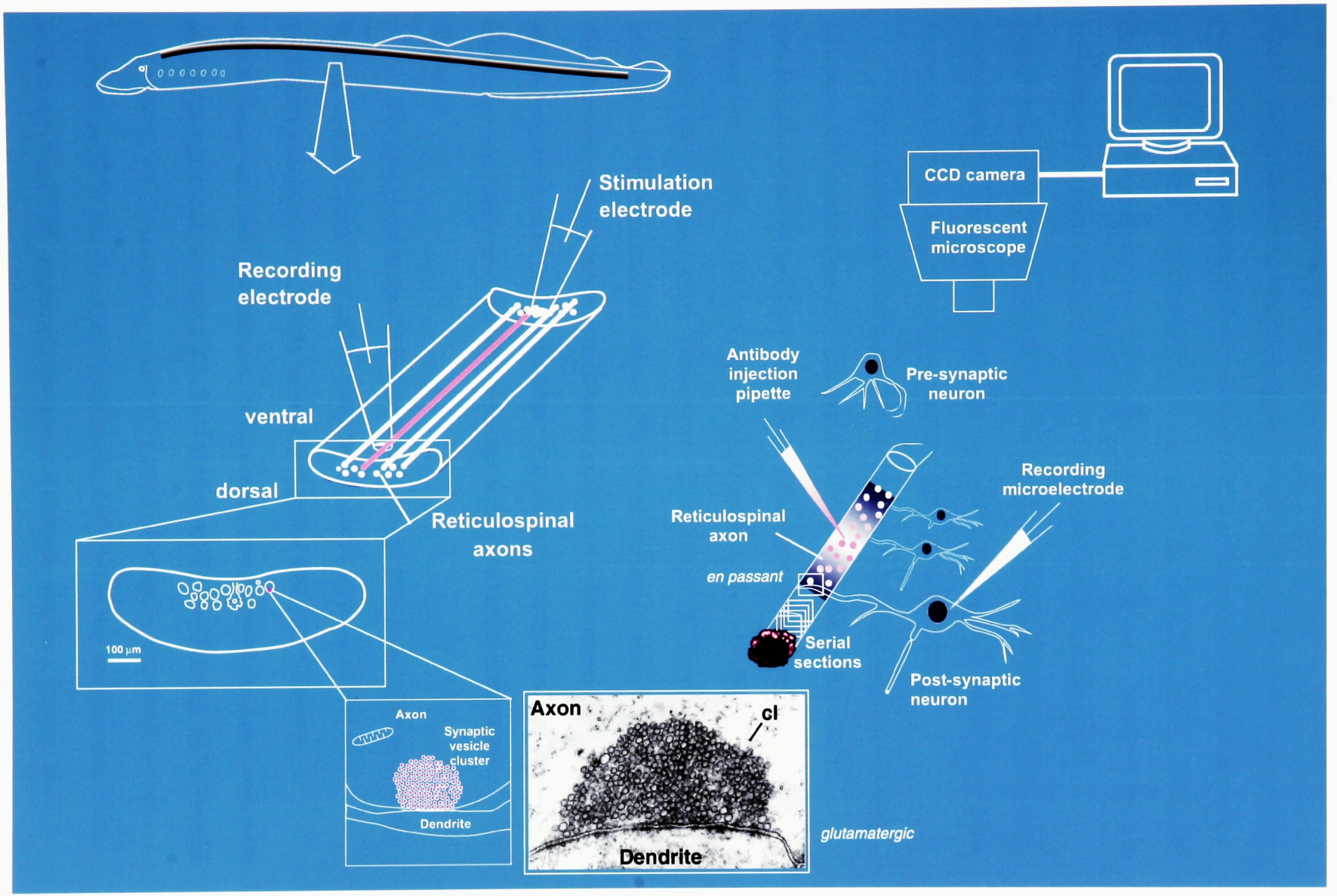
Stimulation electrode
Recording electrode
ventral
dorsal
Reticulospinal axons
100 µm
Axon
Synaptic vesicle cluster
Dendrite
CCD camera
Fluorescent microscope
Antibody injection pipette
Pre-synaptic neuron
Recording microelectrode
Reticulospinal axon
en passant
Serial sections
Post-synaptic neuron
Axon
cl
Dendrite
glutamatergic

necessary for release from filaments and thus remain bound to actin (Meeusen and Cande, 1979). Rabbit S1 fragments purchased from Sigma Chemicals were used to prepare NEM-S1 fragments as described (Lin et al., 1996). Using standard *in vitro* assays, the NEM-S1 fragments were shown to have efficient actin binding activity and deficient ATPase activity (data not shown). For optical monitoring during injection, the NEM-treated S1 fragments were mixed 10:1 with recombinant glutathione-S-transferase (GST), labeled with the Cy5 fluorophore (Amersham Life Sciences, Inc.), according to manufacturer's instructions. Previously, microinjection of GST has been shown to have no effect on synaptic function (Ringstad et al., 1999).

The *Clostridium botulinum* C2 toxin destroys F-actin and sequesters G-actin (Aktories, 1997) (and Figure 9). This toxin is distinct from the widely used *C. botulinum* neurotoxins and derives its effects from a specific ability to ADP-ribosylate monomeric G-actin. ADP-ribosylation traps G-actin, destroys its ability to polymerize, and promotes its accumulation. Thus altered, ADP-ribosylated G-actin joins the fast growing end of actin filaments and prevents further monomer addition. By capping filaments and trapping monomers, C2 toxin results in the destruction of actin filaments and the sequestration of monomeric actin. The active C2 subunit of *Clostridium botulinum* was kindly provided by Dr. Holger Barth, University of Freiburg, Germany.

The specificity of the C2 toxin was tested by *in vitro* assays (data not shown). Briefly, lamprey spinal cord and rat brain homogenates, prepared as described previously (Ringstad et al., 1999), were centrifuged at 500 g for 5 minutes, supernatants were collected and used as substrates. Samples were incubated with 0.1% sodium deoxycholate, 0.2 mM GTP, 5 μM NAD containing 105 dpm [^{32}P] NAD in 35 mM HEPES, pH 7.4 containing 1 mM DTT and 1 mM $MgCl_2$. The samples were incubated at 37 °C for 30 minutes, separated by SDS-PAGE and transferred to PVDF membrane. The PVDF membrane was exposed to X-ray film for 1-3 days. The C2

Figure 9. Mechanism of action of actin-directed compounds

***Clostridium botulinum* toxin (C2 toxin)**

Intracellular actin normally cycles between the globular monomeric form, G-actin, (black darts) and the polymerized filamentous form, F-actin. In the presence of NAD and the active component of *C.botulinum* C2 toxin, G-actin is ADP-ribosylated (red darts). ADP-ribosylated G-actin binds to and caps the fast growing barbed ends of actin filaments, so that no further monomers can be added. This modification disrupts the normal cycling of actin, and a net depolymerization of actin occurs. As G-monomers accumulate in the cytoplasm, they are ADP-ribosylated, so that no further filaments can form ("Monomer Trapping").

***Amanita phalloides* mushroom toxin, phalloidin**

The *Amanita phalloides* mushroom toxin, phalloidin, (red circle) works in an opposing manner. Phalloidin is a small cyclic hexapeptide (mw<800 Da). Phalloidin binds to both short and long actin filaments, with a stoichiometry of one molecule per actin monomer. Phalloidin stabilizes F-actin, shifting the equilibrium between G- and F-actin towards F-actin, and lowering the critical concentration for polymerization. F-actin stabilized by phalloidin still retains many normal interactions, as measured by several experimental parameters.

Adapted from Akatories, (Ed.) Bacterial Toxins. Chapman, & Hall, Weinheim, 1997, page 98 and Molecular Probes Product Information for Phallotoxins, #MP00354.

C2 Toxin (*C. botulinum*)

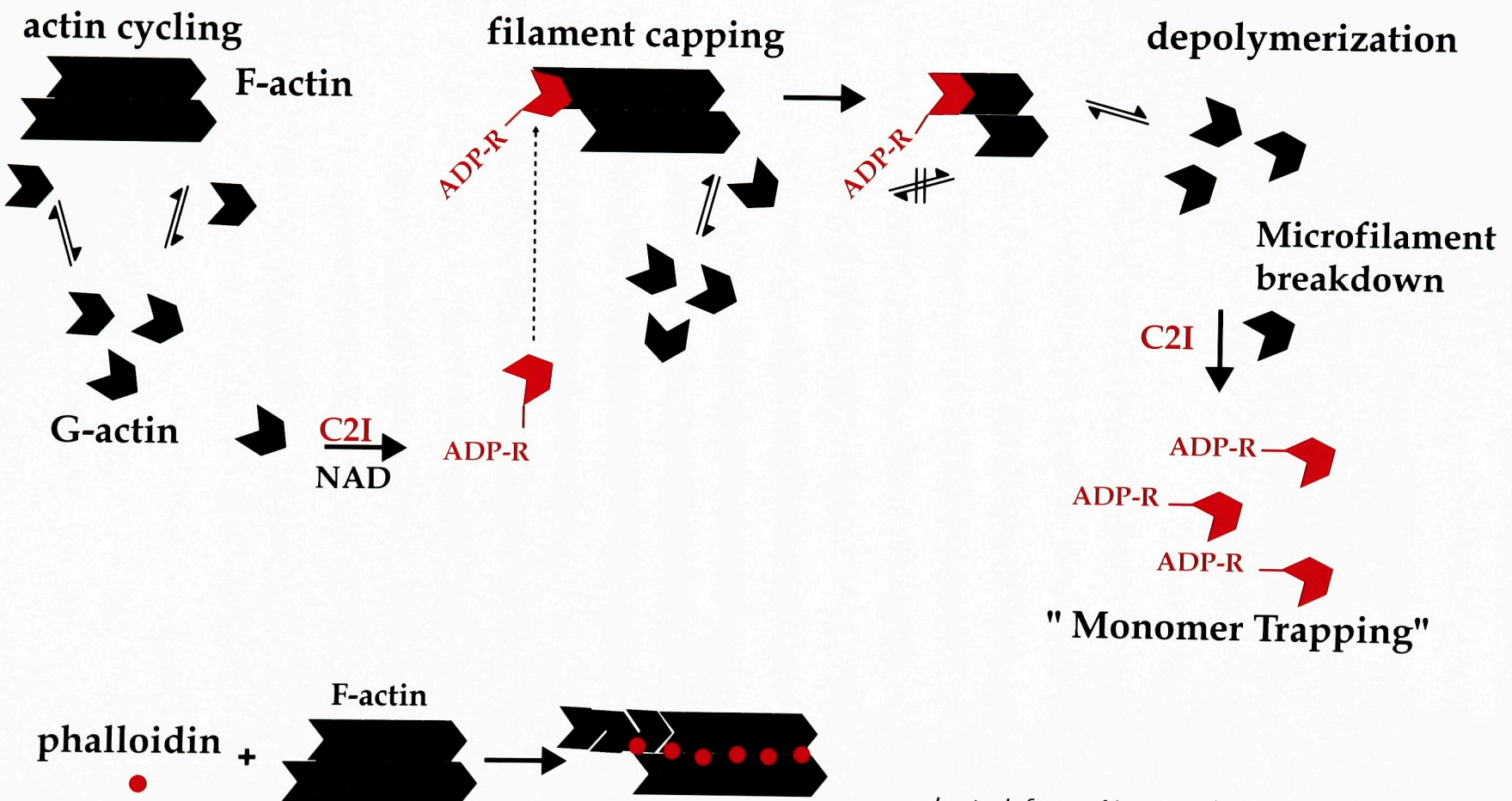

adapted from Aktories (Ed.) Bacterial Toxins. 1997

toxin labeled a band of 43 kDa in both rat brain and lamprey spinal cord, the expected molecular weight for actin (data not shown). For injections, the C2 toxin was mixed with Cy5-labeled GST (Ringstad et al., 1999).

Antibodies

Synapsin

Lamprey synapsins were cloned in the Greengard laboratory as described elsewhere (Kao et al., 1999) and are derived from two genes that give rise to four isoforms via alternative splicing. The primary amino acid sequences and domain structure of lamprey, rat, cow and frog synapsin I are shown in Figure 37. The amino acid alignment was performed using the Clustal alignment method and the known phosphorylation sites were then aligned manually. The highly conserved domains A, C and E were readily identified based on amino acid sequence and were 90, 71 and 69% identical to their human orthologs, respectively (Kao et al., 1999). A "D-like" domain was designated as such on the basis of its high proline content. As shown in Figure 37, most of the phosphorylation sites known to be important in regulating synapsin function in other species are easily identified at appropriate positions in the lamprey sequence. For example, phosphorylation sites corresponding to the following sites are indicated in Figure 37: site 1 for PKA, sites 4, 5 and 6 for MAP kinase, site 3 for CaMKII, as well as candidate sites for the proline-directed kinases. Although there is not an identical sequence corresponding to site 2 for CaMKII, the serine is conserved. Lamprey synapsins also contain the residues required for ATP binding at Lys^{225}, Lys^{269} and Gly^{276} (rat synapsin 1a), which are conserved in all known synapsin isoforms, (except those of *C. elegans* and *Drosophila).*

Anti-synapsin domain E antiserum (G304; (Pieribone et al., 1995) was coupled to an Alexa fluorophore (Molecular Probes) according to the manufacturer's recommendations. To further explore the sub-synaptic localization of synapsin throughout the synaptic vesicle cycle, reagents directed against domain D were developed.

This proline-rich domain has been predicted on the basis of amino acid content to be a highly accessible portion of the molecule (Sudhof et al., 1989) and likely to interact with a number of SH3 domain-containing proteins (McPherson et al., 1994). Domain D of lamprey synapsin I was subcloned into the pGEX vector to produce a GST fusion protein and was purified by standard methods. Antibodies to domain D were generated by immunization of rabbits with the lamprey domain D-GST fusion protein (Cocalico Biologicals, Reamstown, PA). The antigen was coupled to an NHS-activated column and used to affinity purify the antibodies. On a Western blot, the specificity of the affinity-purified antibodies was tested on detergent extracts of lamprey CNS and rat brain, prepared as described previously (Pieribone et al., 1995). The rabbit polyclonal antiserum raised against lamprey domain D detected two bands of the expected molecular weights for lamprey synapsin Ia and Ib in lamprey CNS homogenates specifically (Figure 10). This antibody also exhibited a robust labeling pattern typical for synapses on cryostat sections of the lamprey spinal cord at the light microscope level (data not shown).

SV2

In an effort to compare the cluster localization of synapsin with an integral transmembrane protein of synaptic vesicles, antibodies to the highly conserved synaptic vesicle protein SV2 were used (Bindra et al., 1993). The mouse monoclonal antibody to SV2 was originally described (Buckley and Kelly, 1985) and was obtained from the Developmental Studies Hybridoma Bank maintained at the University of Iowa, Iowa City, Ia. The antibody was obtained as 100 ml of mouse ascites fluid and concentrated to a final volume of 2 ml by centrifugation through a Centricon 10 (Millipore) at 3000 rpm at 4 °C for several hours. On a Western blot of rat brain and lamprey spinal cord homogenates, this antibody recognized a diffuse band running between ~100 and 70 kDa, typical of this protein (Pyle et al., 2000)(data not shown).

Dynamin

Dynamin has been reported to play an essential role in clathrin-mediated endocytosis at the lamprey reticulospinal synapse (Shupliakov et al., 1997). In order to compare its localization with that of synapsin, we used rabbit antiserum raised against the amino terminal domain of rat dynamin I (DG-1) (Shupliakov et al., 1997). The antiserum was kindly provided by Drs. Vladimir Slepnev and Pietro De Camilli, Yale University School of Medicine, New Haven, CT. On a Western blot of lamprey spinal cord extracts, the anti-dynamin antiserum (directed against amino acids 1-750 of rat dynamin I) selectively recognized a band of a similar molecular weight to rat dynamin (data not shown). To confirm the identity of the protein band labeled by the antiserum, the protein was purified on a column containing amphiphysin SH3 domain GST-fusion protein (Shupliakov *et al.* 1997), run and excised from an acrylamide gel and subjected to trypsin cleavage. Peptides were microsequenced at the Core Facility, PAC, Karolinska Institutet, Stockholm, Sweden (data not shown). As described in Results, these antibodies were used to localize dynamin in post-embedding immunoelectron microscopy studies.

Light microscopy

During microinjection experiments, a cooled CCD unit (Princeton Instruments) was used to obtain light microscopic images of axons injected with various compounds. To obtain higher resolution images of reticulospinal axons injected with fluorescent compounds, the living spinal cord was removed from the recording chamber and mounted with the ventral side down on a coverslip. Stimulation was maintained after the specimens had been removed from the recording chamber by changing to a Ringer's solution containing 30 mM K^+ with a corresponding reduction in the concentration of Na^+. The specimens were analyzed with an inverted fluorescence microscope (Nikon Axophot) or a confocal microscope system (Noran Odyssey).

Electron Microscopy

Principles of tissue preparation

In 1932, the electron microscope was invented by physicists, and has subsequently had a profound impact on the biological sciences (reviewed in (Bozzola and Russell, 1992). The transmission electron microscope (TEM) sends a beam of electrons from a high voltage source (60-80 kV filament) through condensor and objective lenses and an ultrathin tissue section (usually less than 100 nm) to produce a two-dimensional image on a phosphorescent screen. A camera is attached to the microscope, so that images displayed on the screen can be captured. The specimen preparation consists of several major stages: primary fixation, washing, secondary fixation, dehydration, infiltration with transitional solvents, infiltration with resin, embedding, and curing. The guiding purpose of these stages is to extract water from the tissue and replace it with progressively nonpolar substances, while preserving the ultrastructural morphology of the cell to the greatest degree possible. When attempting to combine ultrastructural and immunocytochemical techniques, a compromise must be reached between the inherently antagonistic aims of preserving good ultrastructure through the use of harsh fixatives and preserving good antigenicity by minimal denaturation of the tissue. For the best results, every stage must be optimized for a particular biological preparation and experimental interest. The following description is a summary of several technical manuals including: Glauert and Lewis, 1998; Hajibagheri, 1999; Polak and Varnell, 1984.

Primary fixation is the first and perhaps most sensitive step in specimen preparation, since any disruption of the tissue made during this step will be magnified during the progressively harsher subsequent steps. Primary fixation must be optimized to preserve the particular subcellular structure of interest, as various chemicals will differentially affect the preservation and appearance of subcellular elements such as lipids, intracellular or surface proteins, membranes, biogenic amines,

Figure 10. Western blot for synapsin

Protein extracts from lamprey spinal cord and rat brain were analyzed by SDS-PAGE and a Western blot was carried out using synapsin antibodies directed against the highly conserved domain E of rat (G304) or lamprey domain D. G304 recognized proteins of the expected molecular weights in both rat brain and lamprey spinal cord homogenates. Anti-lamprey domain D antiserum was specific for lamprey synapsin I isoforms. The blot is overexposed here to demonstrate the specificity. This antibody exhibited an excellent immunoreactivity by both light and electron microscopy and was therefore used for all post-embedding immunogold localization studies.

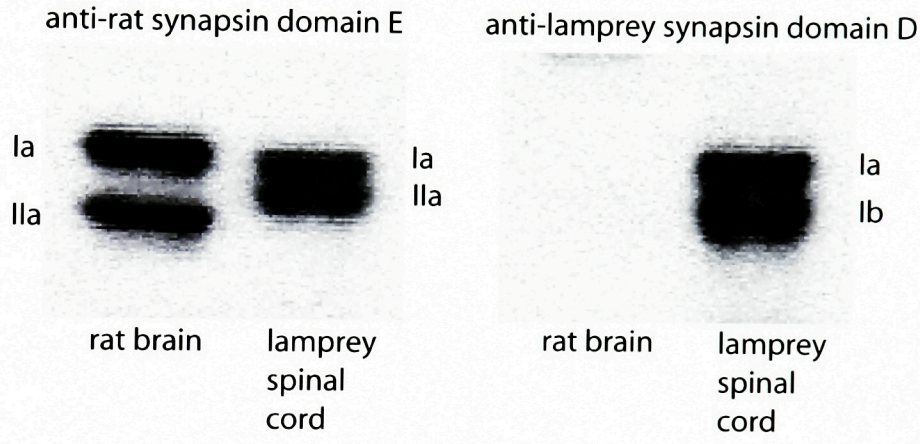
anti-rat synapsin domain E
anti-lamprey synapsin domain D
Ia
IIa
Ia
IIa
Ia
Ib
rat brain
lamprey spinal cord
rat brain
lamprey spinal cord

or cytoskeletal elements. The primary fixative consists of a buffer containing a mixture of 2-4% glutaraldehyde combined with a lower concentration of formaldehyde, prepared freshly. Both act primarily to cross-link proteins to each other via aldehyde linkages, particularly via lysine residues, denaturing many proteins in the process. In addition to reacting with proteins, the fixative reacts to some degree with other cellular constituents such as lipids, carbohydrates, and nucleic acids. The optimal proportion of these two chemicals is highly tissue-specific and purpose-dependent.

As reflected in the protocols used in this thesis, a higher percentage of glutaraldehyde is better for purely ultrastructural studies, while a higher percentage of formaldehyde, which is less denaturing of antigens and enzymatic proteins and penetrates tissues more rapidly, is better for immunocytochemical studies. The prevailing theory of the success of this fixation is that structures are first transiently stabilized by formaldehyde and then irreversibly cross-linked by glutaraldehyde. The three-dimensional architecture of a preparation can greatly alter the proper diffusion of a primary fixative. Empirically, most specimens should be less than 300 μm thick for adequate fixation, which makes the dimensions of the lamprey spinal cord particularly advantageous. Fixatives are commonly mixed with buffers such as phosphate and cacodylate, to maintain a biological pH. Again, buffers must be adjusted for the particular tissue being prepared, as optimum osmolarity and ion concentration can vary and have obvious effects on intracellular structure.

As mentioned earlier, certain intracellular features can be accentuated by addition of specific reagents in the primary fixative or destroyed during the tissue processing. Relevant for this thesis, for example, it has been shown that actin filaments are exceptionally labile and usually destroyed by conventional osmium post-fixation (Maupin-Szamier and Pollard, 1978). The use of tannic acid during primary fixation increases the fixation and contrast of actin filaments, membranes and other constituents of the cytoplasm. Although its precise mechanism of action is unknown, it is thought

that tannic acid coats actin filaments, protecting them from destruction, and also increases the absorption of heavy metals such as lead and uranyl acetate used during tissue processing and counterstaining (LaFountain et al., 1977; Maupin and Pollard, 1983).

Secondary fixation with a buffered solution of the heavy metal osmium (osmium tetroxide, 1-2%) usually follows for ultrastructural studies. It acts as a fixative, reacting with lipids that are not fixed by aldehydes, as well as carbohydrates and proteins. Osmium also enhances contrast of the specimen, by denaturing proteins and thereby promoting exposure of binding sites for heavy metals used for contrast. Osmium tetroxide also reduces to metallic osmium when reacting with organic molecules, increasing in density and therefore appearing denser on the image. As mentioned above, exposure to osmium also causes the extraction of some proteins, so that some cellular constituents must be stabilized against secondary fixation. Osmium post-fixation is omitted for immunocytochemical studies, as its denaturation activity destroys antigenicity.

Further tertiary fixation and staining *en bloc* with uranyl acetate is often performed, as in this thesis. Uranyl acetate stains, as well as fixes, membranes and cellular organelles and is therefore used to enhance the overall contrast of the specimen. Of added relevance for its use in this thesis, uranyl acetate has been indicated to increase contrast of actin filaments (Maupin and Pollard, 1983).

Most embedding resins are nonpolar and therefore not miscible with water. Therefore, dehydration is performed to allow the infiltration of the tissue specimen with resin. As discussed below, for immunocytochemical studies, the use of more hydrophilic resins is of key importance, as it allows for gentler or even incomplete tissue dehydration, leading to greater preservation of antigenicity. As in this thesis, most dehydration steps proceed through a graded ethanol series of increasing strength.

To minimize the shrinkage of tissue that is associated with dehydration, the procedure is performed as quickly as possible and at low temperatures (4 °C).

Infiltration follows dehydration and is defined as the step in which transitional fluids are replaced by plastic monomers. For conventional ultrastructure, nonpolar resins must be dissolved first in nonpolar solvents. As in this thesis, propylene oxide is most commonly used as a transitional solvent, although acetone, which is non-toxic, can often be used in its place. To begin infiltration, the tissue is incubated in propylene oxide, then in a mixture of propylene oxide and the resin, and then finally in the resin alone. For immunocytochemical studies, the propylene oxide step is omitted, as the resins are more hydrophilic and therefore can be dissolved often in ethanol.

Embedding is the process of polymerization of the liquid resin into a solid matrix that completely penetrates the specimen. The plastic monomers are cured under specific conditions of light and temperature. Resins vary by several parameters such as viscosity and hydrophobicity, which dictate such parameters as miscibility with water, rate and uniformity of tissue infiltration, rate of polymerization and uniformity of hardening, quality and ease of sectioning, and stability under the electron beam. Generally speaking, conventional ultrastructural analysis is performed in epoxy resins while immunocytochemical analysis is performed in low viscosity acrylic resins. Generally, epoxy resins suffer from low antigen preservation due to fixation, the heat used for polymerization, or inaccessibility due to high-density cross-linking. In this thesis, Durcapan was used for conventional ultrastructure. For immunocytochemical studies, the acrylic resins Lowicryl, and LR White were tried before making the final choice of the ultra-low viscosity, hydrophilic acrylic resin LR Gold. This choice was made on the basis of empirical observations that LR Gold gave the greatest preservation of ultrastructure coupled to the highest degree of antigenicity (specific signals for all antibodies used were higher in tissue embedded in LR Gold). While heat (45-60°C) in

conventional curing ovens is used to cure epoxy resins, ultraviolet light and low temperature (-50°C) are used for curing low viscosity resins like LR Gold.

Semi-thin sections of 0.5 μm thickness were cut by glass knives in an LKB ultramicrotome from a region of the specimen outside the area of interest. These sections were stained with 1% toluidine blue solution and examined with a light microscope. From this examination, the quality of the tissue preservation was judged. For microinjection experiments, if the tissue preservation was sufficient, the location of injected axons was identified. This identification was accomplished using the information gathered during the microinjection such as position of injected axons relative to the central canal and the pinhole, relative sizes of the injected axons, and depth from the spinal cord surface. After such identification, the blockface was trimmed to a final pyramid shape and serial sections were cut using a diamond knife (Delaware or Diatome Diamond Knives). For standard EM, sections were cut 70-80 nm thick (silver interference color) and collected on copper slot grids. For immunocytochemistry, sections were cut 80-100 nm thick (pale gold interference color) and collected on nickel slot grids. Positive staining, meaning increasing the density of a particular structure relative to the background, was performed with the general stains, uranyl acetate and lead citrate (Hayat, 1975). Sections were examined and photographed using a Philips CM12 or JEOL electron microscope at an accelerating voltage of 80 kV.

To detect the specific localization of intracellular antigens in specimens with a highly preserved ultrastructure, it is necessary to use a postembedding immunogold technique, which detects an antigen labeled by a complex of primary and secondary antibodies on the surface of an ultrathin section. In order to increase antigenic sites exposed to the primary antibody, the first step of the protocol is often to etch away areas of the section, by exposure to chemicals such as hydrogen peroxide, or as in this thesis, sodium borohydride. Several general blocking steps then follow. The primary

antibody is subsequently applied for a period of time, generally 3-12 hours, at RT or 4°C. Following this step, grids are washed, blocked with diluted serum, and incubated for a few hours in a secondary antibody conjugated to colloidal gold particles. Grids are then washed, dried, and stored. For greater visualization of colloidal gold particles, a step known as silver enhancement is often performed. Essentially, this step chemically precipitates silver on the surface of gold particles, slightly enlarging them. This also makes the particles appear darker after heavy metal staining.

Experimental Protocols

Production of formvar coated grids

This procedure was performed in fume hood as follows: Copper or nickel slot grids were stored at RT in small glass vials in 1,2-dichloroethane (Fluka #03530). Clean uncoated glass slides were dipped briefly into a graduated cylinder containing formvar (polyvinyl formate) solution in 1,2-dichloroethane. Formvar film was dried and expelled slowly onto the surface of a glass trough filled with ddH_2O by surface tension. A film was judged to be of correct thickness if it appeared silver on the surface of the water by interference color under a lamp. (A thick film will degrade the image and an overly thin film will break under the force of the electron beam.) Grids were placed on formvar film with rough side down. Parafilm was used to pick up film with grids and placed to dry in a covered glass petri dish for 4-12 hours. Using a dissecting microscope, each grid was examined individually. Grids without holes or dust particles were deemed acceptable and stored in a gridbox for future use.

Heavy Metal Counterstaining (Positive Staining)

All heavy metal counterstaining was performed on fresh parafilm placed in a moist, covered glass petri dish. Throughout these procedures, grids were handled using fine-pointed jewelers' forceps, and each grid was gently placed on a fresh solution droplet with the section side down.

Uranyl Acetate

A stock solution of 2% uranyl acetate (UAc) in ddH_2O was stored at 4°C. Filtered UAc solution was dispensed in 60µl droplets onto parafilm, one per grid. Grids were incubated on drops for three-ten minutes. The incubation time was optimized for each batch of solution and was less for non-osmicated preparations. Grids were washed with cold ddH_2O, dried against filter paper and stored in a gridbox.

Lead Citrate

Several pellets of NaOH were placed the petri dish to avoid contamination of lead citrate with lead carbonate, which can form when lead citrate contacts air. (NaOH pellets absorb CO_2). A saturated lead citrate solution was dispensed in 60µl droplets onto parafilm, one per grid. Grids were incubated for on solution drops for three to six minutes. This time was optimized for each batch of solution and was shorter for non-osmicated preparations. Grids were washed with cold ddH_2O, dried against filter paper and stored in a gridbox.

Specimen processing for ultrastructural analysis (non-immuno-cytochemistry)

As mentioned earlier, during injection experiments, several features of the preparation were recorded in order to facilitate subsequent analysis at the ultrastructural level. These features include: the positions of reticulospinal axons relative to the central canal and the pin in the lateral cell column, the relative size of the axons, the relative amount of reagent injected as indicated by the fluorescence intensity, and the resting potentials of the axons. These features help to identify injected and uninjected axons first in semi-thin sections stained with toluidine blue examined by light microscopy and then on ultrathin sections examined by electron microscopy.

Fixative (3% glutaraldehyde, 0.5% paraformaldehyde, 4% tannic acid in 0.1 M cacodylic acid, pH7.4) was added into the recording chamber at the end of the stimulation protocol, while stimulation was still ongoing. The preparation was fixed in

the chamber for 15 minutes. The spinal cord pinned to Sylgard was then transferred to a vial with fresh fixative. Using a carbon steel razor blade attached to a vibratome, the preparation was cut around the injection site to allow for penetration of the fixative. The preparation was fixed on ice for 45 minutes in tannic acid fixative, and then incubated in the same fixative without tannic acid, for 3-12 hours at 4 °C. Spinal cords were removed from Sylgard and cut into pieces three-four mm long, at least seven mm from the cut end of the preparation (to avoid damage artifacts, (Wickelgren et al., 1985). One piece included the area of the injection site and one included the area far from injection site to serve as a control.

After fixation, the following sequential steps were performed. Preparations were washed for two hours in cold 0.1 M cacodylic acid buffer pH7.4 at 4°C, post-fixed in 1% osmium tetroxide in ddH_2O for one hour at 4°C, and stained *en bloc* with 2% UAc for four hours at 4 °C. Preparations were then dehydrated in a graded ethanol series: (at 4°C) 30% ethanol for five minutes, 50% ethanol for 20 minutes, 70% ethanol for 20 minutes-12 hours; (at RT) 85% ethanol for 20 minutes, 95% ethanol for 20 minutes, 99% ethanol twice for 20 minutes each. At RT on a rotator, preparations were incubated in propylene oxide for one hour, and then infiltrated with a mixture of propylene oxide and Durcapan ACM Resin (1:1) overnight. Lids were then removed from vials to evaporate propylene oxide for an additional four hours. Preparations were incubated in fresh Durcapan resin overnight. Preparations were placed in fresh Durcapan resin in labeled silicon rubber flat molds, ventral side up, and left at RT for one hour so that all air bubbles could escape. Molds were cured at 45°C for three days or until block was sufficiently hard. Preparations were cooled to RT overnight before sectioning.

Specimen processing for immunocytochemical studies

5 Hz 20 minute stimulation ± rhodamine-phalloidin

Tissue was fixed in the chamber after 5 Hz stimulation for 20 minutes with 4% paraformaldehyde/0.5% glutaraldehyde/4% tannic acid in 0.1 M cacodylate buffer (pH 7.4) for 20 minutes. The tissue was cut around the injection site as above, and at 4 °C, incubated in fixative with tannic acid for 45 minutes and without tannic acid for three hours. The preparation was washed in 0.1 M cacodylate buffer overnight, washed for 2 hours in 0.3 M sodium acetate buffer, incubated in filtered 1% UAc in sodium acetate buffer for one hour, and rinsed in sodium acetate buffer for 10 minutes. The preparation was then dehydrated in a graded ethanol series (at 4 °C): 50% ethanol for 20 minutes, 70% ethanol for 20 minutes, and 99.5% ethanol 3 times for 20 minutes each. At RT, the preparation was incubated overnight in LR Gold resin (London Resin Company, U.K.). The specimen was incubated overnight in fresh resin. The resin was changed to include +0.1%(w/v) of the light-sensitive catalyst, BENZIL, and the specimen was incubated again overnight. This last step was repeated once. Preparations were embedded in fresh resin +0.1%(w/v) BENZIL in gelatin capsules and cured by UV light in a Reichert Automatic Freeze Substitution Unit (AFS, Leica) at -50°C for 48 hours. Prior to sectioning, preparations were brought to RT by standing on the bench for 24 hours.

High K^+ v. Low Ca^{2+} Ringer's solution stimulation

Tissue was fixed at 4 °C after incubation for 15 or 30 minutes in the respective Ringer's solution with 4% paraformaldehyde/0.5% glutaraldehyde/4% tannic acid in 0.1 M cacodylate buffer (pH 7.4) for 15 minutes on ice and then for 30 minutes. Preparations were fixed without tannic acid for three hours. Preparations were washed for 3-12 hours in 0.1 M cacodylate buffer and then for 3 hours in sodium acetate buffer. Specimens were incubated in 1% UAc in sodium acetate buffer for 1 hour and washed for 20 minutes in sodium acetate buffer. Preparations were then dehydrated in a graded

ethanol series: 50% ethanol for 10 minutes, 70% for 30 minutes and 99.5% for 10 minutes. Rotating at RT, preparations were infiltrated with a mixture of 99.5% ethanol and LR White Resin (1:2) for 1 hour at 4 °C. Preparations were then infiltrated with LR White Resin (100%) for 1 hour and in fresh LR White Resin (100%) overnight. Preparations were moved to labeled beam capsule molds with vials filled with fresh LR White Resin. Molds were cured at 50 °C for 24 hours. The experiment was also carried out in tissue embedded at 4 °C in Lowicryl resin (not described here) and in LR Gold, using the same protocol described for the specimens stimulated at 5 Hz 20 ± rhodamine-phalloidin. Material embedded in LR Gold had the best labeling efficiency and ultrastructure.

Quantification of High K^+ v. Low Ca^{2+} Ringer solution stimulation

The Morforel Program was used for quantification of synapsin and SV2 labeling (Blackstad et al., 1990). Briefly, a Summasketch III Professional digitizing pad was connected to an IBM computer and used in MSDos mode for the Morforel program. Micrographs were printed at a magnification of 17,000 and enlarged by a factor of three, so that the final magnification was 51,000. Successive equivalent areas of 100 nm in depth were drawn along the length of the active zone. Gold particles were counted in each box and the area of the box was traced. The number of gold particles was divided by the area of the box to yield the density of gold particles/μm^2.

Labeling efficiency may vary between experiments. Therefore, when comparing data from separate experiments, a normalization procedure was performed. The density of gold particles was determined in 100 nm increments from the active zone, within equivalent areas. In most synapses, the labeling density reached a plateau at a distance of 300-400 nm from the active zone. Therefore, the density of gold particles in the first 100 nm shell was normalized against the region of the same cluster 300-400 nm from the active zone. This ratio therefore represents the relative distribution of synapsin labeling within each synapse and allows one to compare labeling done on different

days. Using this ratio, all experiments demonstrated an activity-dependent increase of ~2-fold in the first 100 nm from the active zone.

Postembedding immunolabeling procedure in LR Gold material

Sections were collected onto nickel slot grids. All incubations were performed at RT on parafilm in a covered glass petri dish moistened with filter paper and solutions were used as 60 µl droplets. Grids were etched in four successive rounds of 0.1% sodium borohydride in ddH_2O followed by successive washes in ddH_2O. Grids were incubated for 30 minutes in blocking solution of 50mM glycine/TPBS, 30 minutes in blocking solution of 1% human serum albumin (HSA)/1%bovine serum albumin (BSA) in TPBS, and then overnight at 4 °C in primary antibody diluted in the blocking solution. Primary antibodies were used at the dilution indicated: 1:200 for anti-synapsin domain D, 1:200 for anti-dynamin antibodies (DG-1) or directly for SV2 concentrated supernatant. A solution of 0.005% PEG/TrisCl (0.05 M, pH 7.4) was prepared freshly. Grids were washed in TPBS and dipped in PEG/Tris solution. Grids were incubated in colloidal gold conjugated secondary antibody at RT in the dark for two hours. Secondary antibodies were obtained from Amersham Life Sciences and were used at dilutions as specified: for rabbit polyclonal antibodies (synapsin domain D, DG-1), AuroProbe EM Goat Anti-Rabbit IgG coupled to 5 nm colloidal gold particles RPN 420 (1:50) Batch 126943. For mouse monoclonal antibodies (SV2), Auroprobe EM Goat anti-Mouse IgG+IgM 5nm colloidal gold particles RPN 430 (1:25) Batch 160852. After incubation in secondary antibody, grids were washed in 0.005%PEG /TrisCl (0.05M, pH 7.4), and then in ddH_2O. Excess moisture was removed from grids and they were dried in a gridbox overnight before further processing.

Double labeling experiments were attempted for synapsin D and SV2. SV2 was detected using AuroProbe EM Goat anti-Mouse IgG 10 nm colloidal gold particles (1:20) and synapsin D domain as above. Although labeling with these two antibodies

was consistently overlapping, labeling efficiency was extremely low and therefore the data was not used for localization analyses.

Silver Enhancement

After postembedding immunogold labeling, silver enhancement of gold particles was performed using Amersham IntenSE Silver Enhancement Kit RPN 491, stored at 4 °C. The silver enhancing reagent was mixed immediately prior to use. The reagent was aliquotted into 60 µl droplets and grids were incubated for 2.5-3 minutes. Only three grids were processed at a time, as silver enhancement does not proceed linearly and overexposure will ruin grids. Grids were then washed in a successive series of ddH_2O drops. Excess moisture was removed from grids by filter paper and they were dried in a gridbox overnight at RT before counterstaining.

Ultrathin sectioning

Rough trimming was performed with a glass knife before final sections were cut with a diamond knife. In the case of LR Gold, diamond knife sectioning sometimes proved too difficult, so glass knife sections were collected instead. The cutting speed was 1 mm/sec, 800-1300 Å feed. To cut a ribbon of serial sections, the first sections of the series were cut using a glass knife before switching to a diamond knife. For standard ultrastructure, sections appeared silver on the water surface. For the postembedding immunogold technique, sections were pale gold to white, as thicker sections facilitate better contrast and viewing of structures. Ribbons of serial sections were collected beginning with those closest to the knife, and the first section on each grid was forfeited for use as a kind of "glue" to stick to end of grid, to assist the remainder of the ribbon to fall into place. After collecting sections, grids were dried against a point of filter paper and stored in a gridbox to dry overnight.

SOLUTIONS

Fixatives:

3% glutaraldehyde/0.5% paraformaldehyde in 0.1 M phosphate buffer, pH 7.4

The fixative was always prepared freshly on the day of the experiment. In a fume hood, 0.5 g paraformaldehyde was dissolved in 35 ml ddH_2O and then heated to 60 °C while mixing. 1N NaOH was dropped into the solution until the paraformaldehyde dissolved. The solution was filtered into glass graduated cylinder and 50 ml 0.2 M phosphate buffer (pH 7.4) was added. Then, 12 ml 25% glutaraldehyde was pipetted directly into the cylinder. The final volume of the solution was adjusted to 100 ml with ddH_2O. Tannic acid fixative was mixed 20 minutes prior to use: 2 g tannic acid were added to 50 ml fixative, mixed, and the pH was adjusted to 7.2-7.4 with NaOH. Fixatives with and without tannic acid were stored in glass bottles at 4 °C.

0.5% glutaraldehyde4% paraformaldehyde /4% tannic acid in 0.1 M cacodylate buffer (pH 7.4) This fixative was used for immunolabeling experiments and was prepared essentially as described above with the following modifications: 4 g paraformaldehyde were added to 48 ml ddH_2O, heated to 60 °C while mixing and 50 ml cacodylate buffer (0.2 M, pH 7.4) was added to graduated cylinder. Then, 2 ml 25% glutaraldehyde was pipetted directly into the cylinder. The final volume of the solution was adjusted to 100 ml with ddH_2O. Tannic acid solution was prepared essentially as described above.

Buffers:

sodium acetate buffer:

While stirring, one part 0.3 M acetic acid (pH6.5) was gradually added to one part 0.3 M NaOH.

cacodylate buffer, pH 7.4

0.2 M cacodylate buffer was prepared by adding 2.76g cacodylic acid to 100 ml ddH_2O and the pH was adjusted to 7.4. To prepare 0.1 M buffer, 0.2 M solution was diluted 1:1 with ddH_2O.

sodium phosphate buffer, pH 7.4

For 100 ml of solution, four parts of solution A was combined with one part of solution B until pH reached 7.4. Solutions A and B were prepared separately at a concentration of 0.2 M in ddH_2O as follows: For solution A, 3.56g of ($Na_2HPO_4 \cdot 2H_2O$) was dissolved in 100 ml ddH_2O. For solution B, 2.76g of ($NaH_2PO_4 \cdot H_2O$) was dissolved in 100 ml ddH_2O. The combined solution was stored at 0.2 M at RT. To prepare 0.1 M phosphate buffer, 0.2 M phosphate buffer was diluted 1:1 with ddH_2O.

TrisCl Buffer (0.1 M, pH 7.4)

6.61g TrisCl was dissolved in 400ml ddH_2O and 0.97g TrisBase was dissolved in 50ml ddH_2O. The TrisBase was added to the TrisCl solution until the pH reached 7.4. The final volume was adjusted to 500 ml with ddH_2O. To prepare 0.05M TrisCl buffer, the 0.1 M solution was diluted 1:1 with ddH_2O. Solutions were stored at 4°C.

Tris phosphate buffered saline (TPBS)

100 ml sodium phosphate buffer (0.1 M, pH 7.4) was combined with 200ml Tris/Cl buffer (0.05M,pH7.4), 690ml ddH_2O, 7g NaCl, and 0.4g KCl. Solution was mixed, the final volume adjusted to 1L with ddH_2O, and stored at 4°C.

Postembedding solutions:

etching solution (0.1% sodium borohydride)

0.005g/5ml ddH_2O was mixed immediately prior to use.

blocking solution (50mM glycine in TPBS)

0.0375g/10ml TPBS was mixed on the day of the labeling procedure.

Heavy metal solutions:

Lead Citrate, saturated, pH 12

200ml ddH_2O was boiled for 15 minutes, covered and then cooled to 4°C. In a 100 ml volumetric flask, 2.66g $Pb(NO_3)_2$ and 3.52g sodium citrate ($Na_3(C_6H_5O_7 \cdot 2H_2O)$ were combined. 60ml boiled ddH_2O was added and the solution was mixed by hand for ~ 30

minutes until crystals were dissolved and solution had the appearance of milk. Approximately 0.4-0.6g NaOH was added and the solution was mixed until it turned clear. The volume was adjusted to 100 ml with boiled ddH_2O. The solution was left to stand at 4 °C overnight and the pH was then checked to be pH 12.

Uranyl Acetate, 2% in ddH_2O

2 g uranyl acetate was dissolved in 100 ml ddH_2O, mixed for several hours and stored at 4 °C.

Uranyl Acetate, 1% in sodium acetate buffer

1g uranyl acetate was dissolved in 100 ml in sodium acetate buffer, mixed for several hours, and stored at 4 °C.

osmium tetroxide, 1% in ddH_2O

As osmium vapors can penetrate plastic, all solutions were stored in a dark glass bottle covered with aluminum foil inside a larger glass jar and stored in an isolated refrigerator. In a fume hood, 1.0 g osmium ampoule was broken and dropped into a dark glass bottle with a glass stopper. A volume of 100 ml ddH_2O was added to the bottle and shaken. The bottle was sonicated for approximately 15 minutes.

Ringer's Solutions:

Normal, concentrations in mM: NaCl (109), KCl (2.1), $MgCl_2$ (1.8), glucose (4), HEPES (2), $CaCl_2$ (2.6), glutamine (0.073g/L). These were combined in cold ddH_2O, and the pH was adjusted to 7.4 using 1N NaOH. Immediately prior to use, the solution was bubbled for 20 minutes with O_2 and the pH was checked again.

Low Ca^{2+}, concentrations in mM: NaCl (109), KCl (2.1), $MgCl_2$ (4), glucose (4), HEPES (2), $CaCl_2$ (0.1), glutamine (0.073g/L), prepared as above.

High K^+, concentrations in mM: NaCl (81.1), KCl (30), $MgCl_2$ (1.8), glucose (4), HEPES (2), $CaCl_2$ (2.6), glutamine (0.073g/L). Adjusted pH using 1N KOH and otherwise prepared as above.

III. RESULTS

The hypothesis of synapsin function states that in its dephosphorylated form, synapsin acts to cross-link synaptic vesicles to each other and the cytoskeleton, thereby maintaining the vesicle cluster. When Ca^{2+} flows into an active nerve terminal, CaMKII phosphorylates synapsin, changing its conformation and forcing its dissociation from synaptic vesicles and actin. This dissociation of synapsin, synaptic vesicles and actin diminishes the ability of vesicles to interact with the actin cytoskeleton (Greengard et al., 1993) promoting the refilling of the pool of vesicles proximal to the active zone used during neurotransmission.

Light microscopic visualization of actin with rhodamine-phalloidin

To investigate the localization of actin in the synapse at the light microscope level, we injected the F-actin stabilizing compound, rhodamine-phalloidin, into lamprey reticulospinal axons (n>100 axons). Following injection of rhodamine-phalloidin, we examined injected axons using a 10 X (water-immersion) Nikon lens and a CCD camera and found an intense accumulation of rhodamine fluorescence in spots on the surface of the axons (Figure 11 and Figure 12, top panel), reminiscent of those seen after injection of antibodies to synaptic vesicle proteins (Pieribone et al., 1995). To test if these fluorescent spots accumulated at synaptic vesicle clusters, Cy5 labeled-antibodies to synaptotagmin were co-injected with rhodamine-phalloidin (Figure 12, middle panel). When the illumination of each fluorophore in the same field of view was merged at this resolution, the spots along an axon accumulated from rhodamine-phalloidin and Cy5-anti-synaptotagmin antibodies co-localized, indicating an overlapping distribution of actin and synaptotagmin in living axons (Figure 12, bottom panel).

To address the presynaptic localization of actin more precisely, lamprey reticulospinal axons were co-injected with Alexa-labeled anti-synapsin antibodies (G304) and Oregon Green-labeled phalloidin. The pattern of localization was then

Figure 11. Gallery of reticulospinal axons microinjected with rhodamine-phalloidin

A CCD unit was used to visualize the presynaptic microinjection of rhodamine-phalloidin into living lamprey reticulospinal axons. Six axons from different experiments are shown here. Fluorescent spots accumulated along the surfaces of axons. These spots were stable for several hours and reminiscent of those formed after presynaptic injection of antiserum to synapsin (Pieribone et al., 1995). Variations in the distribution of spots reflect the positions of synaptic contacts on each axon. Variations in fluorescence intensities reflect the local amounts of phalloidin achieved by microinjection.

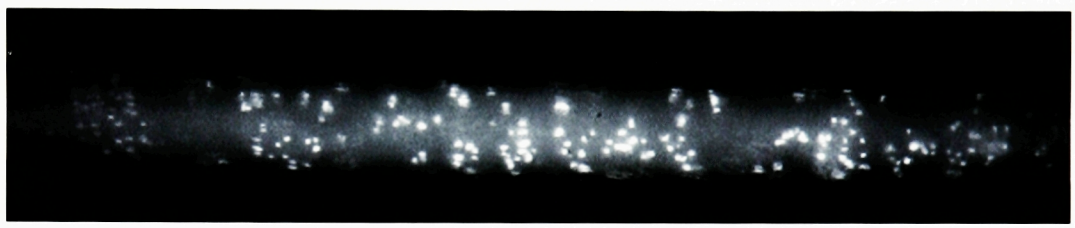

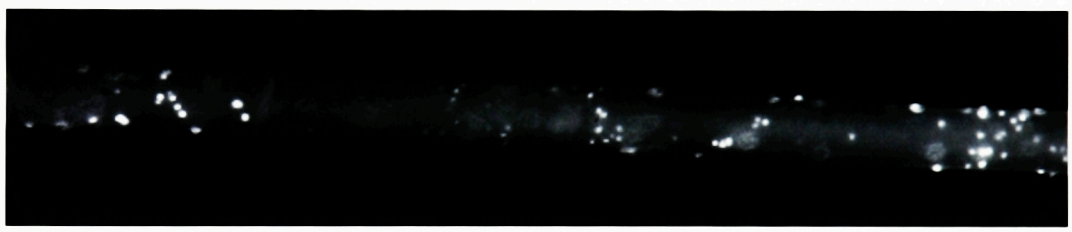

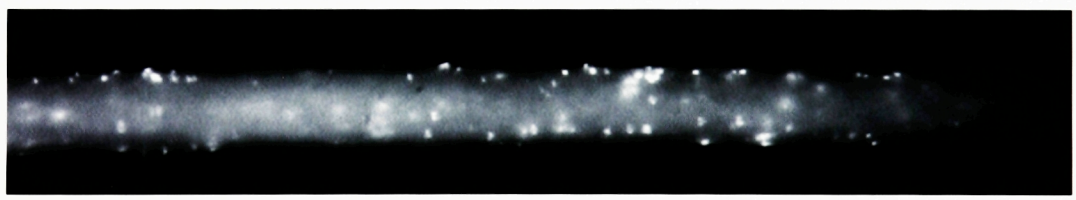

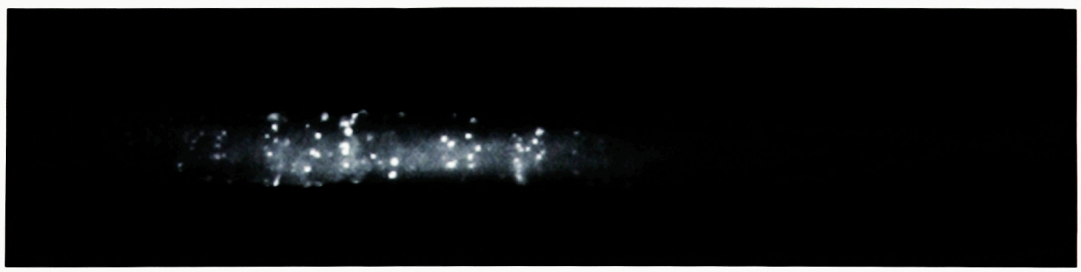

Figure 12. Phalloidin and synaptotagmin co-localize in reticulospinal axons

Presynaptic injection of rhodamine-phalloidin (top panel) and antiserum to the integral synaptic vesicle membrane protein, synaptotagmin (middle panel, Cy5-labeled anti-synaptotagmin antiserum, green) were performed in the same axon. These signals co-localized (bottom panel), suggesting that F-actin is concentrated specifically along the axon at synapses. Scale bar indicates 20μm. Fluorophores were converted to pseudo-color for this image.

Phalloidin labeling in reticulospinal axons

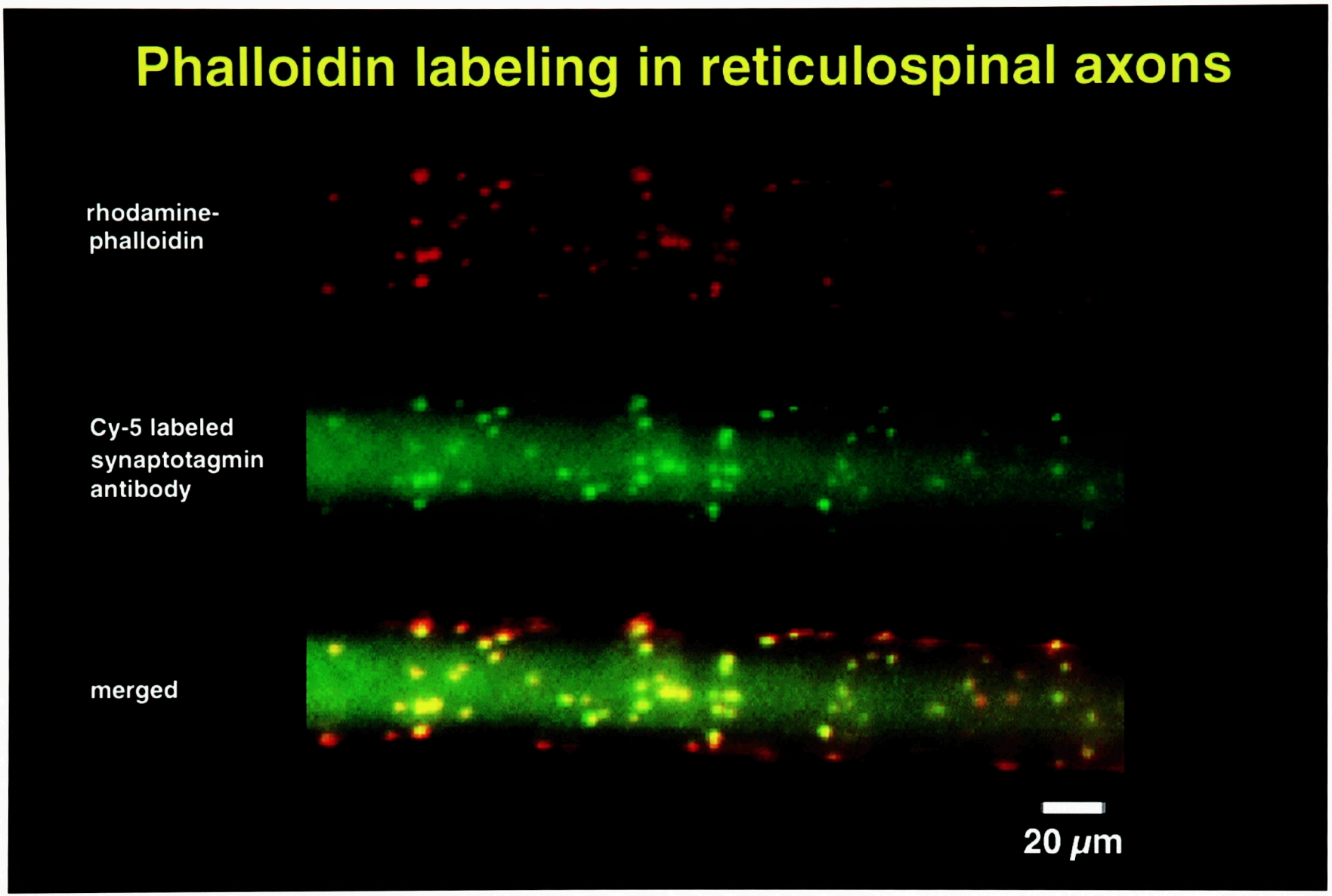

examined using a 60X (oil-immersion) Nikon lens. The use of the 60X oil-immersion lens to image axons injected with phalloidin revealed that the spots of fluorescence observed using the less precise 10X water-immersion lens appeared as hollow rings (Figure 13, left and top right panels). The bright rings were most prominent shortly after microinjection. They diminished variably and gradually 15-60 min post-injection, and were replaced by a diffuse axonal labeling, consistent with the results observed at the ultrastructural level (see below). In contrast, fluorescence accumulation of injected Alexa-tagged anti-synapsin antibodies remained localized to discrete spots (Figure 13, middle right panel). These discrete spots of fluorescence occurred in the center of the Oregon Green-labeled rings (Figure 13, bottom right panel), suggesting that structures containing filamentous actin surrounded, rather than overlapped with, synaptic vesicle clusters. This pattern of labelling was confirmed by confocal microscopy (data not shown).

Electron microscopic visualization of actin with rhodamine-phalloidin

To investigate the ultrastructural correlates of the non-overlapping presynaptic localization of actin and synapsin, results obtained following rhodamine-phalloidin injection were examined by electron microscopy. As mentioned above, lamprey reticulospinal axons contain phasic synapses consisting of 1000-3000 synaptic vesicles densely clustered at active zones of 1-3 μm in diameter separated by areas of vesicle-free axoplasm. In the absence of rhodamine-phalloidin, upon stimulation, vesicle membrane is incorporated into the presynaptic plasma membrane and recycled via clathrin-mediated endocytosis in the area of the plasma membrane lateral to the active zone (Figure 14 and (Wickelgren et al., 1985). In the absence of stimulation, intraaxonal injection of rhodamine-phalloidin did not lead to any observable alterations in the morphology of the nerve terminal (data not shown).

Synapses from axons injected with rhodamine-phalloidin and stimulated at 5 Hz for 20 minutes showed predominantly two kinds of morphological alterations in the nerve

Figure 13. Actin filaments form ring-like structures around synaptic vesicle clusters

A light micrograph of a living axon double-injected with Oregon Green-phalloidin and Alexa-synapsin antibodies (G304) and visualized using a 60X (oil-immersion) Nikon lens. The axon was injected under continuous stimulation at 5 Hz and then transferred into high K^+-containing solution. Ring-like structures are present on the surface of the axon.

Left and upper right panels: Actin ring-like structures are revealed by the injection of phalloidin.

Middle right panel: The same area is shown after switching filters to reveal the fluorescence of the Alexa-tagged anti-synapsin (G304) antibodies.

Lower right panel: Merged images of the top and middle right panels. The ring-like structures formed by filamentous actin surround the spot-like fluorescence revealed by injection of synapsin antiserum.

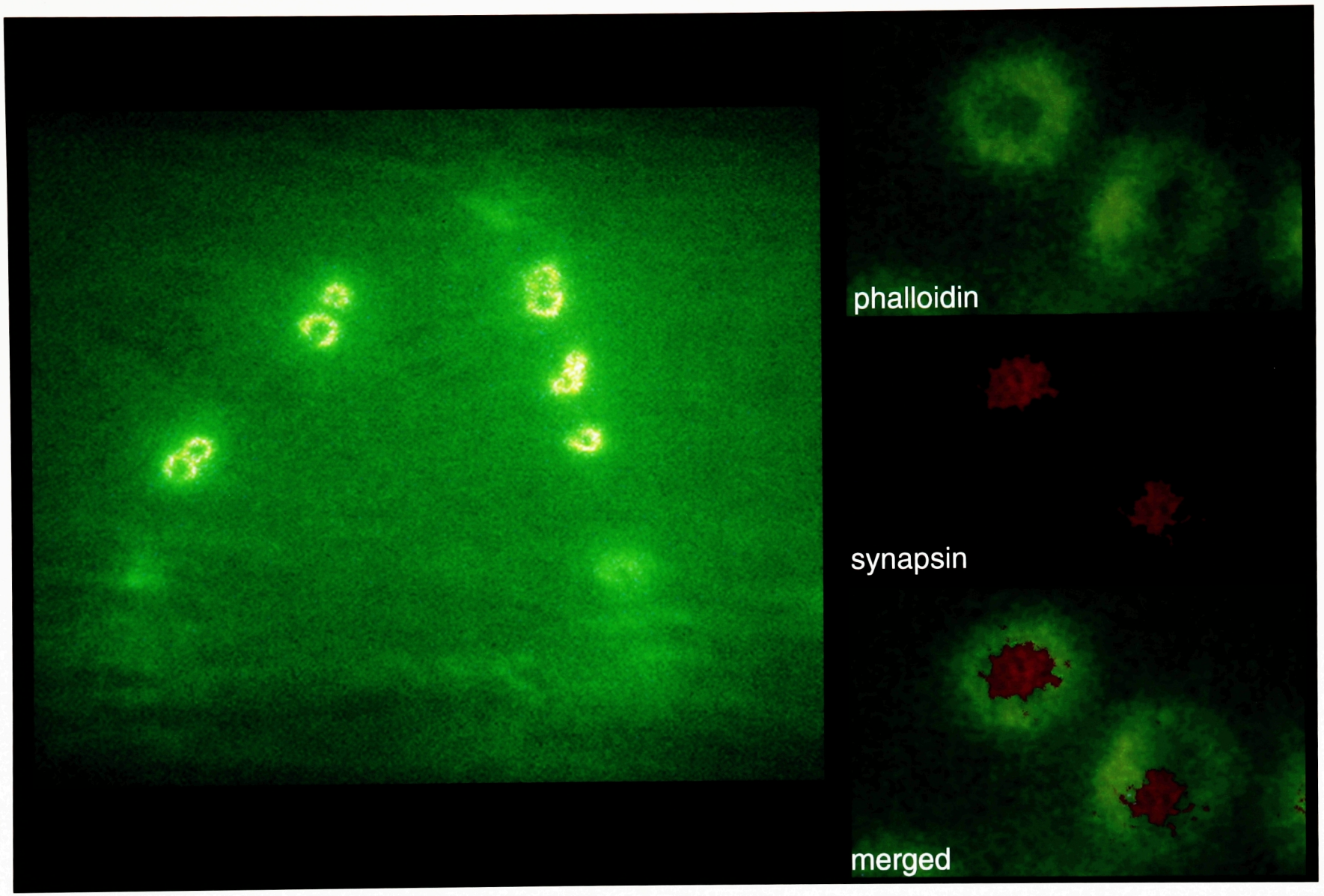
phalloidin
synapsin
merged

terminal (Figures 15 and 16). The first effect indicates a role for actin in a previously undescribed stage of the synaptic vesicle cycle. In many synapses, a filamentous material with an organization resembling the actin matrix nucleated by virus particles (reviewed in (Qualmann et al., 2000) was observed in the axoplasm between the vesicle cluster and the area of the plasma membrane lateral to the active zone, where clathrin-coated endocytosis occurs. The presence of clathrin-coated endocytic intermediates in this area of the plasma membrane was consistent among injected axons, indicating a spatial coupling of endocytic zones and the filamentous matrix. Uncoated clear round vesicles of approximately 50 nm in diameter, indistinguishable in size and overall appearance from those synaptic vesicles within the cluster, were often seen associated with or enmeshed in these filaments (Figure 15).

In other synapses, the overwhelming morphological effect of stimulation following phalloidin injection was a disruption of the clathrin-mediated pathway of endocytosis (Figure 16). This disruption was characterized by the marked accumulation of clathrin-coated endocytic intermediates often accompanied by the heavily-expanded area of the plasma membrane lateral to the active zone. In some cases, the effect was severe enough to cause a dramatic reduction in the size of the synaptic vesicle cluster, presumably since new vesicles could not be recycled within the appropriate time. Furthermore, endocytosis appeared to be blocked at a very specific stage, corresponding to the endocytic Stage 3 as delineated by (Gad et al., 1998), namely unconstricted, invaginated coated intermediates. Endocytic intermediates of this morphology also accumulated after injection of *C. botulinum* C2 toxin, as described below (Figure 20). The preferential accumulation of endocytic intermediates or actin filaments was not apparently related to the distance from the injection site. It is possible that these differential effects of phalloidin could be due to local variations in the ratio of the phalloidin concentration and to the degree of synaptic activity, but that issue remains unresolved.

Figure 14. An electron micrograph of a stimulated reticulospinal synapse

Some axons of a lamprey spinal cord were injected with rhodamine-phalloidin, the cord was stimulated at 5 Hz for 15 minutes, fixed during stimulation, and embedded for analysis by electron microscopy.

An electron micrograph is shown of an uninjected (Control) representative reticulospinal synapse between an axon (ax) and dendrite (d). Indications of nerve terminal activity are present, such as the membrane invaginations (curved arrows) and coated intermediates (arrow) lateral to the vesicle cluster (sv), (enlarged in lower panel). Scalebar indicates 0.1μm.

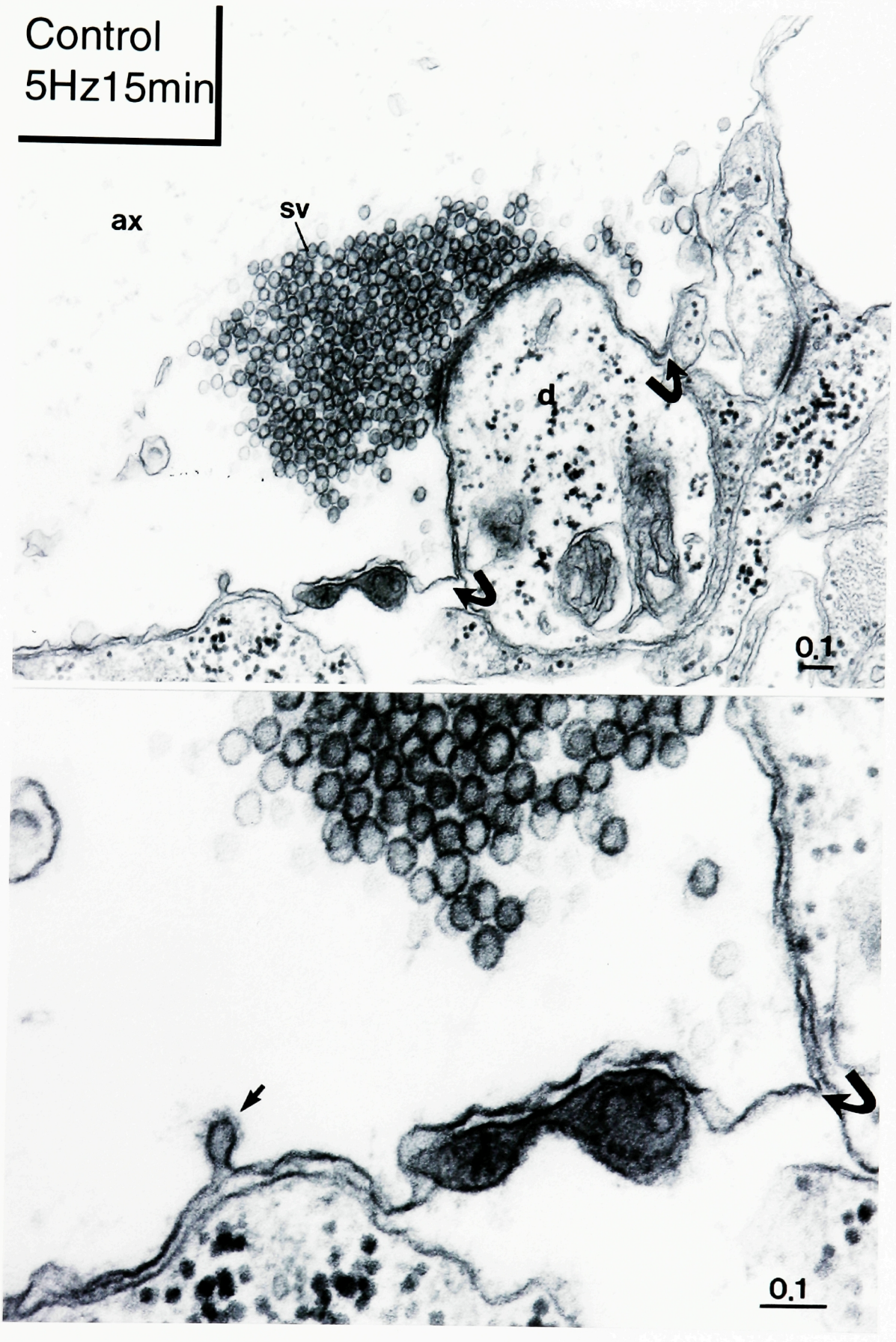
Control
5Hz15min
ax
sv
d
0.1
0.1

Figure 15. Phalloidin injection reveals the cytoskeletal matrix lateral to the active zone

This is an electron micrograph of a synapse between a dendrite (d) and a reticulospinal axon (ax) from the same preparation as shown in Figure 14. This axon was injected with rhodamine-phalloidin and stimulated at 5 Hz for 15 minutes, as indicated by the membrane invaginations (curved arrows). Note the filamentous cytoskeletal matrix (arrows) at the region lateral to the synaptic vesicle (sv) cluster. Distinct filaments are in contact with synaptic vesicles outside of the vesicle cluster.

The lower panel is a higher magnification of the area lateral to the vesicle cluster. Scalebars indicate 0.1μm.

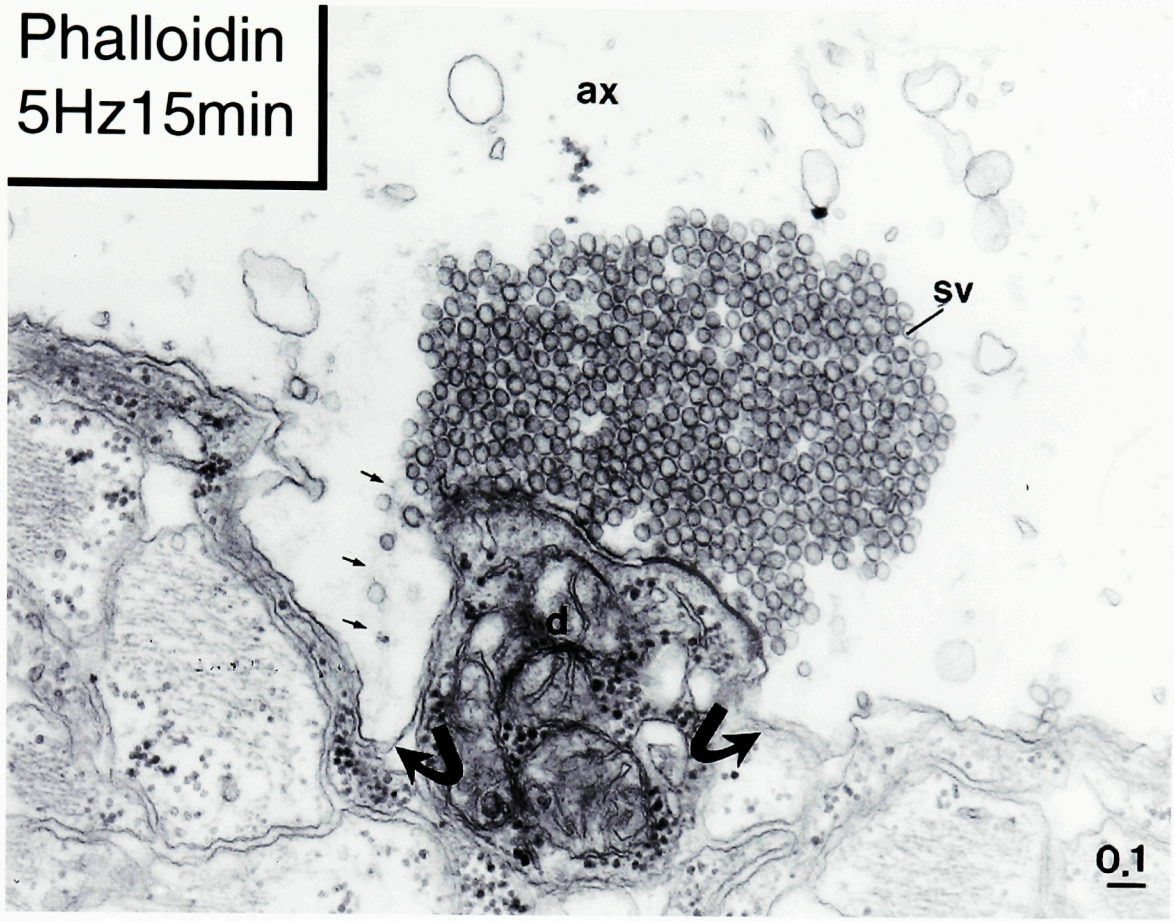
Phalloidin
5Hz15min
ax
sv
d
0.1

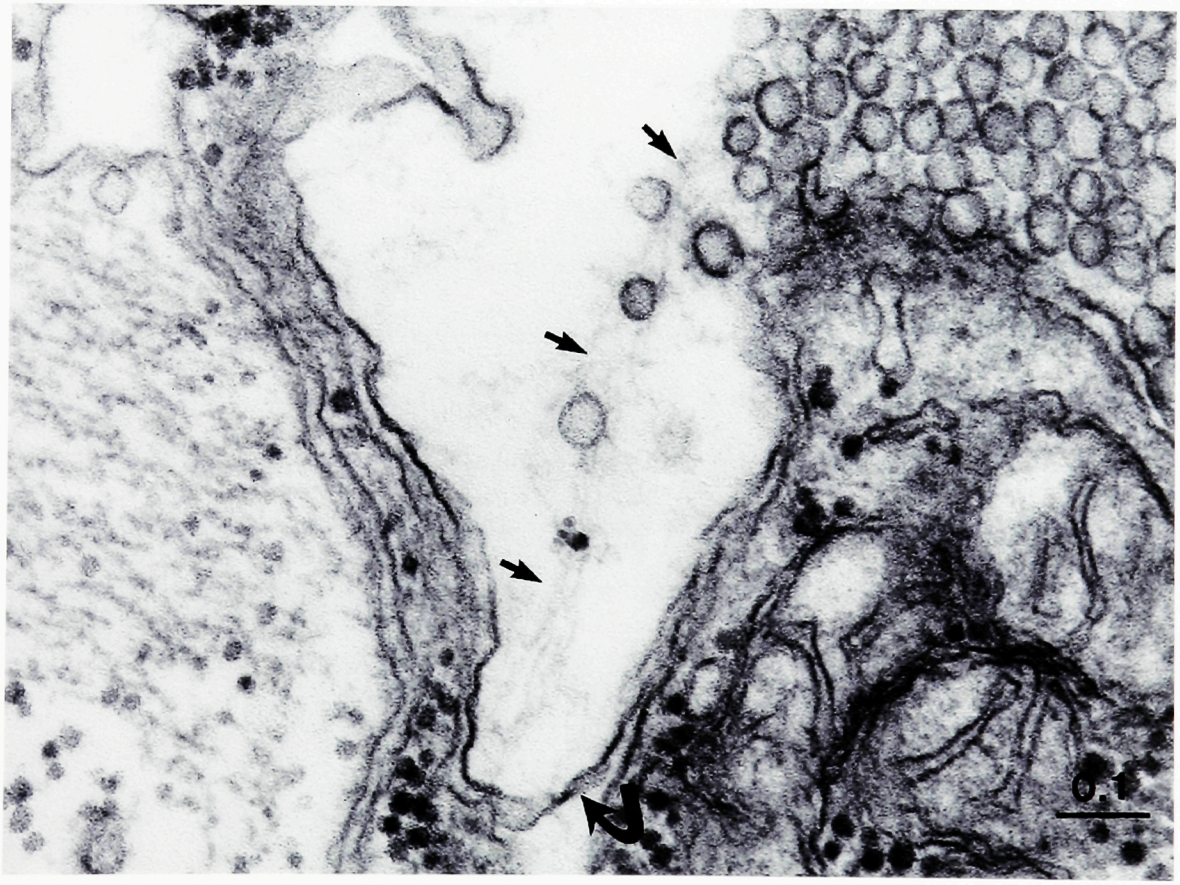
0.1

Three-dimensional reconstruction of actin around vesicle cluster

Looking upon individual electron micrographs, one can consistently observe a few vesicles in contact with the filamentous matrix on each section. To understand if the filaments observed by electron microscopy corresponded to the rings observed by high resolution light and confocal microscopy, and to gain a greater appreciation for the number of synaptic vesicles contacting the actin filaments throughout an entire synapse, we assembled a three-dimensional reconstruction of a phalloidin-injected synapse contained within 30 serial ultrathin sections. As shown in Figures 17 and 18, clustered synaptic vesicles are represented in dark red, filamentous material is yellow, and the plasma membrane is green. By reconstructing 30 serial sections, one can appreciate the accumulation of many synaptic vesicles within a halo of actin-containing filaments surrounding the synaptic vesicle cluster (Figure 17). A transverse section of the reconstruction is shown in Figure 18, (active zone shown in bright red), revealing the clustered vesicles (red), as well as an appreciable number of synaptic vesicles (purple) enmeshed within the filamentous matrix (yellow).

Disruption of actin dynamics and the synaptic vesicle cycle

Since the actin stabilizing compound phalloidin revealed the activity-dependent filamentous matrix, it was reasoned that disruption of actin filament formation should disrupt the transport of recycling synaptic vesicles. Accordingly, the formation of actin filaments was perturbed using the ADP-ribosylating C2 toxin from *Clostridium botulinum* (Aktories et al., 1997) (see Methods). In axons microinjected with C2 toxin and not stimulated, presynaptic morphology appeared unaltered (Figure 19, top). However, in synapses from axons injected with C2 toxin and stimulated at 5 Hz for 30 minutes, neither vesicles nor the associated filamentous matrix was observed in the

Figure 16. Phalloidin injection disrupts endocytosis pathway and leads to a depletion in the synaptic vesicle cluster

In the same preparation as described in Figure 14-15, some axons injected with rhodamine-phalloidin and stimulated at 5 Hz for 15 min exhibited a dramatic disruption of the endocytic pathway. The upper panel shows such an example, with only a small portion of the synaptic vesicle cluster (sv) intact. Large membrane expansions were present lateral to the active zone (curved arrows) and deep pockets of axoplasm lateral to the cluster were filled with clathrin-coated intermediates, a filamentous matrix, and synaptic vesicles (short fat black arrows). Open arrow indicates apparent demarcation of endocytic region. Mitochondria (m) are present within the axon. Scale bar indicates 0.1μm.

The lower panel shows an enlargement of the right third of the top panel. Larger arrow indicates the accumulation of unconstricted clathrin-coated intermediates and small arrows point to filamentous material presumed to be actin.

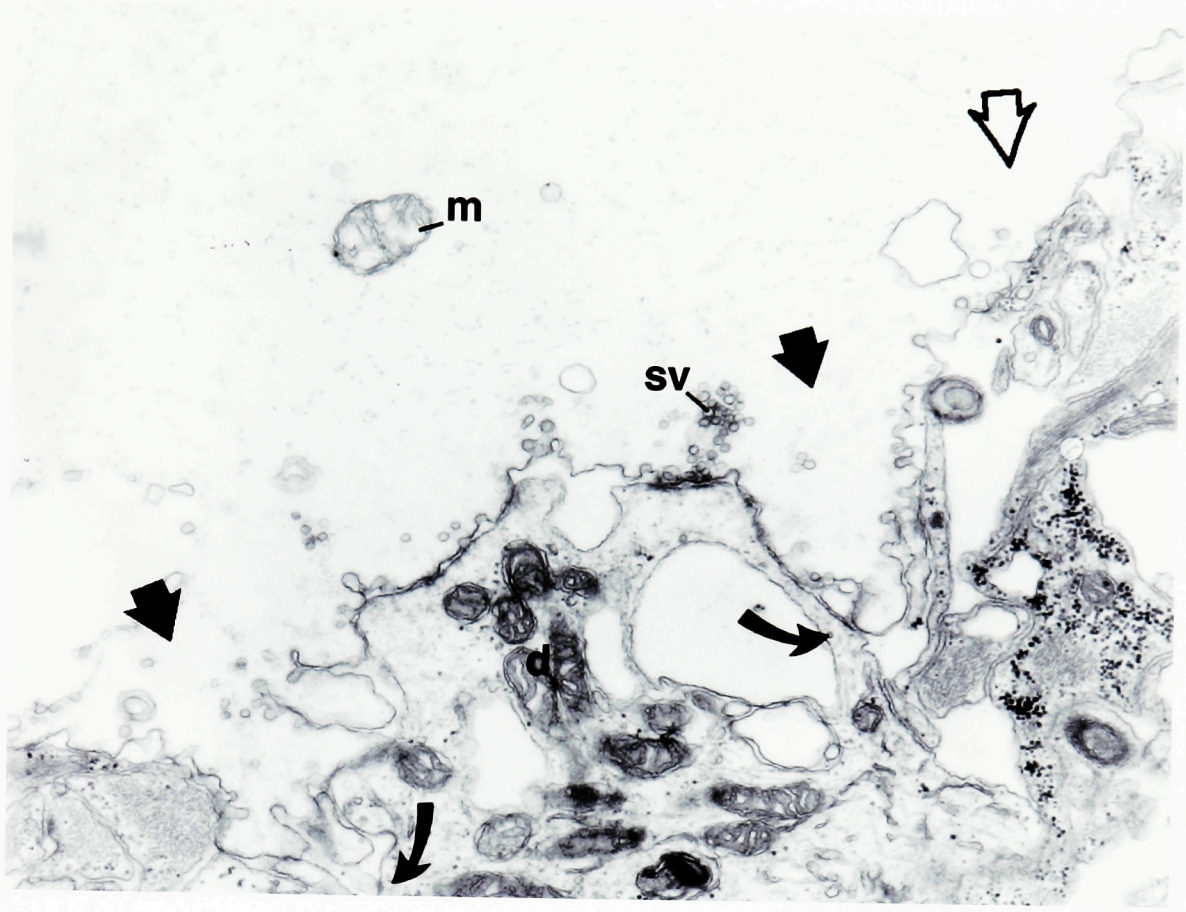
m
sv
d

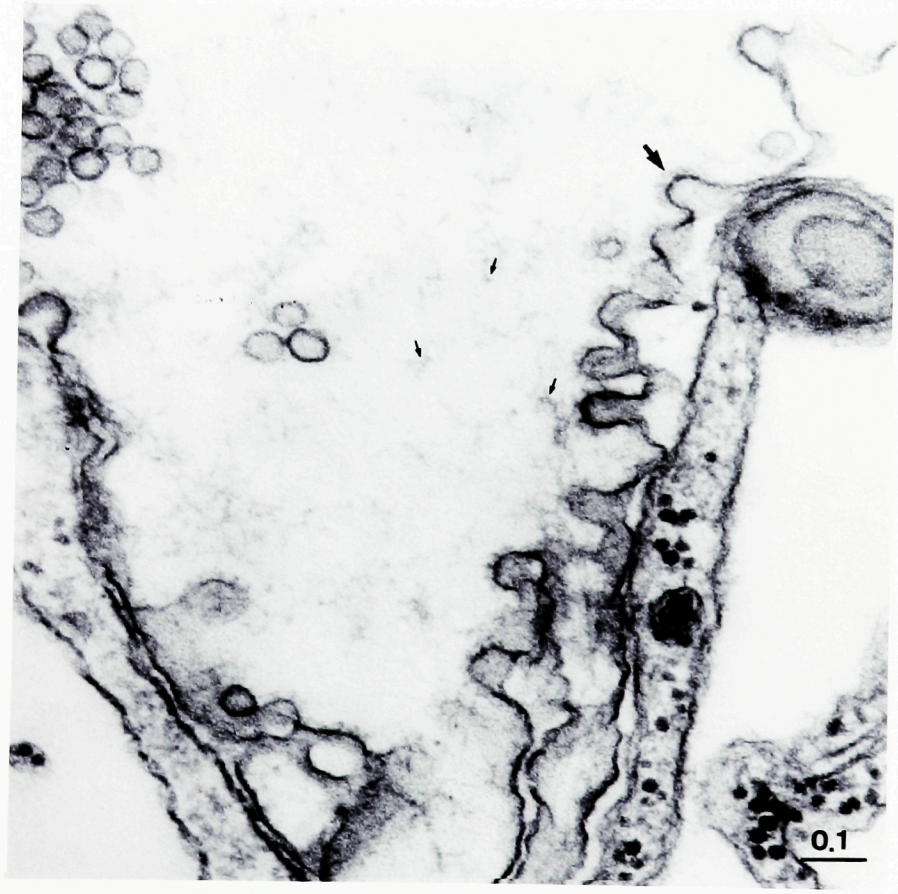
0.1

Figure 17. A three-dimensional reconstruction reveals a ring of actin surrounding the synaptic vesicle cluster

A lamprey reticulospinal axon microinjected with rhodamine-phalloidin was stimulated at 5 Hz for 15 minutes and fixed during stimulation. A complete synapse from this axon was reconstructed from 30 serial sections using FormZ software (Auto-des-Sys, Inc.). Clustered synaptic vesicles (red) are surrounded by a halo of actin (yellow) which is in contact with the plasma membrane (green).

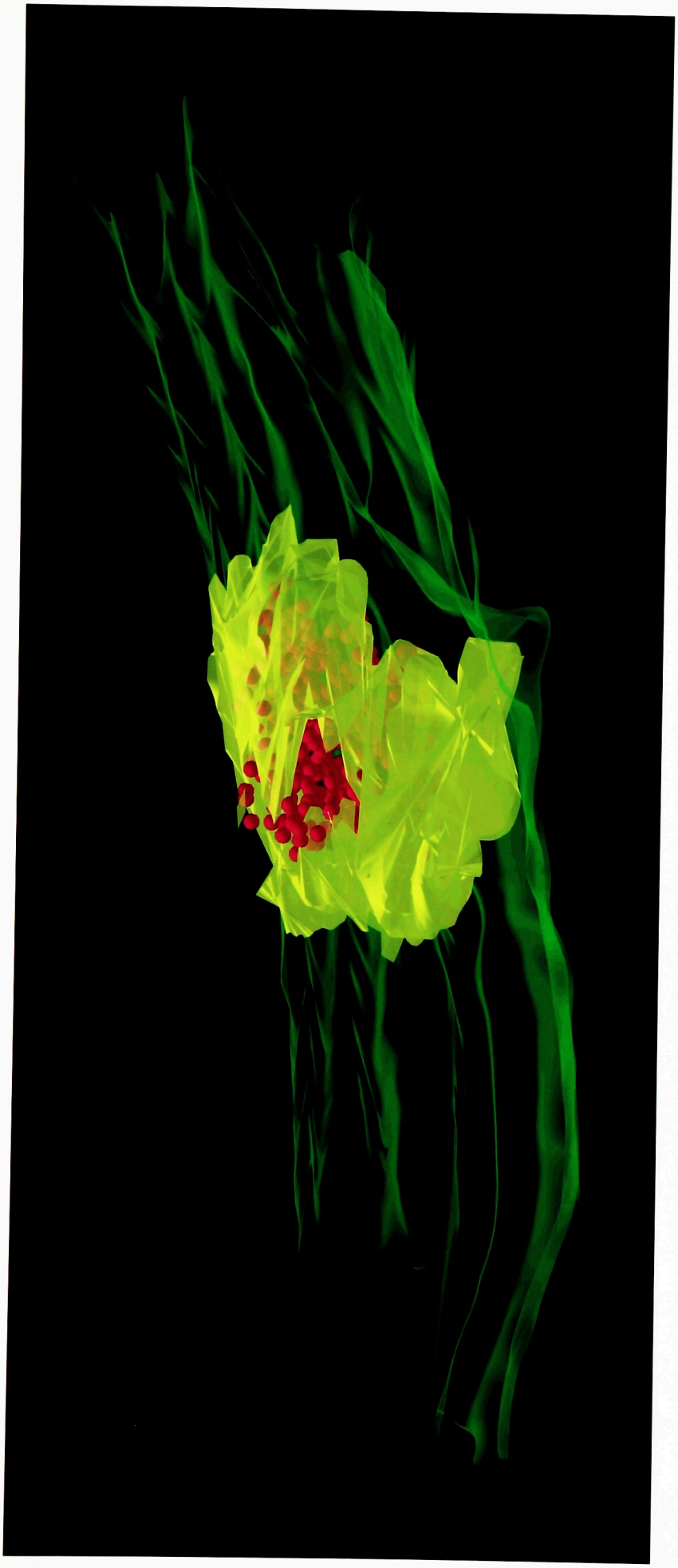

Figure 18. A transverse section through the middle section of the three-dimensional reconstruction

A transverse section through the reconstructed synapse shows that clustered synaptic vesicles (red) are surrounded by the actin matrix (yellow), while some synaptic vesicles outside of the cluster (purple) are enmeshed within the actin matrix. The active zone is shown in this view (bright red line) to delineate the cluster and the plasma membrane (green) is clearly in contact with the actin matrix.

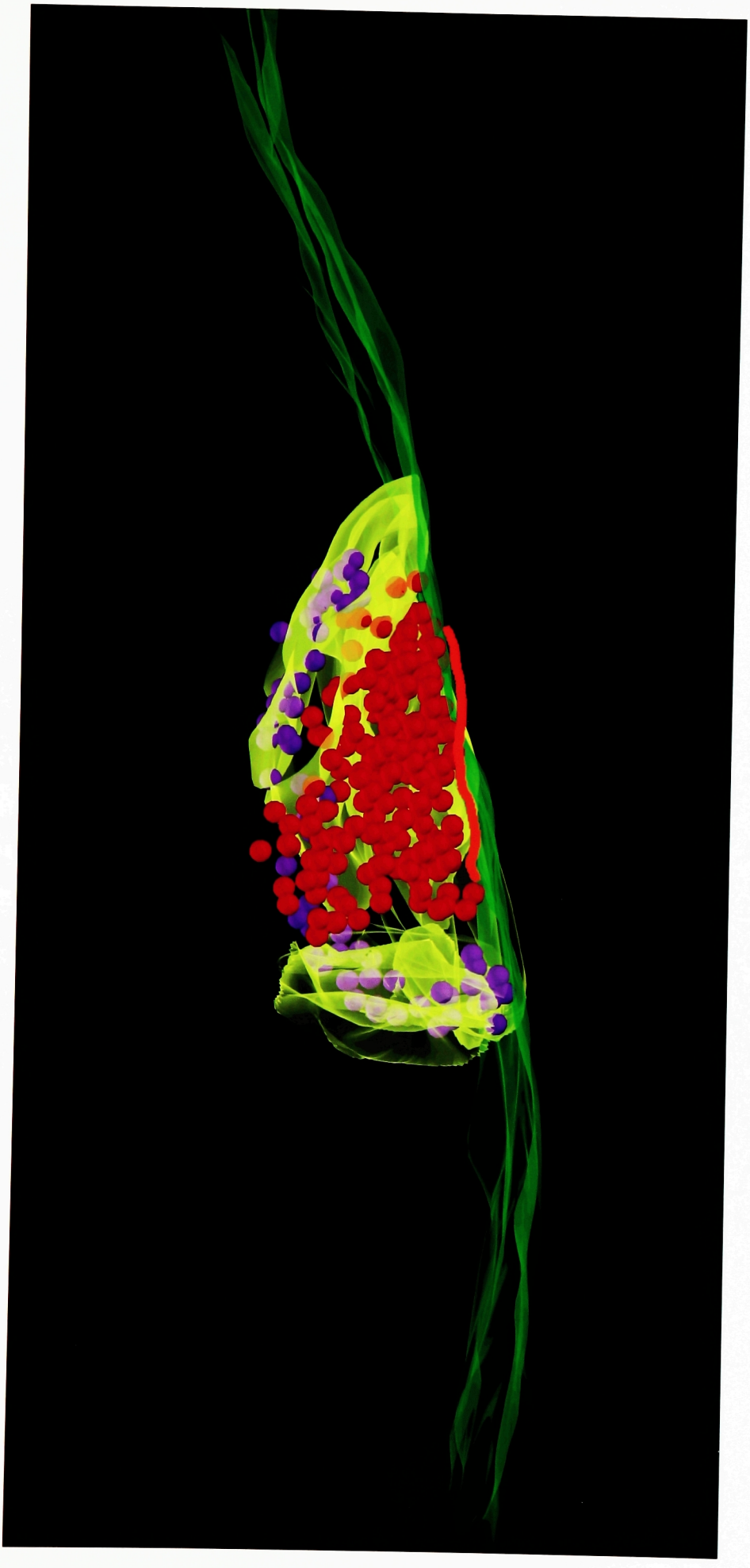

axoplasm lateral to active zones (Figure 19, bottom). Concomitantly, synaptic vesicleclusters were dramatically reduced in size. In the presence of C2 toxin, synaptic vesicles were counted in regions outside of the cluster where endocytosis occurs. As shown in Table I, the number of synaptic vesicles found outside the cluster in stimulated synapses was altered by C2 toxin in a time-dependent manner.

Table I. Effect of C2 Toxin on Number of Vesicles in Axoplasm Lateral to Vesicle Cluster

Area Lateral to Active Zone	Control ±SEM	C2 Toxin (15min) ±SEM	C2 Toxin (60min) ±SEM
0-0.5μm	13±5	15±5	0.4±0.4
0.501.0 μm	1.1±0.5	7±4	0.3±0.3
n (synapses)	6	4	3

As with phalloidin, in some synapses injected with *C. botulinum* C2 toxin, there was a marked accumulation in the number of clathrin-coated pits was observed. The proportion of clathrin-coated intermediates with an unconstricted morphology was increased in a dose-dependent manner, as compared to synapses from uninjected, stimulated axons (Figure 20). The effects on endocytosis were specific for toxins that affect actin polymerization, as bath-application of the microtubule-depolymerizing compound nocodazole (100 μm) for more than 1 hour followed by stimulation at 5 Hz for 20 minutes had no detectable effect on the synaptic structure or distribution of stages of clathrin-coated intermediates, as defined by Gad et al., 1998) (see Table II). Thus, similar to the F-actin-stabilizing toxin phalloidin, the actin-depolymerizing C. *botulinum* C2 toxin disrupted both endocytosis and post-endocytic transport of synaptic vesicles. The reduced size of synaptic vesicle clusters was attributed to a combined action of the toxin at both actin-dependent steps of the synaptic vesicle cycle.

Figure 19. Injection of C. *botulinum* C2 toxin disrupts clathrin-mediated endocytosis

Reticulospinal axons were microinjected with C2 toxin, stimulated at 5 Hz for 30 minutes, fixed during stimulation, and embedded for analysis by electron microscopy.

Panel A: A synapse between a dendrite (d) and an axon (a) that was microinjected with the C. *botulinum* C2 toxin, maintained at rest for 30 min, fixed, and embedded for analysis by electron microscopy. No morphological alterations are apparent.

Panel B: A synapse between a dendrite (d) and an axon (a) that was microinjected with the C. *botulinum* C2 toxin and then stimulated at 5 Hz for 30 min, fixed during stimulation, and embedded for analysis by electron microscopy. Note the depletion of the synaptic vesicle cluster (sv), the lack of observable actin-like filaments (arrow) and expanded periactive zone membrane. Some larger cytoskeletal elements, such as neurofilaments, are apparent in the axon. Scale bar indicates 0.1 μm.

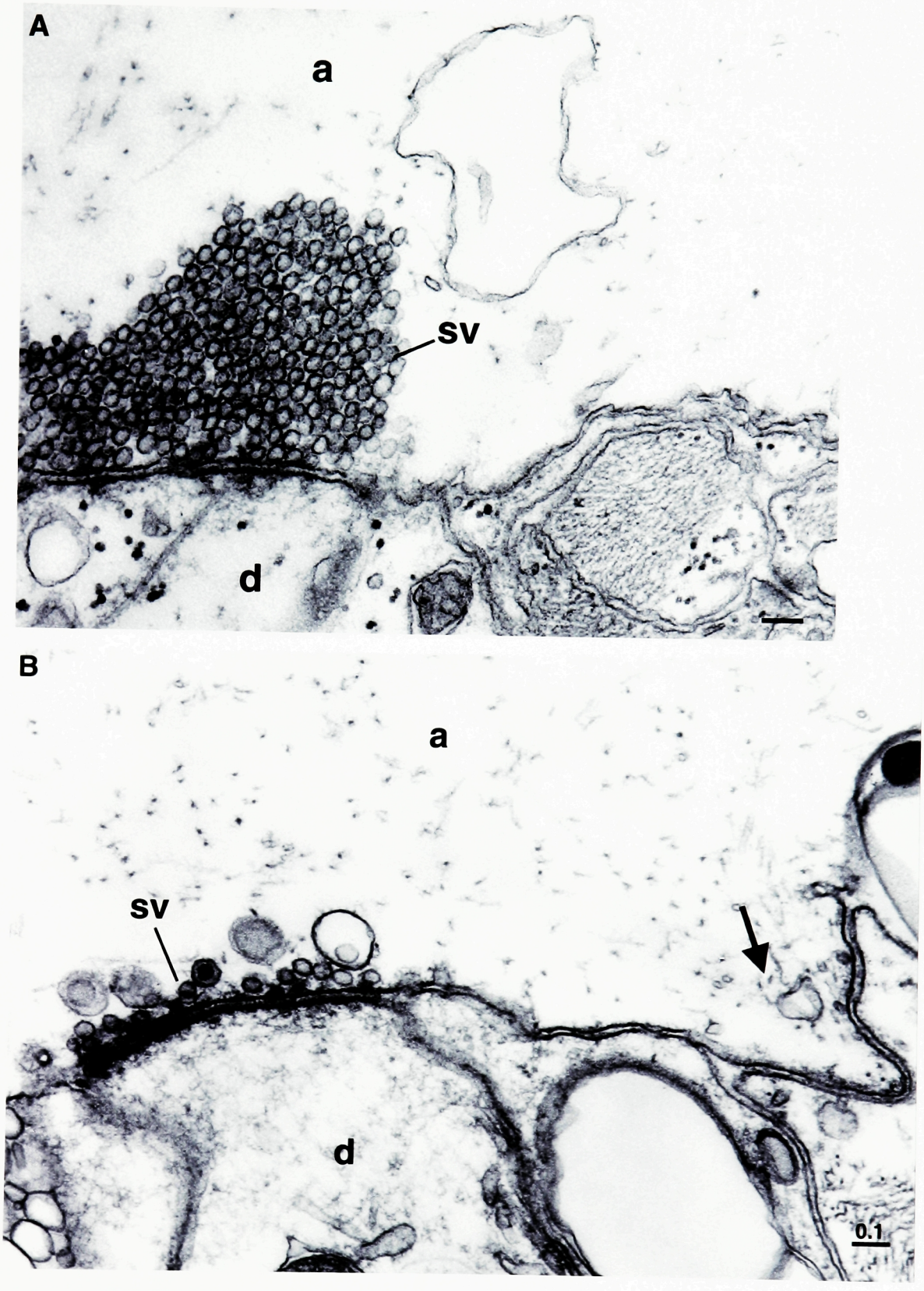
A
a
sv
d
B
a
sv
d
0.1

Figure 20. *C. botulinum* C2 Toxin increases the number of coated intermediates and changes the relative abundance of different stages of coated intermediates.

Synapses from axons injected with *C. botulinum* C2 toxin, stimulated at 5 Hz for 30 minutes, and fixed for analysis by electron microscopy. Clathrin-coated intermediates in these synapses were classified into four groups as performed in (Gad et al., 1998). The groups were classified according to morphology: (1) partly invaginated; (2) invaginated but unconstricted; (3) constricted; (4) constricted with an electron-dense ring. The distribution of intermediates in these stages has been shown to change over time. In normal stimulated synapses, intermediates are most commonly found corresponding to group 3. In the presence of C2, the number of coated intermediates increases (top panel) and the stage distribution changes, with stage 2 becoming the most common.

C2 Toxin Increases Number of Coated Intermediates

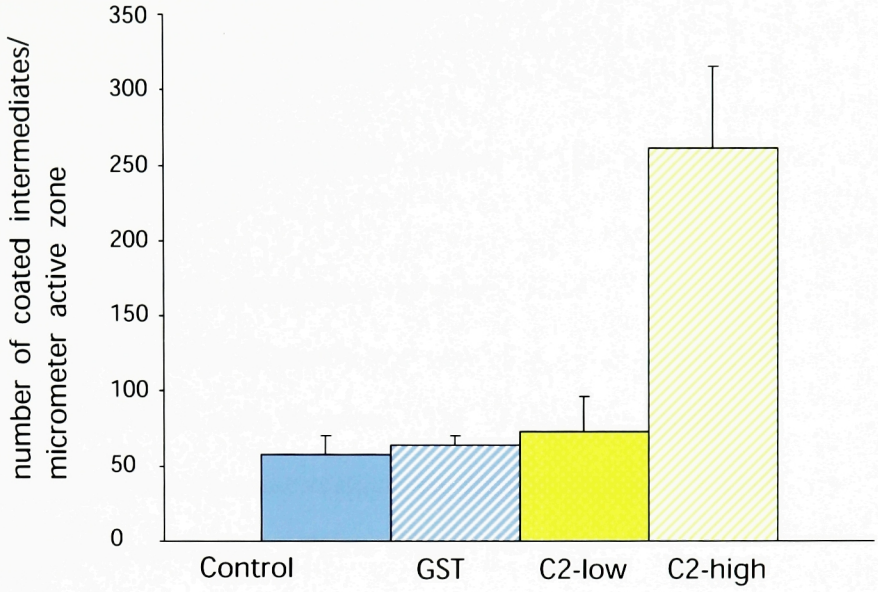

C2 Toxin Changes Shape Distribution of Coated Intermediates

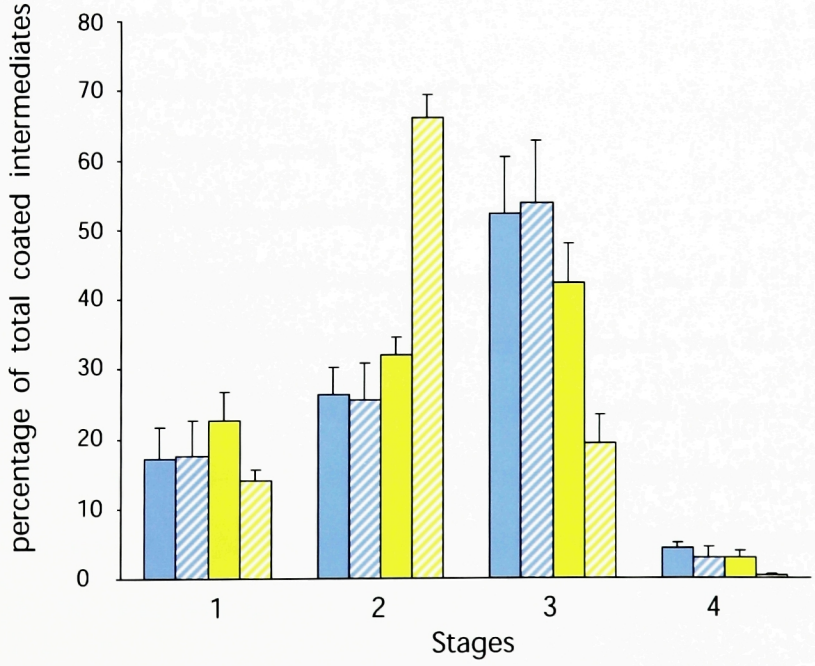

Table II. Effects of nocodazole on stage distribution of coated intermediates: Percentage of Total Coated Pits Per Synapse in Stages 1-4, as described by Gad *et al.*, 1998

Stage Number	Nocodazole
1	16
2	25
3	55
4	2
n (synapses)	7

NEM-S1 disrupts synaptic vesicle cycling in an activity-dependent manner

To further characterize the role of actin in vesicle transport, another reagent that interacts with actin filaments was used. The subfragment 1 (S1) of meromyosin selectively binds actin filaments. The sulfhydryl reagent N-ethylmaleimide (NEM) reacts with two cysteine sulfhydryls that are located in the ATPase sites of S1 myosin fragments, abolishing ATPase activity (Meeusen and Cande, 1979). This modification produces S1 fragments that are irreversibly bound to F-actin, as they cannot complete the ATPase cycling which normally induces their release from actin filaments (Lin et al., 1996; Meeusen and Cande, 1979). Axons maintained at rest after microinjection of NEM-S1 had a normal structure with large synaptic vesicle clusters (Figure 21A). Microinjection of NEM-treated S1 fragments followed by stimulation had a dramatic effect on synaptic vesicle trafficking. At intermediate concentrations of NEM-S1, aggregates of synaptic vesicles accumulated in the area lateral to the synaptic vesicle cluster (Figure 21B). The size of synaptic vesicle clusters was reduced. A moderate expansion of the presynaptic plasmalemma also occurred, but the number of clathrin-coated pits was similar to that in control axons. In axonal regions containing a higher S1 concentration, (as judged by the intensity of a co-injected fluorescent marker), the release sites were almost entirely depleted of synaptic vesicles (Figure 21C&D). In

these regions, synaptic vesicles were scattered in the periphery of the area normally occupied by the synaptic vesicle cluster.

Synapsin and actin in the synaptic vesicle cycle

A novel actin-dependent step is described above which appears to mediate the transport of synaptic vesicles from the sites of endocytosis to the synaptic vesicle cluster during synaptic vesicle cycling. Studies of other vesicle trafficking systems suggest that the dynamics of such a system should be tightly regulated by actin binding proteins associated with the cargo vesicles (see Discussion). Synapsins are among the most well characterized synaptic vesicle proteins and have the ability to interact simultaneously with both G- and F-actin (see Introduction and Discussions). After the presence of an activity-dependent actin-based translocation pathway was detected, experiments were designed to investigate if synapsin was present on the translocating vesicles. The hypothetical co-localization of synapsin and actin in the translocation network would provide a novel setting for the *in vivo* interaction of these two presynaptic proteins and serve to reconcile many previous studies of synapsin function. To investigate this hypothesis, the localization of synapsin in relation to the synaptic vesicle cycle was examined under conditions consistent with the visualization of the activity-dependent actin matrix.

Synapsin antibodies (G304) affect synaptic vesicle organization

Lamprey reticulospinal axons were injected with synapsin antibodies, (G304), stimulated at 1 Hz for 12 min, maintained at rest for 1.5 hours, and then fixed for analysis by electron microscopy (Pieribone et al., 1995). Using the same preparations, serial ultrathin sections of synapses located far from the injection sites (at distances greater than 100 μm) were examined. In synapses from such axons, synaptic vesicle clusters appeared to be breaking down, with areas of axoplasm observed in the gaps between vesicles within the cluster (Figure 22). Isolated vesicles were sometimes observed closer to the center of the axon, consistent with a passive drift of synaptic

Figure 21. Stimulus-dependent disruption of synaptic vesicle cycling by myosin subfragments

Synapse between dendrites (d) and axons (a) that were microinjected with NEM-treated myosin S1 fragment and fixed after varying conditions of activity are shown here.

Panel A: This axon was microinjected with NEM-treated S1 fragment, maintained at rest for 30 min and then fixed for analysis by electron microscopy. Note the absence of vesicles and filaments in the area around the vesicle cluster. Scalebar indicates 0.1μm.

Panel B: This axon was microinjected with NEM-treated S1 fragment, stimulated at 5 Hz for 2 min and fixed for analysis by electron microscopy. Note numerous vesicles (arrow) halted outside the synaptic vesicle cluster (sv). Scalebar indicates 0.1μm.

Panels C&D: These synapses are from axons that were microinjected with NEM-treated S1 fragment, stimulated at 5 Hz for 30 min and fixed for analysis by electron microscopy.

Panel C: The synaptic vesicle cluster (sv) is drastically depleted and a group of vesicles contacting filaments are present at the lateral border of the area usually occupied by distal portion of the synaptic vesicle cluster (arrow).

Panel D: In this synapse, the synaptic vesicle cluster is less severely depleted (right) and a group of synaptic vesicles can be seen in contact with a filamentous network that coincides with a clathrin-coated pit (left).

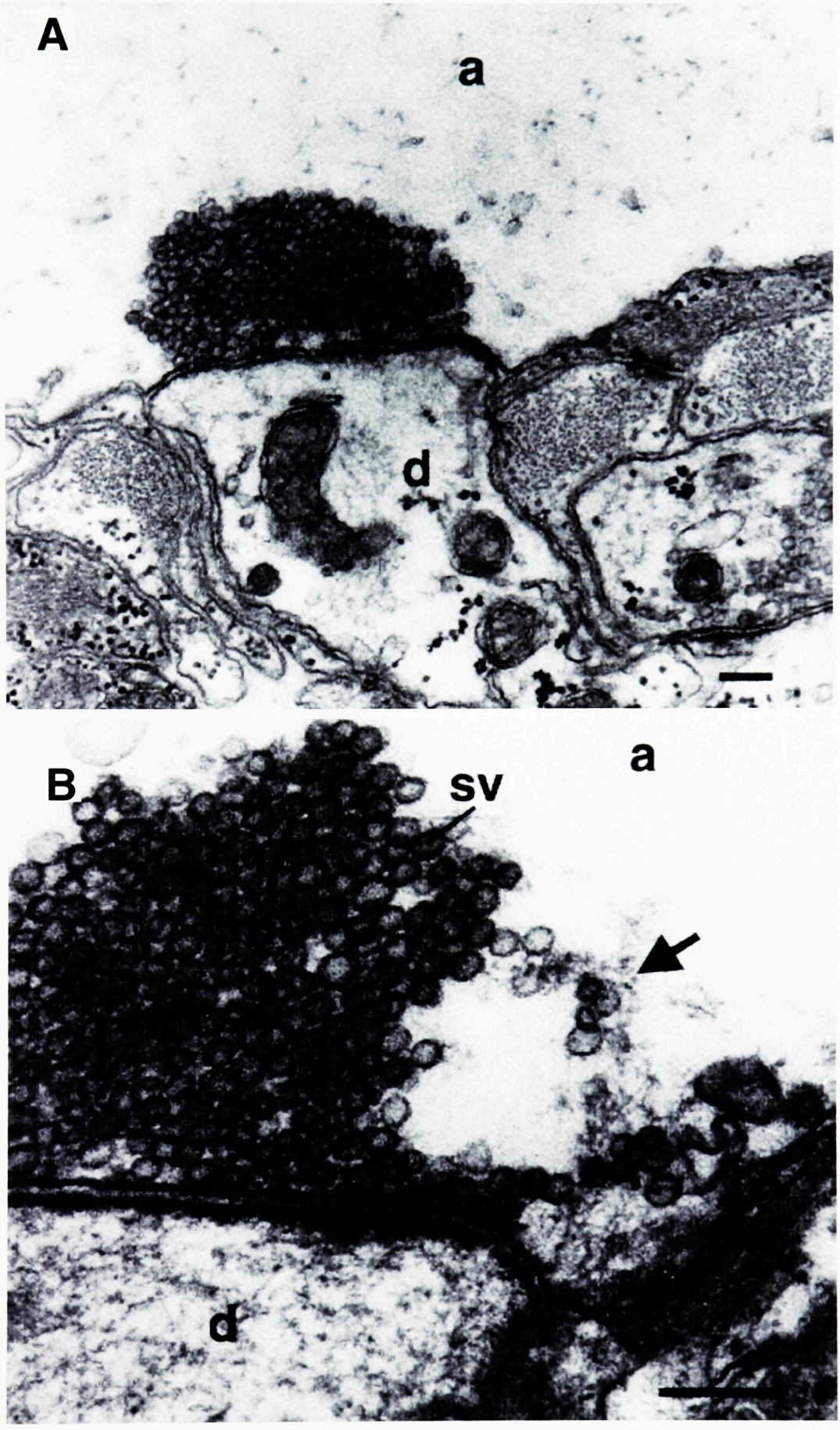
A
a
d
B
sv
a
d

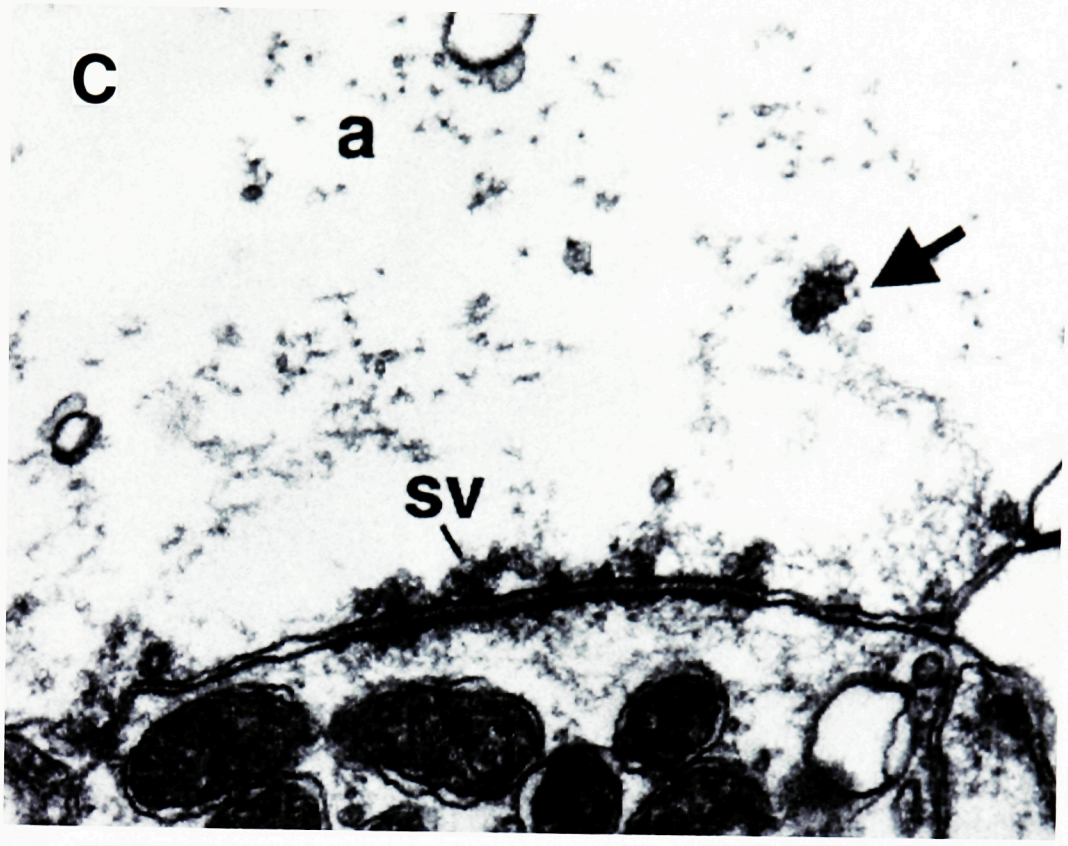
C
a
sv

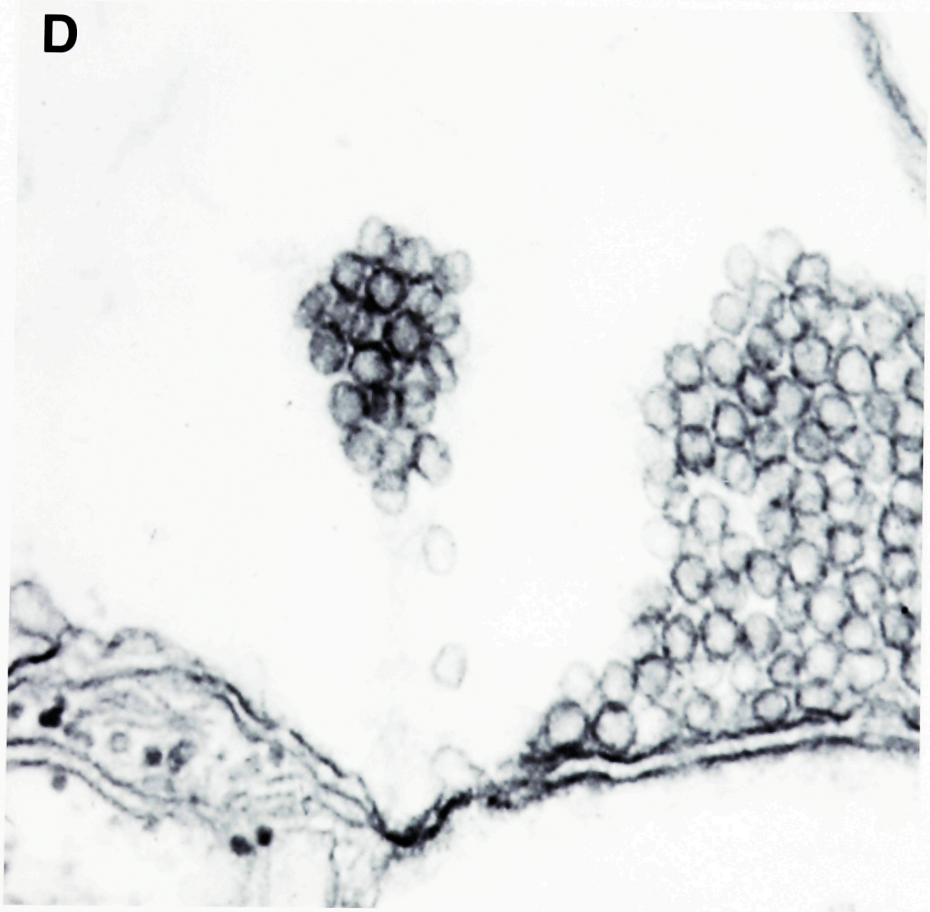
D

Figure 22. Disintegration of synaptic vesicle clusters after injection of synapsin antibodies and brief low frequency stimulation

Electron micrograph of a lamprey reticulospinal synapse from an axon injected with anti-synapsin domain E antibodies (G304), stimulated at 1 Hz for 12 minutes, maintained at rest for 1.5 hours and then fixed for analysis by electron microscopy. The cluster appears to be dissolving, and synaptic vesicles are often separated by axoplasm. Synaptic vesicles are sporadically found far from the apparent boundaries of the cluster, towards the center of the axon (top). Note the accumulation of synaptic vesicles (arrow) in the area between the presynaptic plasma membrane and the vesicle cluster.

Scale bar indicates 0.1μm.

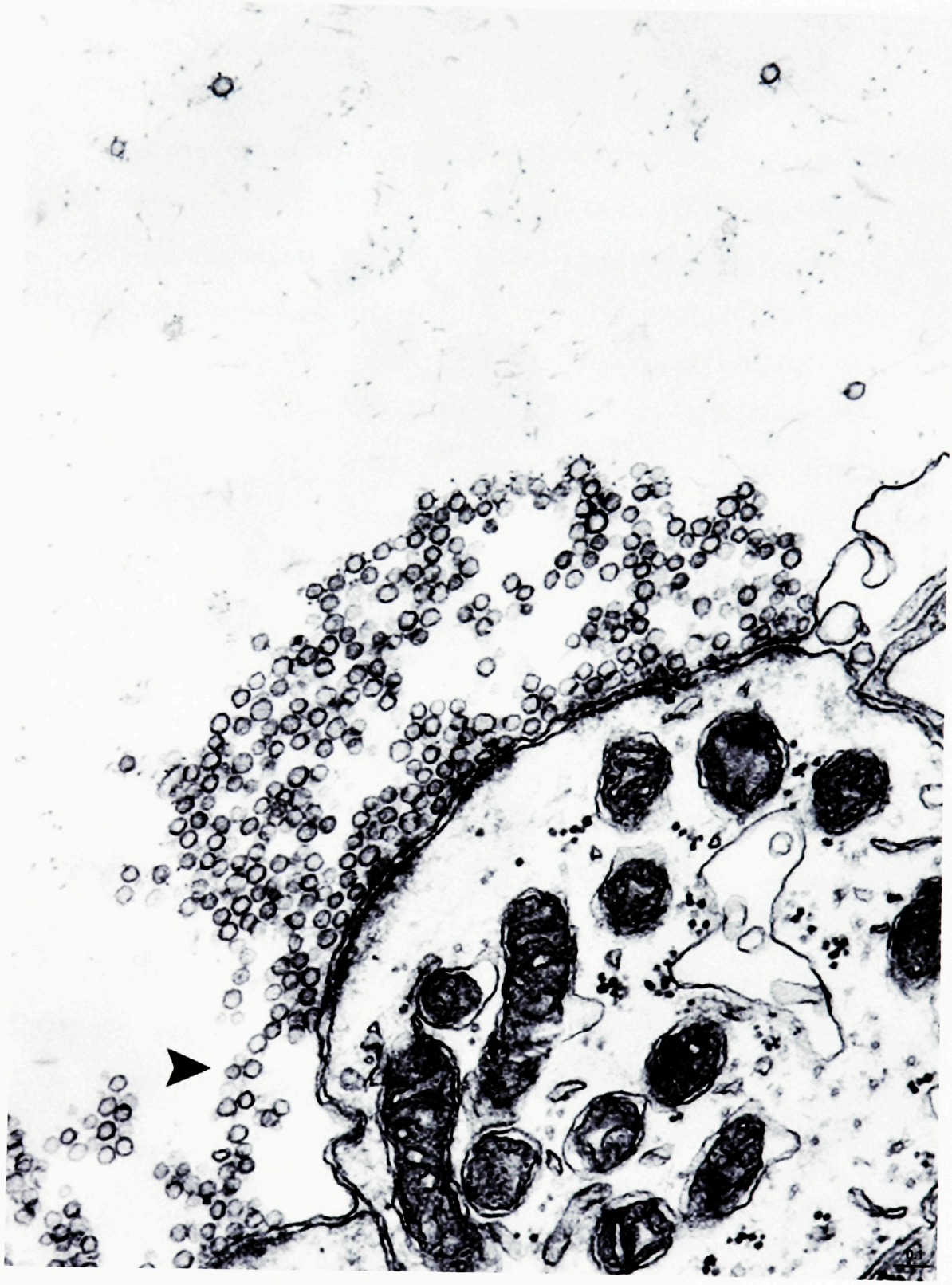

vesicles from the dispersed clusters. Strikingly, groups of synaptic vesicles were often present in the area of axoplasm directly between the synaptic vesicle cluster and the plasma membrane lateral to the active zone (arrowhead).

The localization of synapsin in the synaptic vesicle cycle

In previously published studies of synapsin localization, this protein was found primarily within the distal portion of the cluster in unstimulated lamprey reticulospinal synapses (Pieribone et al., 1995). To investigate the sub-synaptic localization of synapsin throughout the synaptic vesicle cycle, the distribution of synapsin was quantified in vesicle clusters of resting and active nerve terminals. For this localization of synapsin, antibodies were raised against the proline-rich domain D of lamprey synapsin (see Methods), which has been predicted on the basis of amino acid content to be an accessible portion of the molecule (Sudhof et al., 1989). Western blot analysis of lamprey spinal cord extracts showed that this antibody was specific for lamprey synapsin (Figure 10). Under the present experimental conditions, the antibody to domain D provided the high labeling efficiency needed to identify the sub-synaptic localization of synapsin (see Methods).

Synapsin is present on vesicles throughout the synaptic vesicle cluster

To investigate the localization of synapsin in resting and active synapses, a lamprey spinal cord was dissected into pieces of equivalent length (~2 cm), and incubated in Ringer's solution containing 4 mM Ca^{2+} (Low Ca) or 30 mM K^+ (High K^+) Ringers for 15 or 30 minutes. Spinal cord pieces were then fixed and processed for postembedding immunogold electron microscopy, as described in Methods. Under resting conditions, the synaptic vesicle cluster is concentrated discreetly at densely packed active zones and synapsin is present predominantly within the distal pool of synaptic vesicles, greater than 100 nm from the active zone (Figure 23, upper panel), confirming previous observations (Pieribone et al., 1995). After 15 minutes of tonic stimulation with 30mM K^+ Ringers solution, large clusters of synaptic vesicles were

observed that were tightly packed and a 2-fold increase in synapsin labeling less than 100 nm from the active zone was measured. Results from a representative of three experiments are shown in Figure 23, lower panel and Table III. This activity-dependent change in synapsin labeling was specific, as there was no change observed for the labeling pattern of an integral synaptic vesicle membrane protein, synaptic vesicle protein 2 (SV2; n=7 synapses, data not shown).

Table III. Activity-dependent increase in synapsin labeling in the proximal vesicle pool. Values are listed as gold particles/μm^2

Synapse Group	Distance from Active Zone (nm)	
	0-100	100-200
Resting	33 ± 3	65 ± 10
n=8 sections		
Stimulated K^+15min	60±12	70± 8
n=12 sections		

After 30 minutes of tonic stimulation, an almost complete depletion of the synaptic vesicle cluster was observed. Synapsin labeling was detected on the vesicles that remained close to the active zone, typically considered to be the readily releasable pool (Figure 24, upper and lower panels). Synapsin labeling was sporadically observed on clathrin-coated intermediates, (n=19/248 coated pits), indicating that *in vivo*, the majority of synapsin dissociates from synaptic vesicles before vesicle fusion with the active zone.

Dynamin

In an effort to confirm the specificity of the lack of synapsin labeling on clathrin-coated intermediates, the localization of dynamin was investigated. Dynamin is a GTPase known to play a role in clathrin-mediated endocytosis and antibodies to rat dynamin (DG-1) detected the lamprey ortholog isolated from lamprey spinal cord homogenates (data not shown). In preparations stimulated for 15 or 30 minutes with

High K^+(30mM) Ringer's solution, a majority of clathrin-coated intermediates were readily labeled for dynamin. The clathrin-coated pits observed under these conditions ranged in shape from shallow ("early" stage) to deeply invaginated ("late" stage) coated pits (Gad et al., 1998). As shown in Figure 25, dynamin was localized to deeply invaginated ("late") coated intermediates at sites of endocytosis. Unexpectedly, however, dynamin labeling was also associated with shallow ("early") coated pits (Figure 26).

The actin recycling matrix can be visualized in the absence of phalloidin

In order to localize synapsin in relation to the actin recycling matrix, this matrix had to be visualized under conditions compatible with immunocytochemistry. To perform this task and to address the possibility that the filamentous matrix was artificially induced by the presence of phalloidin, preparations were stimulated by an extracellular electrode at 5 Hz for 20 minutes and fixed using methods designed to enhance the preservation of actin filaments and to be compatible with immunocytochemistry (see Methods). In such preparations, stimulated axons consistently contained a filamentous matrix in the area of the axoplasm lateral to the active zone (Figure 27, 3 panels of serial sections). Small clear uncoated synaptic vesicles were commonly observed in contact with the matrix. As shown in Figure 27, the matrix typically coincided with areas of clathrin-mediated endocytosis. Based on the consistent observation of this matrix in active synapses fixed under several conditions, we conclude that the actin-based matrix is present in normal active synapses and is not an artifact produced by improper tissue processing or the presence of phalloidin.

Synapsin is associated with the perisynaptic plasma membrane during activity

Although synapsin is tightly associated with synaptic vesicles, it is not an integral transmembrane protein. Therefore, we were not surprised that synapsin did not accumulate within the expanded plasma membrane of active terminals. However, if

Figure 23. Synapsin distribution is activity-dependent in reticulospinal synapses

Upper panel: An electron micrograph of a middle section of a synapse maintained at rest. Note the majority of synapsin labeling in the portion of the cluster greater than 100 nm from the active zone. Scalebar indicates 0.1μm.

Lower panel: An electron micrograph of a middle section of a synapse stimulated tonically for 15 min. Note the increased presence of synapsin labeling less than 100 nm from the active zone. This micrograph shows a gap junction in the middle of the active zone. A clathrin-coated pit is present on the right side of the cluster and a small amount of filamentous matrix is present on both sides of the cluster, in contact with the plasma membrane. A small amount of synapsin labeling is present in the area of the filaments. Scalebar indicates 0.1μm.

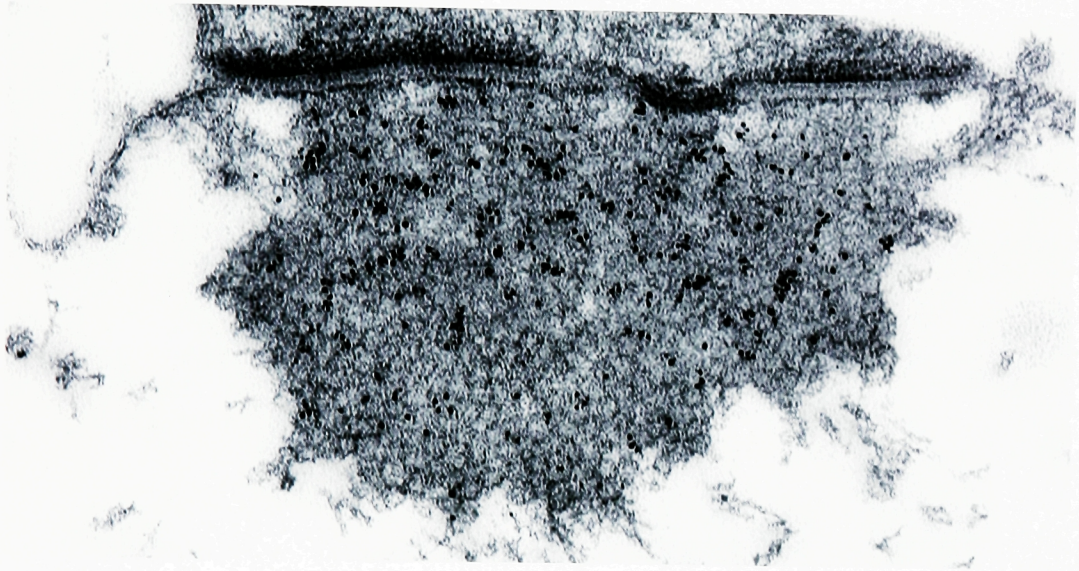

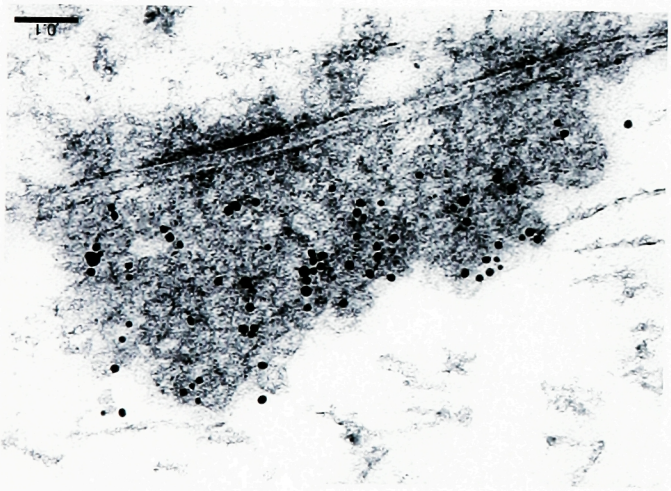
0.1

Figure 24. Synapsin is found on the pool of synaptic vesicles proximal to the active zone

Electron micrographs of two synapses stimulated tonically for 30 minutes in High K^+ (30mM) Ringer's solution.

Upper panel: The number of synaptic vesicles clustered at the active zone decreased dramatically (box) with prolonged tonic stimulation and the plasma membrane lateral to the active zone was greatly expanded. The vesicles present in close apposition to the active zone were labeled for synapsin (box). Many clathrin-coated intermediates were present in the expanded region (arrowheads). Scalebar indicates 0.1 μm.

Lower panel: A micrograph of another tonically stimulated synapse shows the labeling of the scarce synaptic vesicles (sv) close to the active zone (darker electron dense material), but not clathrin-coated intermediates (cp). The presence of coated intermediates so close to the active zone is sometimes observed in such drastically stimulated synapses.

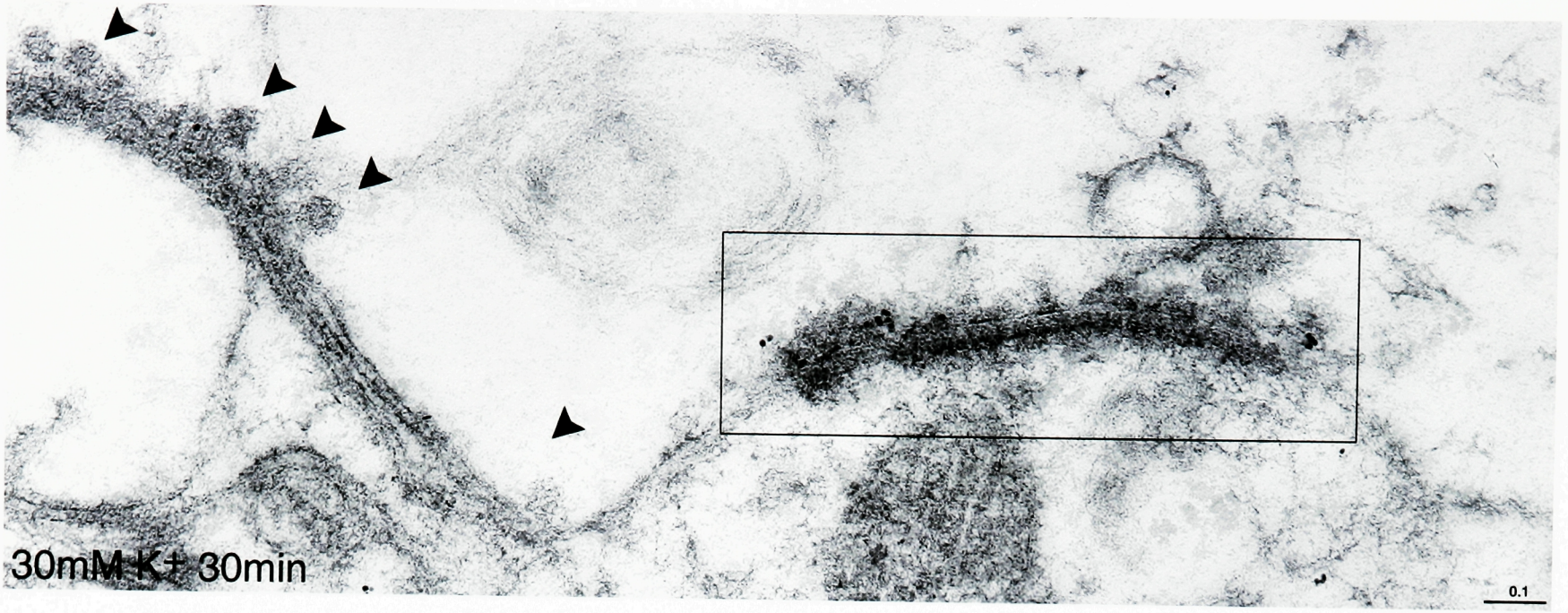
30mM K+ 30min
0.1

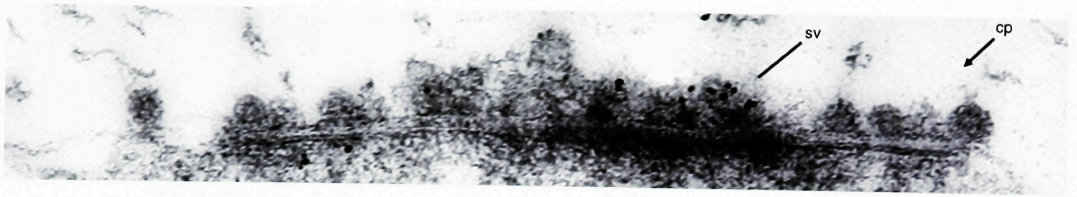
sv
cp

Figure 25. Dynamin is localized to deeply invaginated clathrin-coated pits

Portions of three synapses of lamprey reticulospinal axons stimulated tonically with high K^+ (30mM) Ringer's solution are shown here. As expected, deeply invaginated clathrin-coated intermediates were labeled by anti-dynamin antibodies (DG-1). This suggests that the absence of labeling of clathrin-coated intermediates by synapsin antibodies was specific and did not represent an inaccessibility of these structures to labeling using the post-embedding immunogold method.

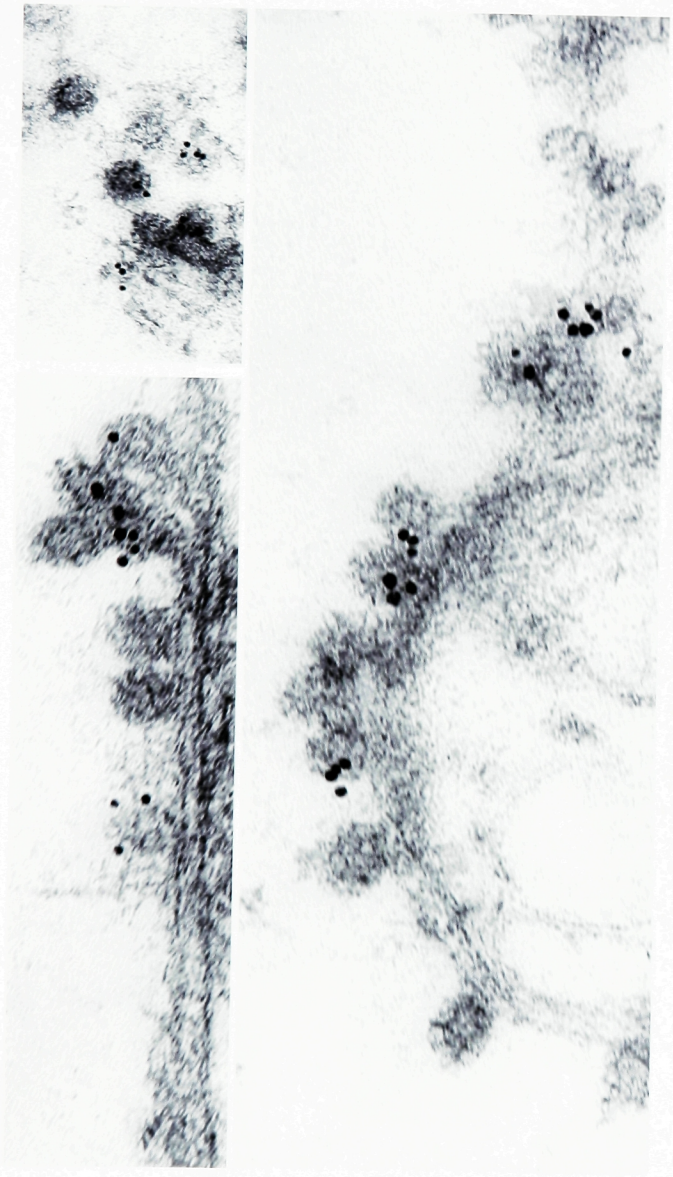

Figure 26. Dynamin is localized to shallow clathrin-coated pits

This material is taken from the same preparation shown in Figure 25.

Three electron micrographs are presented from a grid containing 17 serial sections that contained a high proportion of shallow clathrin-coated intermediates. Surprisingly, these shallow intermediates were labeled consistently by the dynamin antibody, indicating that dynamin is present at early, as well as late stages of clathrin-mediated endocytosis. Scale bar indicates 0.2 μm.

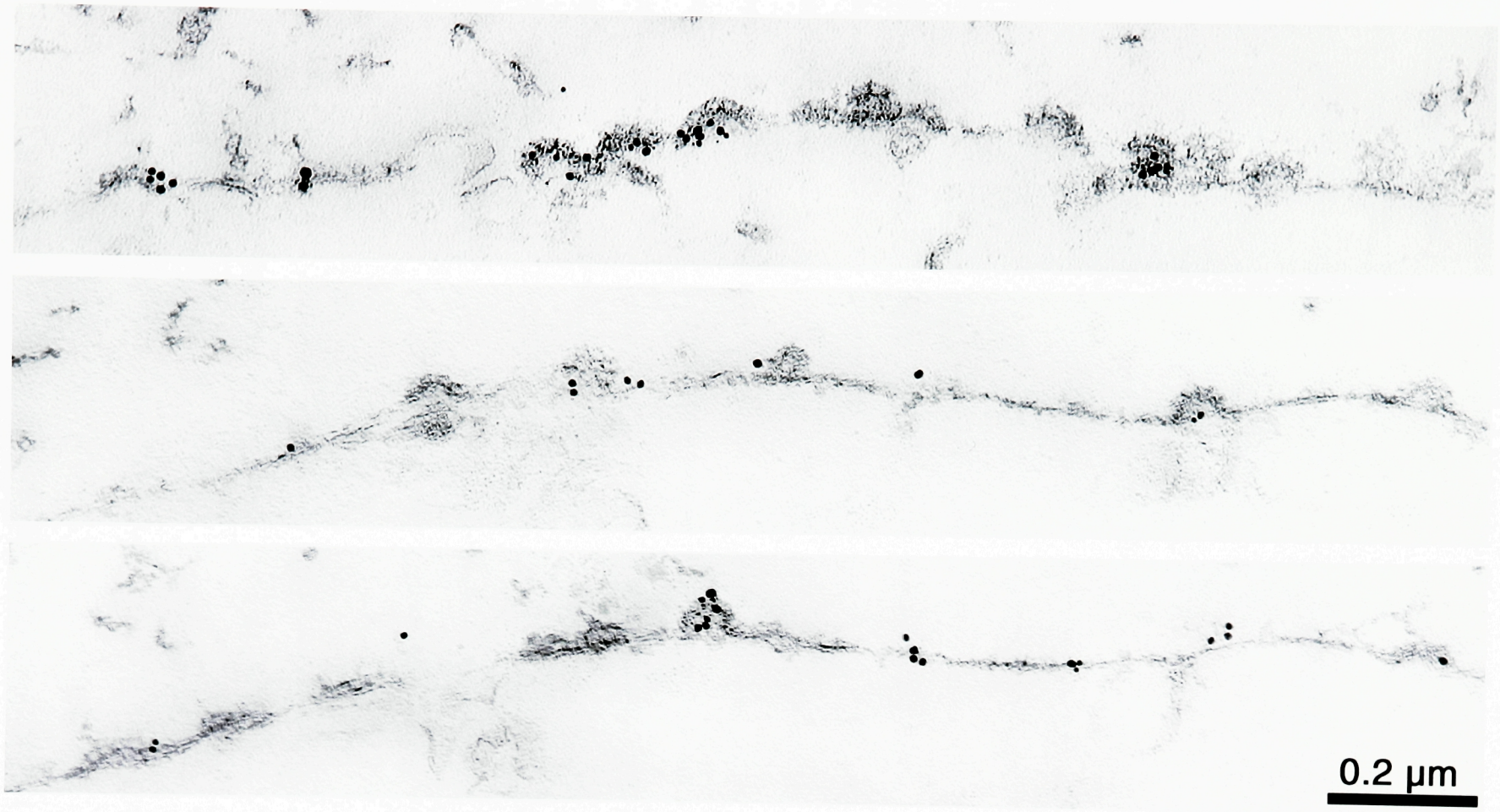
0.2 µm

synapsin is present on synaptic vesicles close to the active zone, but not on the membrane incorporated from synaptic vesicles, then it must dissociate from synaptic vesicles prior to or during fusion. In synapses stimulated at 5 Hz for 30 minutes, non-vesicular synapsin labeling was often present immediately adjacent to the plasma membrane, less than 1μm from the active zone, where clathrin-mediated recycling of synaptic vesicles and the actin matrix are observed (Figure 27, n=12/19 micrographs).

To localize synapsin in relation to the actin-based transport matrix described above, the stimulation paradigm used to discover the actin-based movement of post-endocytic synaptic vesicles (5 Hz for 20 minutes) was used in combination with postembedding immunoelectron microscopy methods. Lamprey giant axons were either uninjected or injected with rhodamine-phalloidin and stimulated at 5 Hz for 20 minutes. As expected with this stimulation protocol, large synaptic vesicle clusters were observed in both the presence and absence of phalloidin (Figures 29 and 30, respectively). Indicative of synaptic activity, we observed occasional clathrin-coated structures of varying shapes in the plasma membrane lateral to active zones. Synapsin labeling was observed on post-endocytic vesicles enmeshed in the actin-containing post-endocytic transport system, in both the presence and absence of phalloidin (n=35 sections). Synapses were examined on serial sections, allowing for the distinction between vesicles within the borders of the cluster and those associated with the filamentous matrix located in the area of the plasma membrane lateral to the vesicle cluster.

As mentioned above, previous studies have shown that synapsin is able to bind directly to purified F-actin and induce the formation of networks of filaments (Greengard et al., 1994). Since synapsin was present on vesicles enmeshed in the actin-containing filamentous matrix used for the transport of post-endocytic vesicles, we wondered if the ability of synapsin to interact with F-actin might be relevant to the regulation of the cytoskeletal

Figure 27. The actin matrix is visualized in the absence of phalloidin

On the following three pages, twelve serial sections are displayed from a synapse between a dendrite (d) and an axon (a) that was stimulated at 5 Hz for 20 minutes and embedded in LR Gold according to the protocol described in Methods.

The first page (panels 1-4), shows approximately the middle section of the synapse, indicated by the large active zone and vesicle cluster (sv). The second (panels 5-8) and the third pages (panels 9-12) show almost the entire half of the synapse. Clathrin-mediated endocytosis is occurring lateral to the cluster and clathrin-coated pits of varying morphology can be seen (arrowhead). The actin matrix is shown in the same area where endocytosis is occurring on both sides of the vesicle cluster (arrows on the top section of each page), in the area corresponding to the glial cell apposition. The matrix becomes more prominent with increasing distance from the middle section. Sections were photographed at 17,000x.

1-4

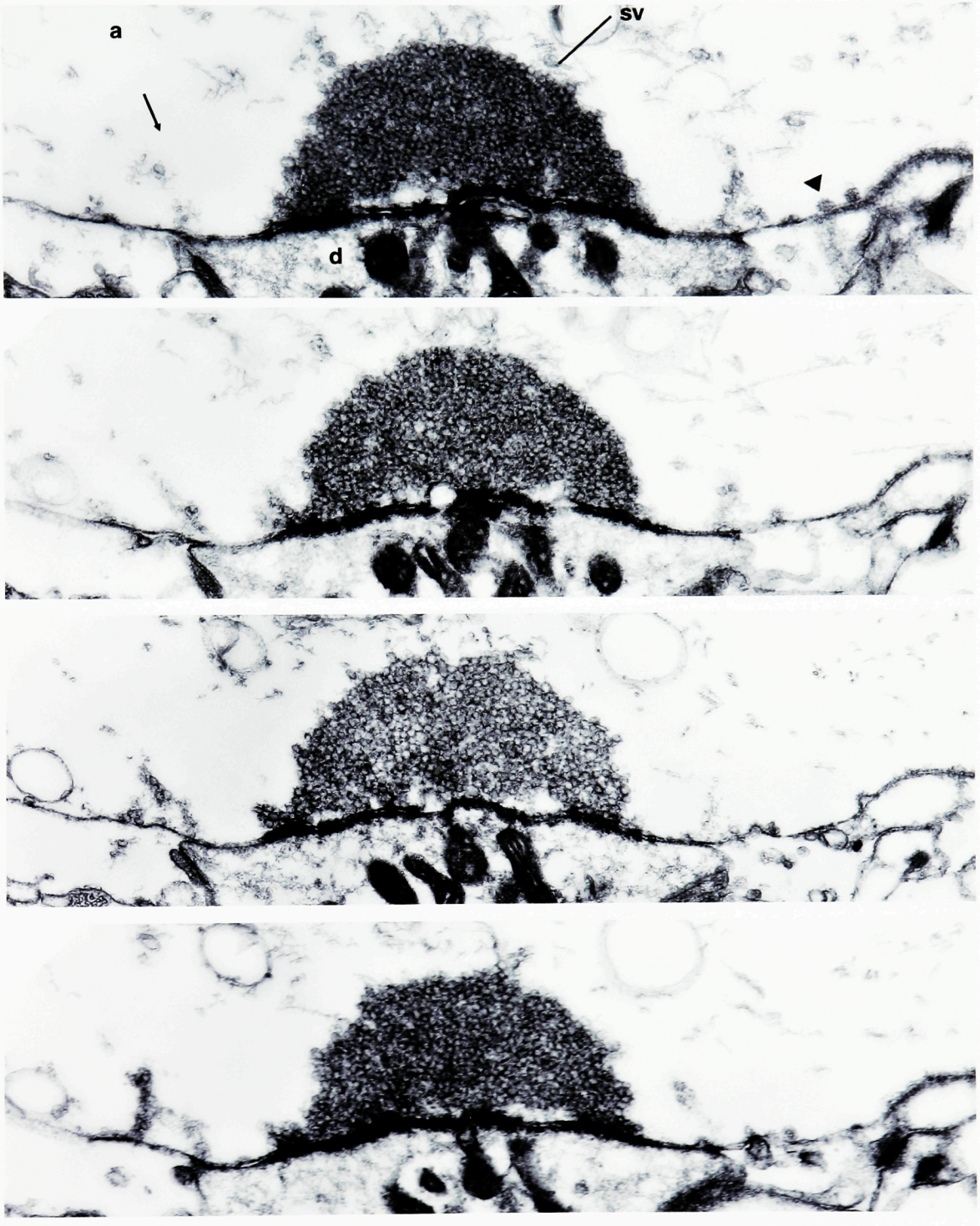

5-8

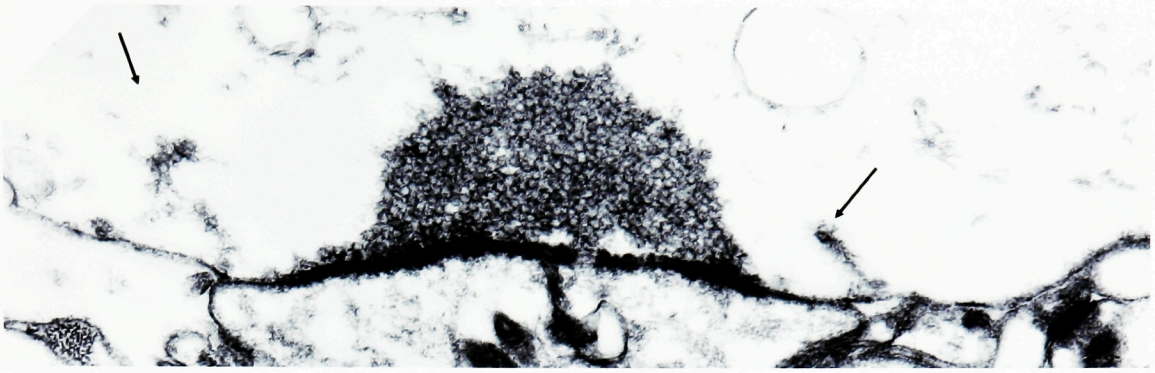

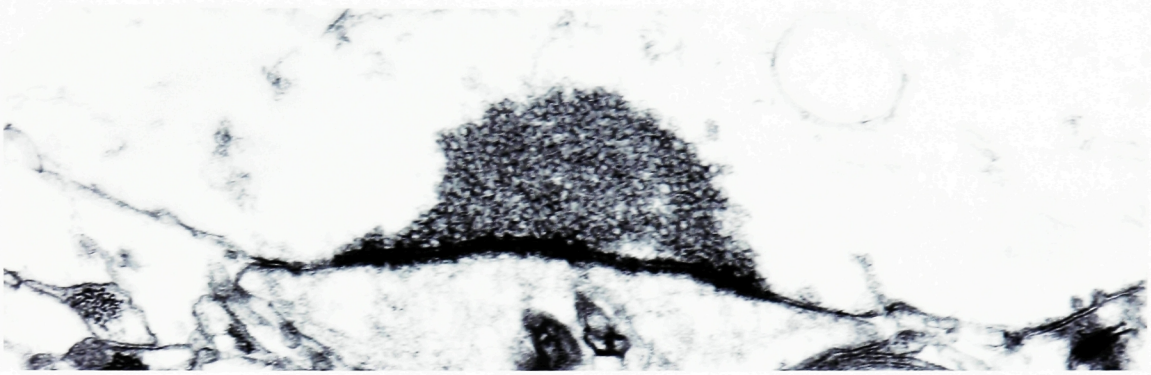

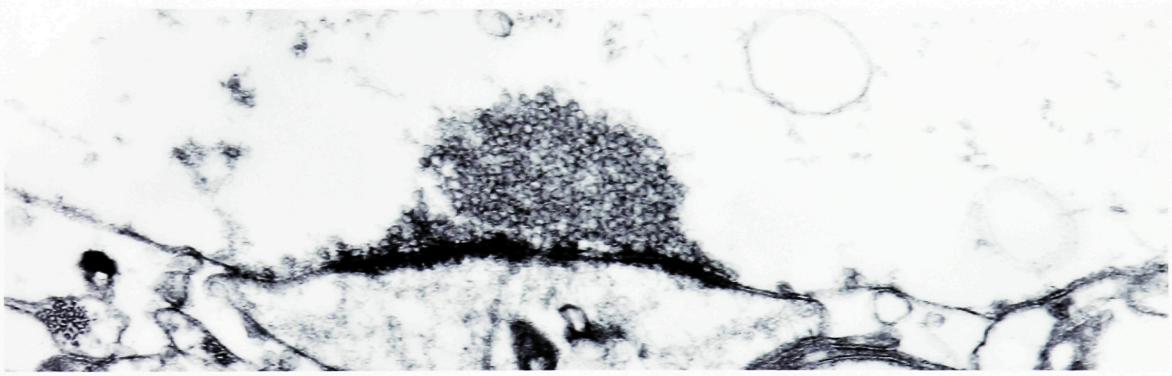

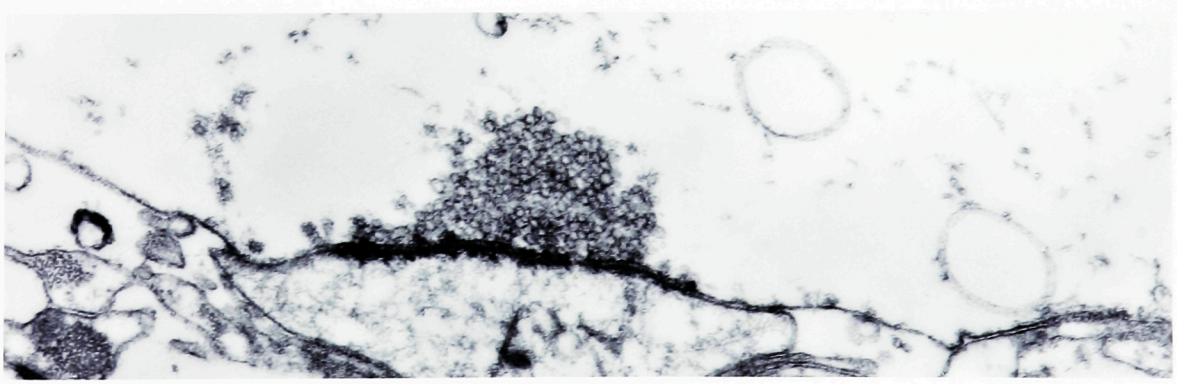

9-12

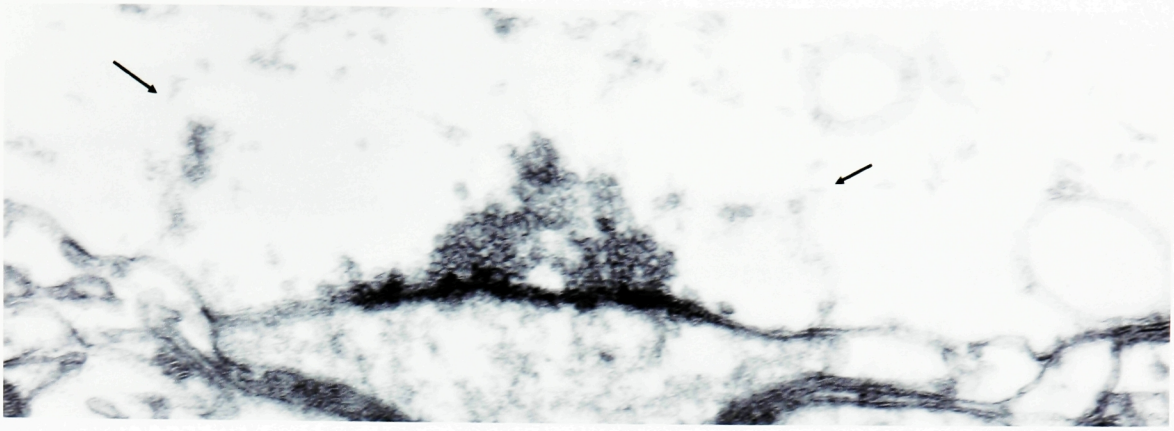

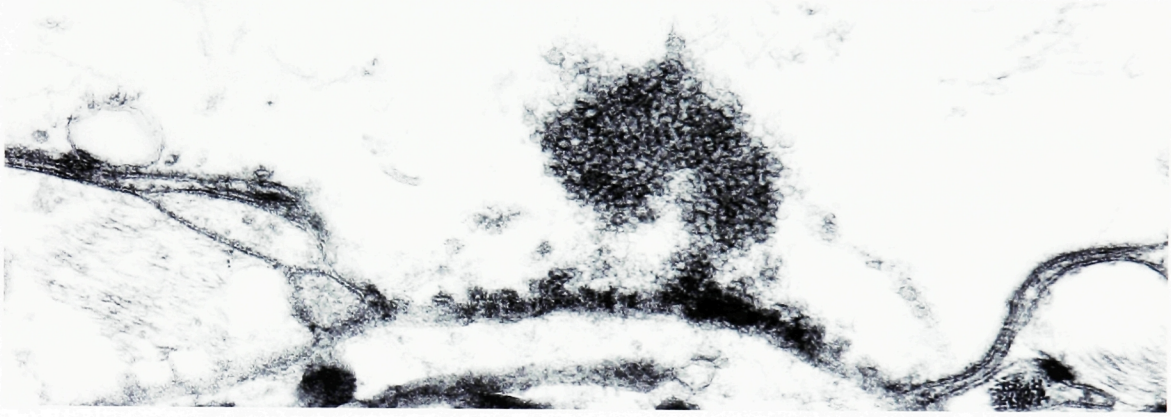

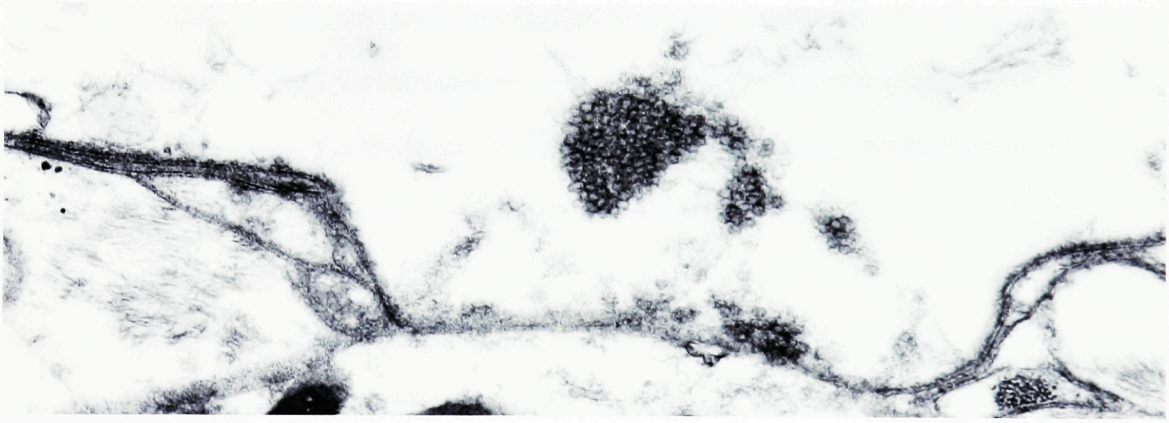

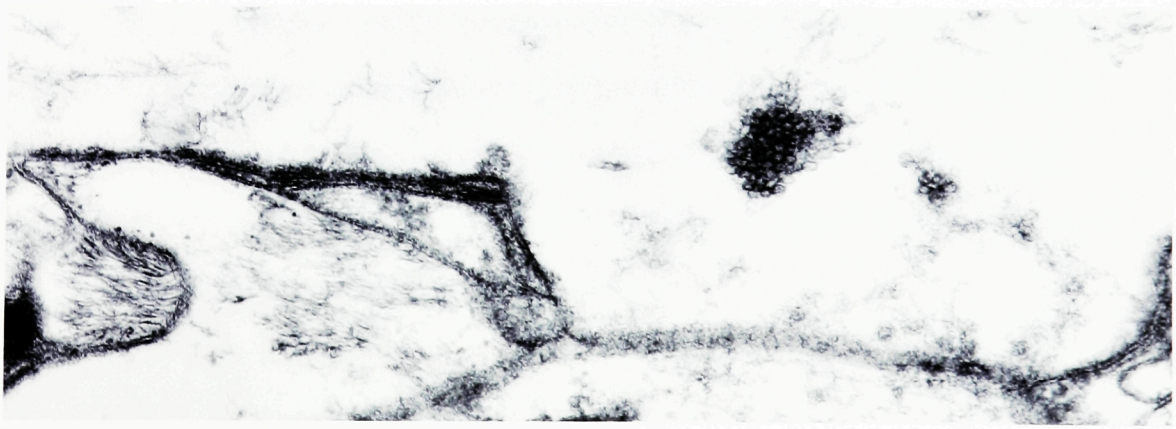

presence of synapsin on the filamentous matrix was investigated. As shown in Figures 32 and 33 respectively, synapsin labeling was consistently observed within the filamentous matrix itself, in both the presence and absence of phalloidin. This supports the hypothesis that the transportation of post-endocytic synaptic vesicles may be a relevant physiological setting for the well-established biochemical interactions of synapsin and F-actin.

To better understand the distribution and association of the various components of the presynaptic architecture that were labeled for synapsin, a three-dimensional reconstruction was made from ten serial ultrathin sections of a synapse in an uninjected axon that had been stimulated at 5 Hz for 20 minutes (see Experimental Procedures). Figure 34 shows one of the ten sections used for the reconstruction and displays labeling for synapsin on vesicles in the cluster as well as the actin matrix. Figure 35 shows a reconstruction of ten serial sections and elements of the synapse are represented as follows:synaptic vesicles (red), synapsin (blue), filamentous material (yellow), clathrin-coated intermediates (bright blue) and plasma membrane (green). The synaptic vesicles labeled for synapsin in contact with filaments were clearly distinct from those within the vesicle cluster. In agreement with the other reconstruction shown in this thesis, the filaments were localized to the endocytic zones and together formed a halo, or ring, around this portion of the vesicle cluster. While the entire synapse was not contained on the sections collected, ten sections that are each 90 nm thick are roughly equivalent approximately to one-half of a synaptic vesicle cluster of average size. Thus, the three-dimensional reconstruction of a stimulated synapse establishes that synapsin is localized on several distinct elements of the actin-containing filamentous transport system used for the essential local recycling of synaptic vesicles: synaptic vesicles, the filamentous matrix, and the plasma membrane lateral to the active zone to which the filament network is physically connected.

In the experiments described above, it was shown that the actin-based transport of post-endocytic synaptic vesicles participates in maintaining the vesicle cluster during synaptic activity. Furthermore, the localization of synapsin on synaptic vesicles within this recycling pathway has been visualized. Therefore, a new hypothesis can now be proposed: the simultaneous association of synapsin, synaptic vesicles, and actin in the translocation network outside of the synaptic vesicle cluster may contribute directly to synapsin's critical role in sustaining the necessary supply of synaptic vesicles during nerve terminal activity.

Figure 28. Synapsin is present on plasma membrane lateral to the active zone

This electron micrograph shows a synapse from an uninjected axon stimulated at 5 Hz for 20 minutes. Note the presence of synapsin labeling along the plasma membrane lateral to the vesicle cluster (arrowhead). This may coincide with the nucleation of the actin matrix. Scalebar indicates 0.2 μm. Two mitochondria (dark, round) are embedded within the vesicle cluster close to the active zone.

0.2

Figure 29. Synapsin is present on a mixture of post-endocytic vesicles and on the actin-containing matrix in stimulated axons injected with rhodamine-phalloidin

This axon was microinjected with rhodamine-phalloidin, stimulated at 5 Hz for 20 minutes and fixed for analysis by electron microscopy. These are two serial micrographs of a synapse. Note the labeling of vesicles within the vesicle cluster (arrow) as well as outside of the vesicle cluster. The location of actin filaments with vesicles coincides with areas of clathrin-mediated endocytosis and the sites of glial cell apposition. Scalebar indicates 0.1μm.

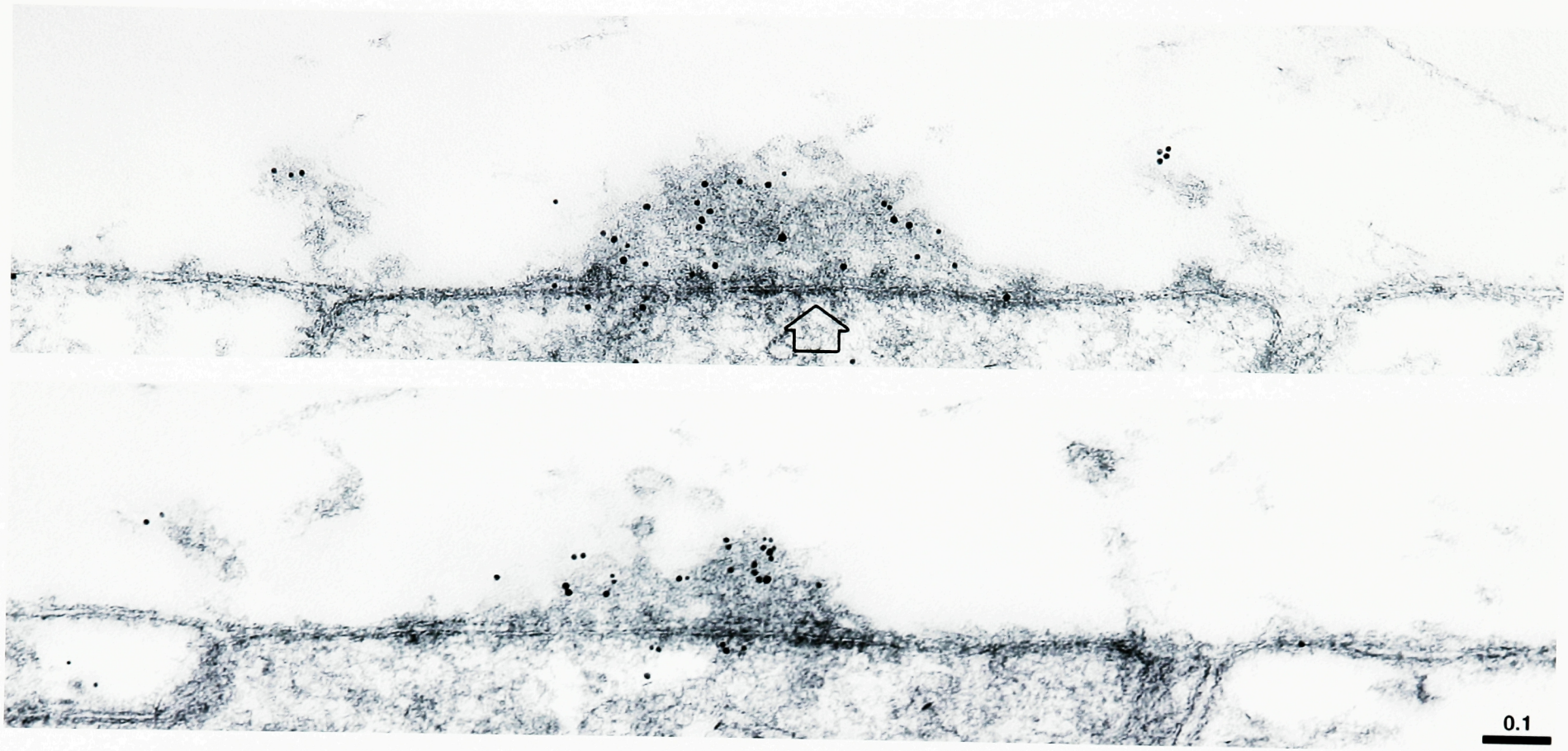
0.1

Figure 30. Synapsin is present on mixture of post-endocytic vesicles and the actin-containing matrix in uninjected, stimulated axons

Electron micrographs of two adjacent sections of a synapse from an axon that was not injected with rhodamine-phalloidin but stimulated at 5 Hz for 20 minutes and fixed for analysis by electron microscopy (from the same preparation as shown in Figure 27). The presence of synapsin is demonstrated on synaptic vesicles within the cluster as well as outside of it, in contact with actin filaments lateral to the active zone. Scalebar indicates 0.1μm.

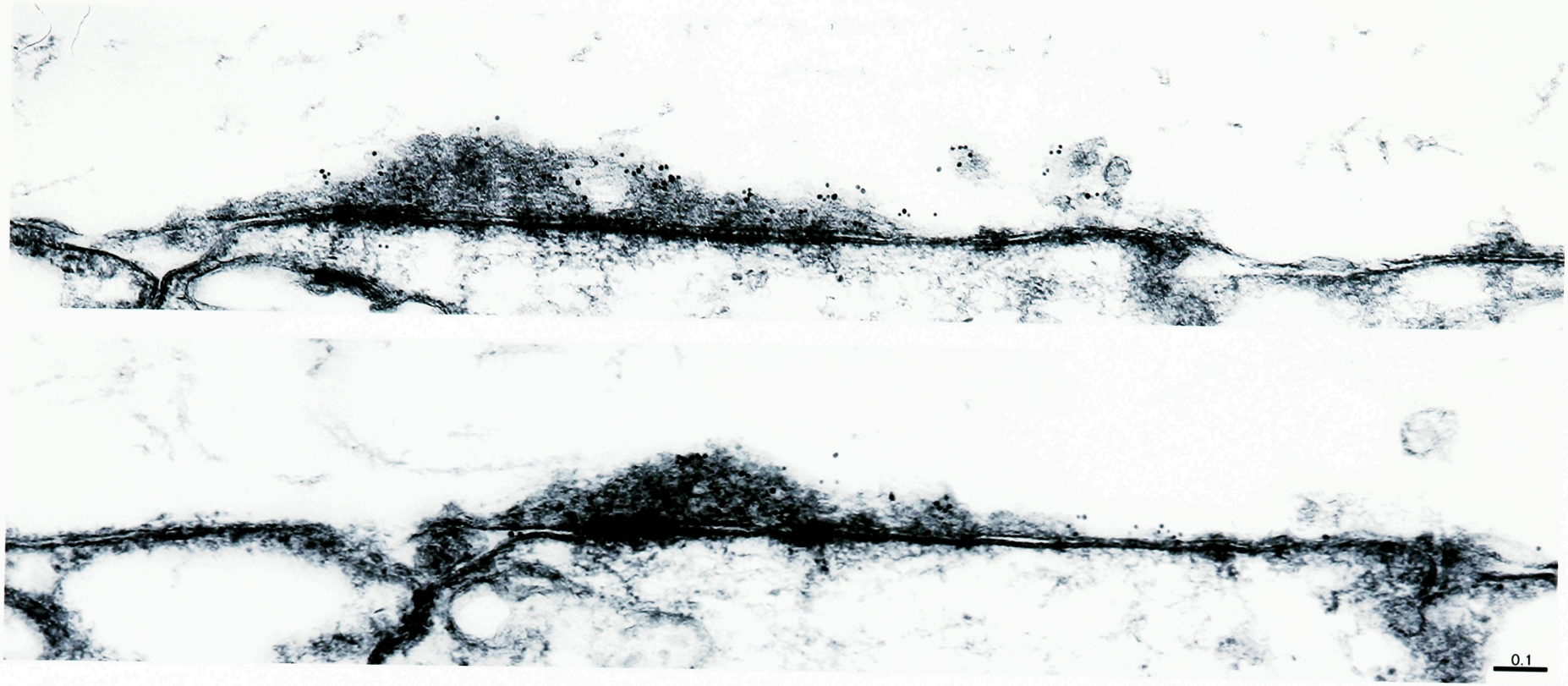
0.1

Figure 31. A second example illustrating the presence of synapsin on the mixture of post-endocytic vesicles and actin-containing matrix in uninjected, stimulated axons

Electron micrographs of two adjacent sections of an additional synapse from an uninjected, stimulated axon showing a filamentous matrix lateral to the active zone. Upper panel: Note the presence of synapsin on synaptic vesicles in contact with the actin filament matrix lateral to the active zone. Lower panel: Note the presence of clathrin-coated intermediates in the area corresponding to filamentous region of the upper panel. Scalebar indicates 0.1μm.

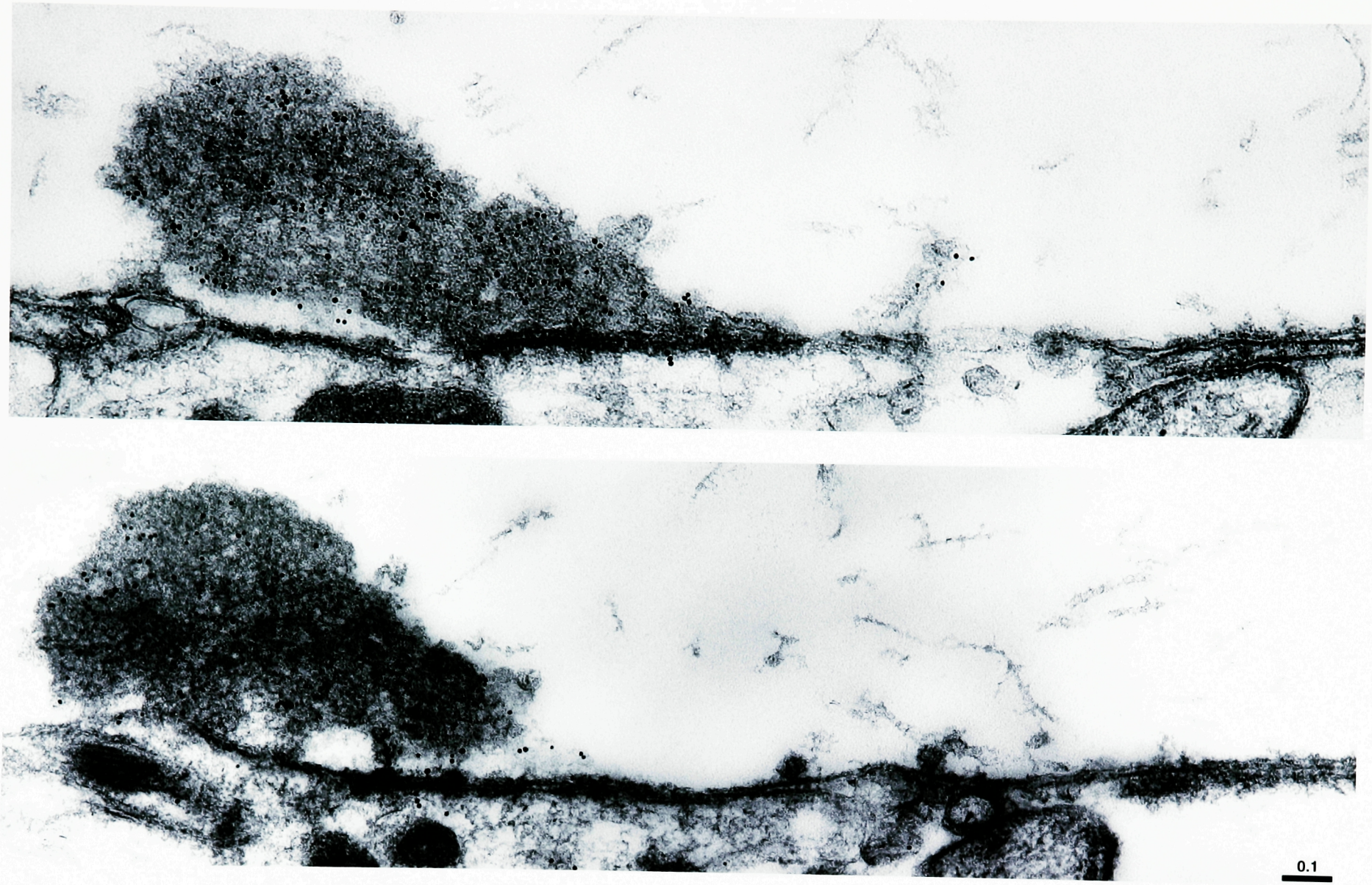
0.1

Figure 32. Synapsin is associated with the actin-containing matrix lateral to the active zone

These are electron micrographs of two nearby sections of a synapse between a dendrite (d) and an axon (a) that was injected with rhodamine-phalloidin, stimulated extracellularly at 5 Hz for 20 minutes, and fixed for analysis by electron microscopy.

Panel A: Synapsin labeling is present on actin filaments lateral to the active zone. Clathrin-coated endocytic intermediates in the region are not labeled while uncoated vesicles in the axoplasm are labeled for synapsin.

Panel B: Note the position of the vesicle cluster (sv) at the active zone (arrow) relative to the actin filaments (af) at the lateral edges of the synapse.

Scalebar indicates 0.1μm.

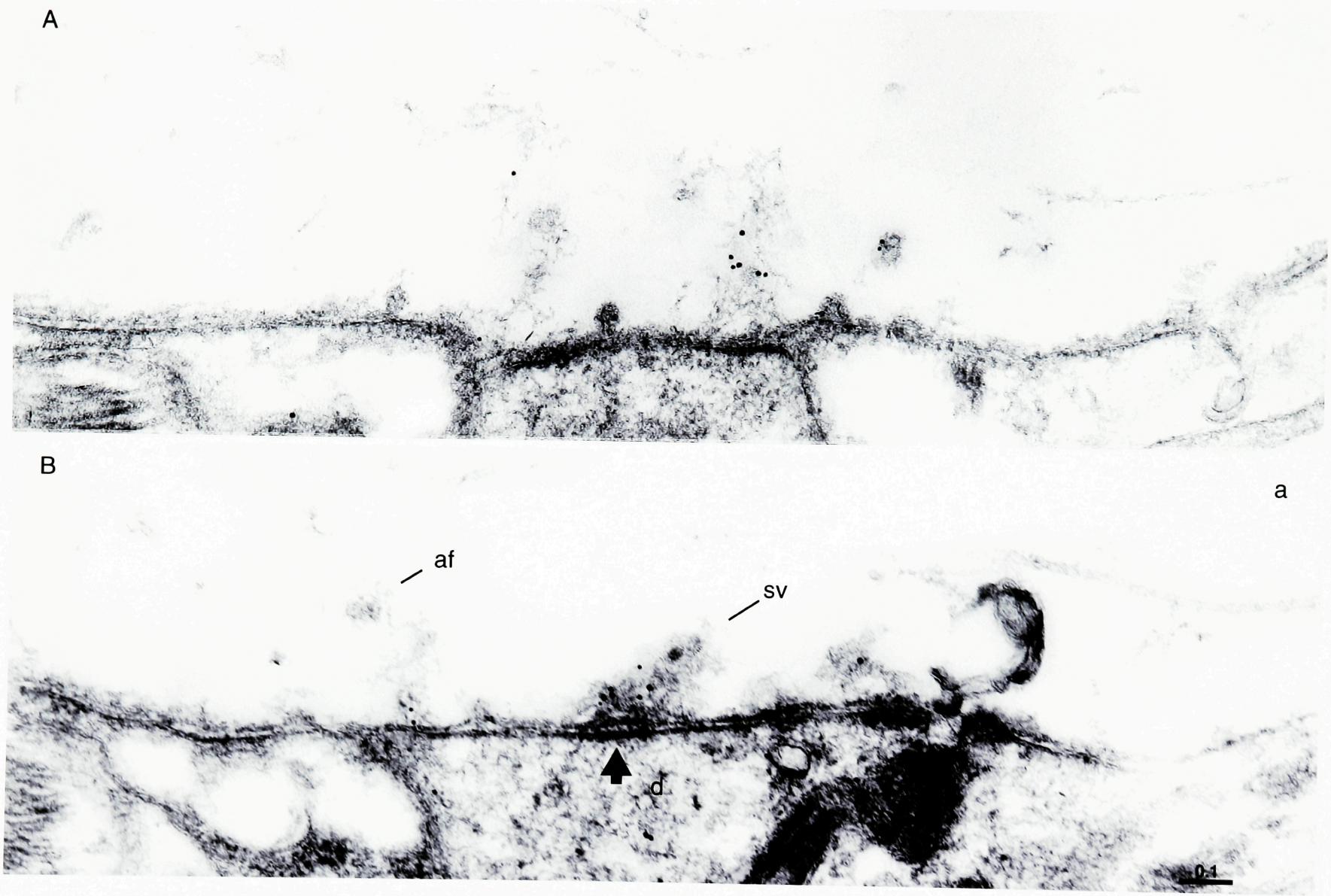
A
B
a
af
sv
d
0.1

Figure 33. Three serial sections show labeling of synapsin on the filamentous actin network

These are electron micrographs of three serial sections (A-C) of a synapse from an uninjected axon (a) that was stimulated at 5 Hz for 20 minutes and then fixed for analysis by electron microscopy. Clustered synaptic vesicles (cl) are present in the middle of each section as well as a network of actin filaments (af) lateral to the synaptic vesicle cluster are robustly labeled for synapsin. Scale bar indicates 0.1μm.

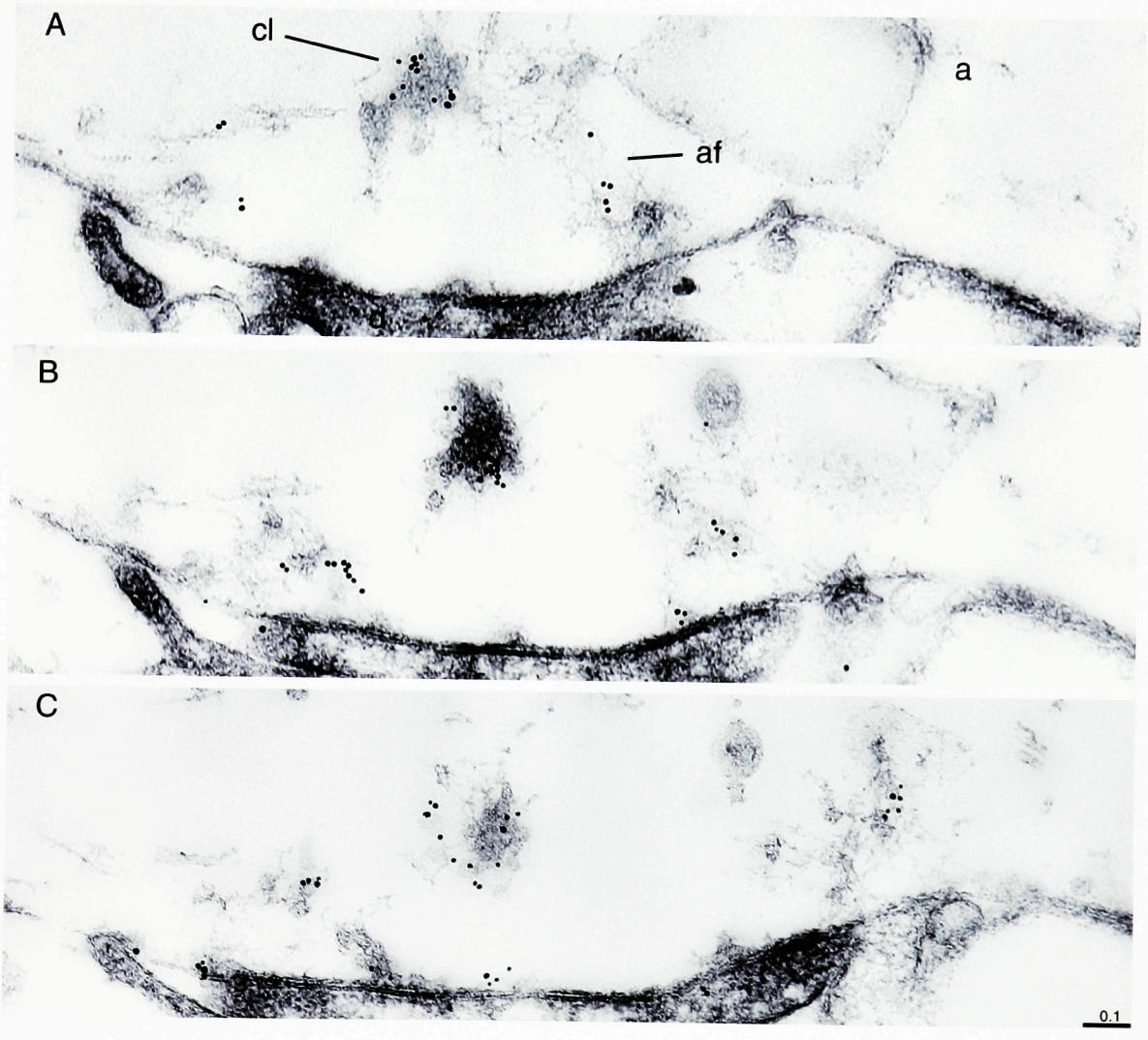
A
cl
a
af
B
C
0.1

Figure 34. Synapsin is present on vesicles within the cluster and within the actin matrix

This is an electron micrograph of a section from the synapse reconstructed in Figure 35, showing synapsin labeling of vesicles within the cluster as well as synaptic vesicles in contact with actin filaments. Scale bar indicates 0.1μm.

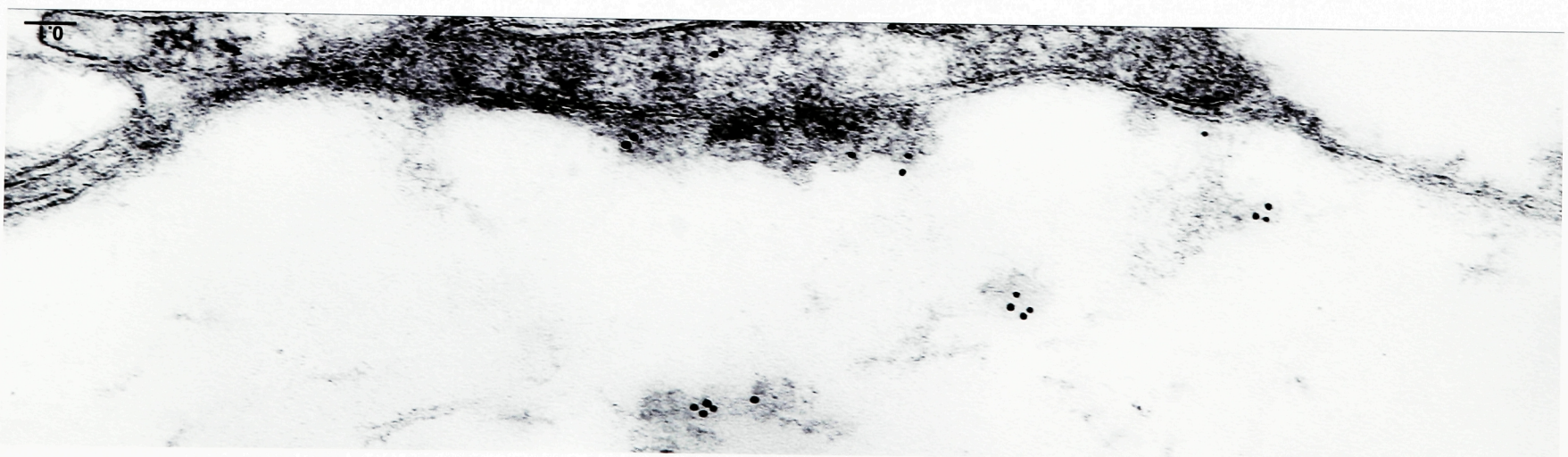
0

Figure 35. Three-dimensional Reconstruction of a Stimulated Reticulospinal Synapse Labeled for Synapsin

Approximately half of a synapse was captured on serial sections and labeled for synapsin. As in the previous reconstruction, sections were photographed, relevant features were traced on transparencies, and fed into a MacIntosh G4 computer using a Wacom digitizing tablet. The synapse was reconstructed using FormZ software.

The actin filaments lateral to the vesicle cluster are shown in yellow. The plasma membrane is shown in green. All synaptic vesicles (50 nm) are shown in red. Synapsin labeling by the colloidal gold method is represented here as small blue spheres. Clathrin-coated endocytic intermediates are shown as flat blue discs on the plasma membrane. In addition to its localization on clustered synaptic vesicles, note the presence of synapsin on three distinct elements of the vesicle transport system: the plasma membrane, the actin filaments, and the vesicles within the actin filaments.

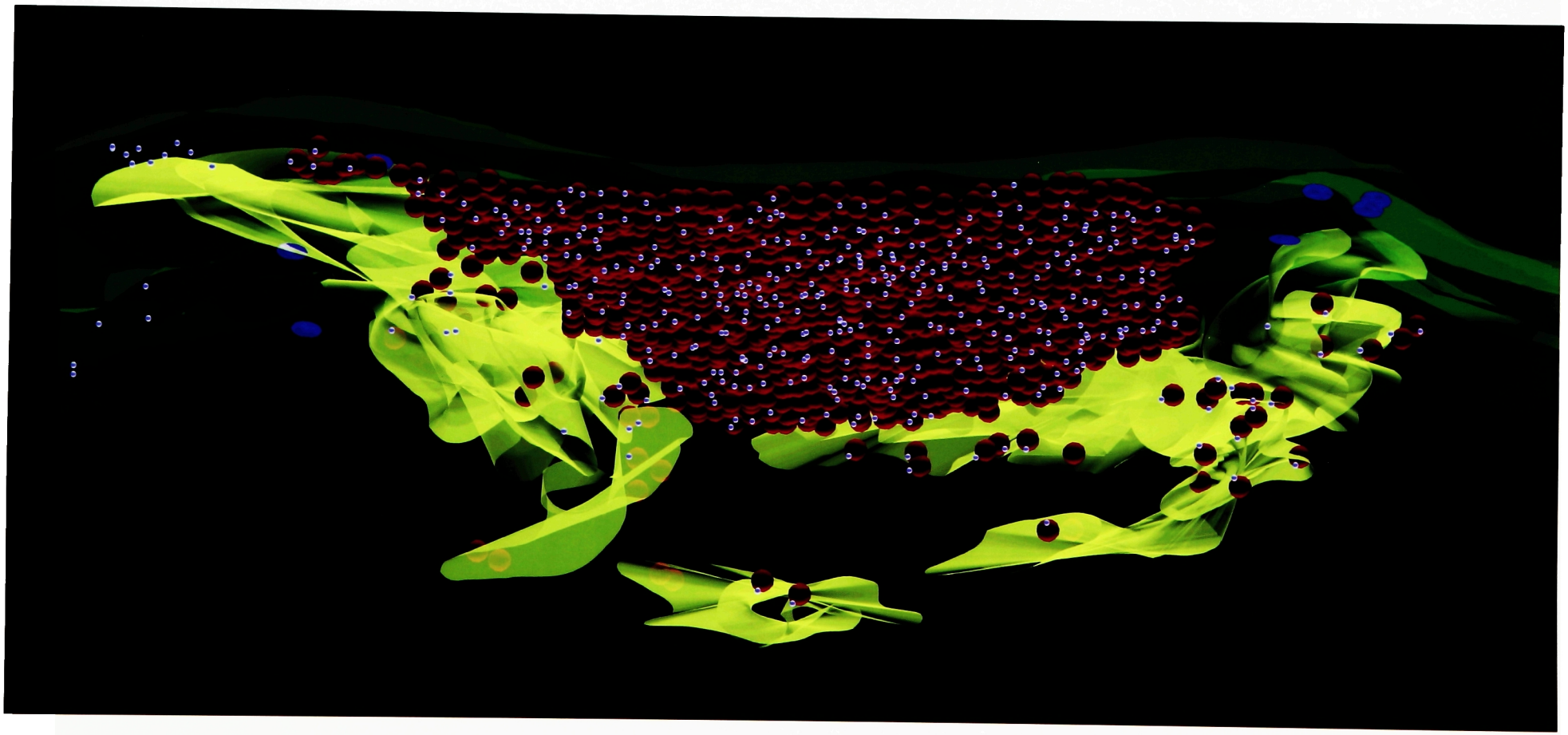

IV. DISCUSSION

Based on its *in vitro* interactions with actin and synaptic vesicles, synapsin has been proposed to serve as a cross-linker of synaptic vesicles to an actin cytoskeleton beneath the vesicle cluster (reviewed in (De Camilli and Greengard, 1986). As described in the Introduction, several *in vitro and in vivo* studies have supported this hypothesis.

An actin-based mechanism is implicated in the transport of synaptic vesicles

In addition to the classic ultrastructural studies of the frog NMJ reviewed in the Introduction, more recent studies have demonstrated that clathrin-mediated endocytosis around active zones is an essential step of the synaptic vesicle cycle in a variety of nerve terminals (Gonzales-Gaitan and Jackle, 1997; Nonet et al., 1999; Ringstad et al., 1999; Ryan et al., 1993; Ryan et al., 1996b; Shupliakov et al., 1997; Turner et al., 1999). It is evident from all of these studies that synaptic vesicles which have been recycled by endocytosis return quickly (on the order of one minute) to the synaptic vesicle cluster. By necessity, the route of newly recycled synaptic vesicles should span the sites of clathrin-mediated endocytosis and the synaptic vesicle cluster. However, neither the pathway nor the mechanism of this movement has been defined.

Presently, an actin-based pathway has been visualized between endocytic zones and synaptic vesicle clusters and implicated in the movement of recycling synaptic vesicles. The visualization of this pathway was greatly facilitated by the unique features of the reticulospinal axon. The large size of the axon permitted microinjection of concentrated actin-disrupting compounds, and the discrete organization of synapses made it possible to monitor vesicle traffic around individual synaptic vesicle clusters.

The actin-based local transport pathway was observed after microinjection with two actin filament-binding compounds, phalloidin and NEM-S1, under conditions when synaptic vesicle cycling was perturbed but not completely blocked (see also

Methods). Based on the ultrastructural analysis, the pathway appeared to traverse the region of the axoplasm between the periactive zone of the presynaptic membrane, where clathrin-mediated endocytosis occurs, and the synaptic vesicle cluster. Since lamprey reticulospinal synaptic vesicle clusters are characteristically shaped like a dome, the actin network appeared at the light microscope level as a ring or horseshoe-like structure surrounding the vesicle cluster. By electron microscopy, synaptic vesicles were detected within these ring-like structures of actin. Pathways preferential to the distal or proximal portions of the cluster could not be detected by this method and are not expected, based on previous studies that indicated a random mixing of HRP-labeled vesicles (reviewed in (Ceccarelli and Hurlbut, 1980b). Endosomes were not observed along the course of this pathway, consistent with the single-step budding model of synaptic vesicle recycling (Murthy and Stevens, 1998; Takei et al., 1996).

The massive depletion of synaptic vesicles from active synapses in the presence of NEM-S1 indicates that the actin-mediated pathway is the dominant route for synaptic vesicle recycling in the reticulospinal synapse. The existence of additional pathways via transient fusion cannot, however, be ruled out entirely, as highlighted by Ceccarelli and colleagues (reviewed in (Ceccarelli and Hurlbut, 1980b; Heuser, 1989). For instance, it is possible that a synaptic vesicle may cycle once or twice by an alternate route (Ceccarelli et al., 1973; Fesce, 1999; Klingauf et al., 1998) before entering the actin-dependent translocation pathway.

Historical evidence for a dynamic actin matrix used in synaptic vesicle recycling

During the past fifty years of ultrastructural investigations of the synapse, several studies have commented upon the presence and purpose of filamentous material in association with synaptic vesicles or coated intermediates in presynaptic terminals. In one of the very first descriptions of the synapse, Robertson noted that his observations of the organization of the synapse were distinct from those of Palade and

DeRobertis and Bennett by only one feature, the attachment of synaptic vesicles to a "tenuous filamentous tail..."(Robertson, 1955).

Previous ultrastructural analyses of the synapse indicated that the actin-mediated translocation of locally recycled synaptic vesicles demonstrated here in the lamprey reticulospinal synapse may extend to other types of synapses as well. In their landmark study of the synaptic vesicle cycle in the frog NMJ, Heuser and Reese noted the presence of an activity-dependent filamentous structure in precisely the same location and with many of the same characteristics as the actin matrix presented here (Heuser and Reese, 1973)(see Figure 36). In their paper, they wrote: "Cisternae were often connected to one or more coated vesicles and even when not joined to a coated vesicle were usually covered with a filamentous material which appeared similar to that around coated vesicles...In addition, coated vesicles were often connected to the plasma membrane in regions of the nerve terminal covered by a Schwann process, especially just at the edge of the synaptic cleft. In these regions, resting nerve terminals contained a filamentous material forming what appeared to be empty baskets, while stimulated terminals contained increased numbers of coated vesicles and coated pits." In the legend for their Figure 11, as well as those reprinted here in Figure 36, the authors further elaborated upon this observation: "Filamentous material, either faint whisps or discrete empty baskets (arrow), that surrounds some cisternae is associated with coated pits and vesicles in various stages of formation along the surface where Schwann process (s) invaginates." In essence, it appears that Heuser and Reese visualized the actin translocation pathway already in 1973, but in noting its association with clathrin-coated intermediates, misjudged its significance and came to the reasonable conclusion that this material was 'unpolymerized' clathrin.

Additional studies have reported the presence of actin in presynaptic terminals. A biochemical study designed to improve purification of synaptic vesicles from

Figure 36. Evidence for actin in recycling of synaptic vesicles as seen in frog neuromuscular junction

These panels are reproduced from The Journal of Cell Biology, 57:315-44, Heuser, J. E., Reese, T. S. *Evidence for recycling of synaptic vesicle membrane during transmitter release at the frog neuromuscular junction*, by copyright permission of The Rockefeller University Press.

The presence of a 'filamentous material' was noticed in various figures of this landmark paper describing local synaptic vesicle cycling. The authors observed that the filamentous material was always localized to the areas of the plasma membrane where endocytosis occurred and contacted clathrin-coated intermediates. The appearance and localization of this matrix is strikingly similar to the actin translocation network described in this thesis and most likely represents the same structure.

Original Figure Legends:

Figure 12*: (Only the top right corner is presented here, rotated 90° from original figure.) Cross section of a large terminal stimulated for 1 min. Synaptic vesicles are not obviously depleted, mitochondria are slightly expanded, and a cisterna has formed. However, even at this early stage the cisterna lies far away from the plasma membrane and appears to have formed indirectly by the coalescence of coated vesicles (inset; not shown here). X50,000; inset X100,000

Figure 13: Cross section of an unstimulated terminal. A filamentous material (f) extends from the cluster of synaptic vesicles to the lateral edges of the terminal covered by Schwann processes, where it appears to participate in forming organized coats (arrow) on the plasma membrane. X90,000.

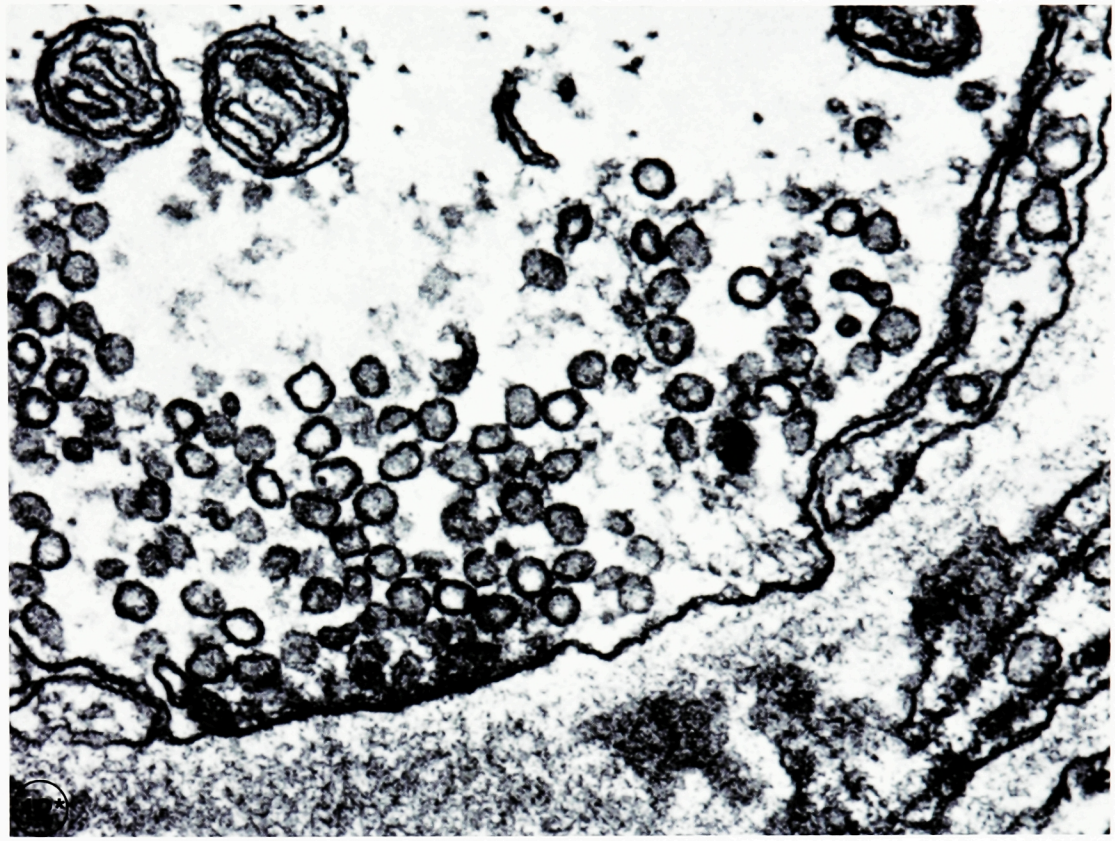

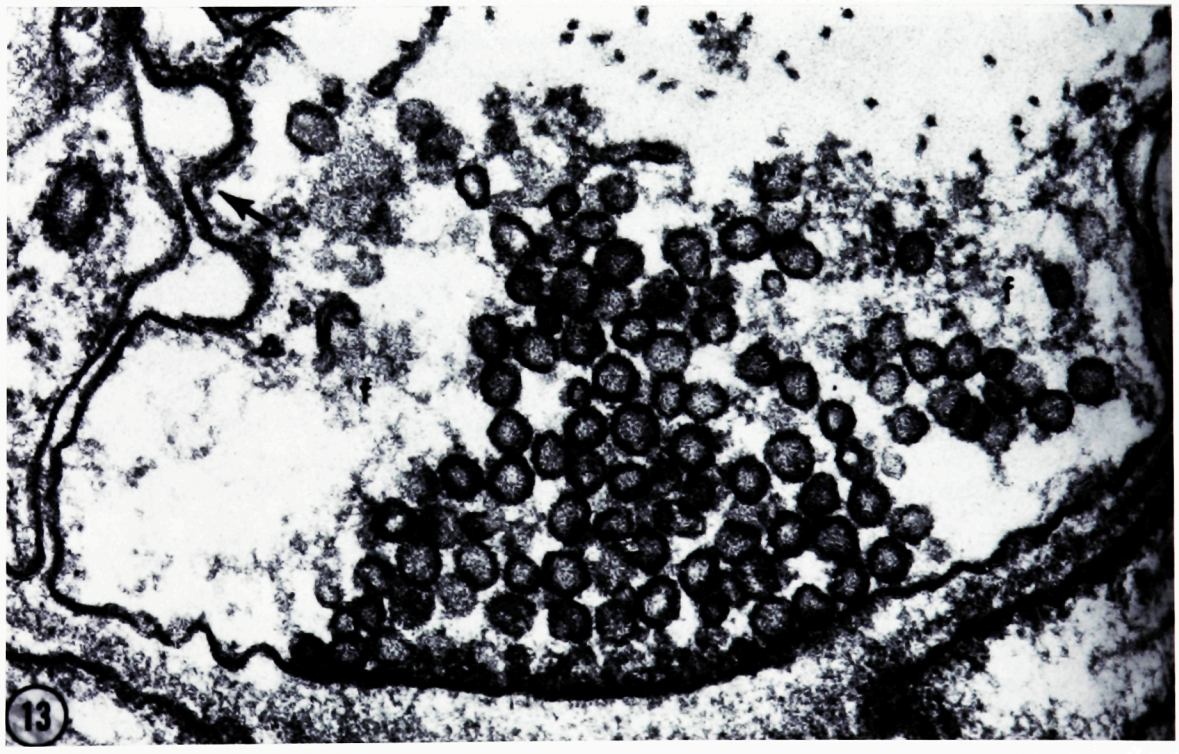
f
f
f
13

Torpedo marmorata also detected the presence of actin in synaptic vesicle fractions (Tashiro and Stadler, 1978). In an early study on the mechanism of action of BWSV, Gorio and Mauro echoed early hypotheses of presynaptic actin function, commenting in their discussion of neurotransmitter release that "contraction of actomyosin filaments could pull vesicles towards the plasma membrane, leading to exocytosis" (Gorio and Mauro, 1979). In cat forebrain synaptosomes, a brief ultrastructural study reported the presence of an actin network similar in appearance to that presented in this thesis (Inestrosa et al., 1976). Decorated with heavy meromyosin, actin filaments formed a random "...three-dimensional feltwork." Furthermore, it was noted that decorated actin filaments were often in contact with the membrane or synaptic vesicles. This network of actin filaments was discussed in relation to axonal transport.

There are discrepancies between the two studies that used quick freeze deep etch methods of freeze fracture to investigate the presence and distribution of actin-like fibers in the pre-synaptic terminal, as discussed in (Gotow et al., 1991). In one study, synaptic vesicles in a variety of nerve terminals were shown to contact randomly running filaments (Hirokawa, 1989; Hirokawa et al., 1989). It is possible that terminals considered to be "resting" were actually activated during the process of saponization or homogenization used for isolation of the tissue so that vesicles considered to be clustered were in fact recycling. In another study using similar methods to investigate presynaptic architecture, the authors observed smaller filaments associated between vesicles, which they postulated could be synapsin, and longer filaments anchored to the presynaptic plasma membrane, which could be actin (Landis et al., 1988). The authors acknowledged that their previous studies indicated that actin filaments in the axoplasm immediately adjacent to the active zone were unlikely.

In an elegant study of the lamprey reticulospinal synapse by Wickelgren and colleagues, the activity-dependent presence of a filamentous matrix was also described but again its purpose was not recognized: "Typically an area of presynaptic cytoplasm

in the vicinity of the differentiated membrane in a stimulated synapse was devoid of neurofilaments, which are common throughout the axonal cytoplasm, and contained a fuzzy substance (see Figs. 3B and 6B of (Wickelgren et al., 1985). We assume this area is the space occupied by the cluster of synaptic vesicles before their release; thus the fuzzy substance could represent some aspect of the cytosketelal structure that normally holds the synaptic vesicles in such focused arrays." The structure referred to in their Figure 3B appears to be clathrin, while the "fuzzy substance" visualized in Figure 6B is a filamentous matrix localized to membrane invaginations where recycling is occurring, identical in appearance to that described in this thesis.

Functional studies supporting a role for actin in synaptic vesicle recycling

Several studies are consistent with an active role for actin in the synaptic vesicle cycle. In addition to their early biochemical characterizations of actin in the presynaptic terminal, Puszkin and Kochwa provided some evidence for a dynamic role of actin in neurotransmitter release (Puszkin and Kochwa, 1974). In rat brain synaptosomes, they observed that enhanced glutamate release was stimulated from synaptic vesicles in the presence of synaptosomal membrane actin in a Ca^{2+}-dependent manner. The authors suggested that an actomyosin-dependent mechanism mediated neurotransmitter release.

Dynamic changes of the actin-like matrix in presynaptic regions have been observed after stimulation. In a series of studies performed in synaptosomes and then in neuronal cultures, Bernstein and Bamburg showed that K^+-evoked depolarization modified the organization of presynaptic actin (Bernstein and Bamburg, 1985; Bernstein and Bamburg, 1989; Bernstein and Bamburg, 1987; Bernstein et al., 1998). They hypothesized that actin in the presynaptic terminal may play a role in vesicle movement. In agreement with these findings, bath-applied actin toxins have been reported to modify synaptic transmission (Kim and Lisman, 1999; Wang et al., 1996). However, optical imaging of vesicles labeled with styryl dyes have reported either

partial (Kuromi and Kidokoro, 1998) or no effects of actin toxins on the re-entry of recycled synaptic vesicles to vesicle clusters (Betz and Henkel, 1994; Job and Lagnado, 1998). The lack of effects may be explained by low potencies, insufficient intracellular concentrations, or differential sensitivity to the actin-directed compounds used (Lamaze et al., 1996; Lamaze et al., 1997), as discussed in (Fujimoto et al., 2000). Structural and functional differences between synapses might also contribute to the observed differences. For instance, the ribbon-type synapse used in the study by Job *et al.*, appears to differ from conventional synapses in several ways, including the absence of synapsin (Mandell et al., 1990; von Gersdorff and Matthews, 1994), and may thus utilize other mechanisms for synaptic vesicle transport.

Actin in vesicle trafficking in non-neuronal cells

Recent studies in non-neuronal cells have provided insight into the mechanisms by which newly budded plasma membrane- and Golgi-derived vesicles enter the cytoplasm (Merrifield et al., 1999; Rozelle et al., 2000). By using GFP-actin, it was shown that actin tails or comets form at the site of vesicle budding. These tails remain in contact with the vesicle as it moves through the cytoplasm. Tumor cells transfected with GFP-actin show spontaneous formation of actin tails at sites of vesicle budding (Merrifield et al., 1999). Massive formation of such tails associated with pinosomes can be induced in fibroblasts by overexpression of phosphatidyl inositol-5-kinase and inhibition of tyrosine phosphatases (Rozelle et al., 2000).

The intracellular movement of some pathogens as well as organelles in non-neuronal cells has been shown to be actin-mediated (Damsky et al., 1977; Merrifield et al., 1999; Rozelle et al., 2000), reviewed in (Qualmann et al., 2000). The exact mechanism generating actin-based movement of newly budded vesicles or pathogens remains elusive. Actin tails may produce vesicle movement directly, or they may operate together with motor proteins (Geli et al., 2000), reviewed in (Machesky and Gould, 1999). Although these cargoes are often much larger than the average diameter

of synaptic vesicles (50 nm), some aspects of the molecular elements used for intracellular motility of larger cargo may be shared. The actin network observed in the present study of synaptic vesicle cycling is somewhat similar in appearance to the actin tails induced by *Listeria*, *Shigella* and *Vaccinia* virus (Cudmore et al., 1995; Cudmore et al., 1997; Machesky and Gould, 1999; Machesky et al., 1999). The regulation of other non-neuronal intracellular actin-based transport, both under normal conditions and in the presence of pathogens, has been found to involve the N-WASP-Arp2/3 signaling pathway (Frischknecht et al., 1999a; Machesky and Gould, 1999; Rozelle et al., 2000). It is presently unclear whether the N-Wasp-Arp2/3 signaling machinery is used at the synapse.

Other roles of actin in the nerve terminal

Actin is likely to have other functions in the nerve terminal, in addition to its role in synaptic vesicle transport (reviwed in (Doussau and Augustine, 2000). The axonal plasma membrane is covered by a cortical actin cyctoskeleton which takes part in maintaining the shape and tension of the plasma membrane. When lamprey reticulospinal axons were exposed to phalloidin for several hours, a proliferation of cortical actin was observed (data not shown). This effect may be responsible for the apparent inhibition of clathrin-mediated endocytosis (Fujimoto et al., 2000). A direct involvement of actin filaments in clathrin-mediated endocytosis is, however, also supported by several studies, as described below.

Several proteins involved in synaptic vesicle endocytosis also have interactions with actin pathways. For example, dynamin, which is critical for synaptic vesicle endocytosis (Koenig and Ikeda, 1983), reviewed in (Brodin et al., 2000) can interact with N-WASP (Qualmann et al., 1999). Furthermore, disruption of the phosphoinositide phosphatase synaptojanin, which is involved in lipid dynamics, can induce expansion of the actin-like matrix at presynaptic regions (Cremona et al., 1999), (and see below).

Actin and endocytosis

Studies performed in yeast clearly support a role for actin in endocytosis. Among the yeast mutants which harbor defects in endocytosis (END genes), several of them have been shown to involve actin (Benedetti et al., 1994; Kubler and Riezman, 1993). Abnormal endocytosis was also reported in mutants of several genes whose products interact with actin, including END3-END7/Act1 (Benedetti et al., 1994; Kubler and Riezman, 1993; Munn et al., 1995; Raths et al., 1993).

In vitro studies of actin dynamics in mammalian cells

In mammalian cells, the role of actin in endocytosis remains controversial, although biochemical studies have shown that clathrin is able to bind to actin directly (Puszkin et al., 1982). This controversy may stem from variations between compounds and experimental systems, as mentioned above and in (Fujimoto et al., 2000).

Several studies have suggested a role for actin in receptor-mediated endocytosis, based on studies of transferrin and transferrin receptor cycling (Durrbach et al., 1996; Gottlieb et al., 1993; Holm et al., 1993; Lamaze et al., 1997; Maples et al., 1997). Sandvig and Van Deurs found that cytochalasin D, which caps and depolymerizes actin filaments, had no effect on endocytosis of transferrin in African Green Monkey Kidney cells (Sandvig and van Deurs, 1990). However, Gottlieb *et al.* showed that actin filaments were important for transferrin endocytosis at the apical surface in polarized epithelial cells (Gottlieb et al., 1993). Using electron microscopy, they found that treatment with cytochalasin D greatly increased the number of coated pits at the apical surface, apparently unable to pinch off from the plasma membrane. In another study, cytochalasin D inhibited endocytosis in a mouse hepatoma cell line and depolymerization of F-actin decreased transferrin internalization and increased its presence on the cell surface. These authors hypothesized that actin could interact with dynamin on clathrin-coated pits (Durrbach et al., 1996).

More recently, Lamaze *et al.* reported that actin is needed for receptor-mediated endocytosis in mammalian cells. In perforated cells, they showed that high concentrations of thymosin B4, which binds and depolymerizes F-actin, were able to inhibit endocytosis of transferrin. The same was true for DNAse I, which increases the depolymerization rate of F-actin. In intact cells, the same study showed that exposure to latrunculin B, a membrane-permeable, actin-disrupting toxin, was able to inhibit transferrin endocytosis. By ultrastructural analysis, they demonstrated that this defect was not in clustering of transferrin receptor into coated pits. The authors concluded that actin must be involved in later stages of endocytosis such as coated pit constriction, vesicle detachment, or both (Lamaze et al., 1997).

Myosins in the synaptic vesicle cycle

The potent block of clusterotropic synaptic vesicle transport induced by NEM-S1 presented here does not prove but is consistent with an actomyosin mechanism in synaptic vesicle translocation. In the present study, arrowhead-like structures, which are typical of bundled actin filaments *in vitro* labeled with myosin S1 (Hirokawa et al., 1989) were not observed. Since the compound was capable of binding actin filaments *in vitro* (data not shown), and affected functional aspects of actin-based stages of the synaptic vesicle, the absence of arrowhead structures may be due to technically related issues such as an insufficient concentration of S1 or ratio of S1 to actin filaments. More likely, the lack of S1 arrowhead structures may reflect a real difference in the organization between actin nucleated lateral to the active zone and actin structures in cellular locations that are labeled by S1 in the arrowhead pattern. Studies using the squid giant axon have demonstrated actomyosin-dependent organelle transport in extruded axoplasm (Langford, 1995; Langford, 1999), and (Kuznetsov et al., 1992). The relation between this process and the transport of newly budded vesicles is not yet clear.

As mentioned in the Introduction, the biochemical purification of myosins from the brain several decades ago provoked many hypotheses on its local function (Puszkin et al., 1968). During the past decade, several studies have attempted to assign particular roles to specific members of the myosin superfamily present in neurons. Screening of a brain cDNA library with antisera raised against synaptic plasma membranes identified a member of the myosin I family (Sanders et al., 1992). Members of this family have been demonstrated to play a role in actin polymerization (Geli et al., 2000). Some studies also suggest a role for myosins in intracellular vesicle movement (Bahler, 1996) and myosins II and V were suggested to function in neurons (Cheung and Reisler, 1992; Espreafico et al., 1992). Evidence for the distribution of myosin II in the CNS has been largely contradictory (Miller et al., 1992; Mochida et al., 1994). Intracellular microinjection of anti-myosin IgG or inhibitors of myosin light chain kinase (MLCK) activity inhibited synaptic transmission (Mochida, 1995). A more recently discovered class of unconventional myosins, myosin V, was co-purified biochemically with synaptic vesicle proteins (Prekeris and Terrian, 1997). However, many of the vesicular structures shown to contain both myosin V and synaptic vesicle markers were not identical to synaptic vesicles but with larger vesicles that appeared to be destined for axonal transport, thus containing some synaptic vesicle proteins (Bridgman, 1999).

Several lines of evidence have suggested a possible connection between the roles of myosin V and synapsin in the nerve terminal. It was shown that brain myosin V binds to synaptic vesicle-bound CaMKII (Costa et al., 1996), reminiscent of synapsin's interaction with vesicular CaMKII (Benfenati et al., 1992b). In an optical study of vesicle mobilization, the presence of myosin light chain kinase inhibitors led to a defective recycling phenotype quite similar to that of the synapsin I knockout mice (Ryan, 1999). Ryan suggested that while the substrate was not known, MLCK was a potential link between the influx of Ca^{2+} leading to vesicle fusion and the refilling of the

distal pool. Later that year, Costa *et al.* showed that brain myosin V, which contains several calmodulin light chains, binds to CaMKII and stimulates its kinase activity, and was more effective than calmodulin alone (Costa et al., 1999). The authors proposed that upon nerve terminal depolarization, Ca^{2+} influx could promote the transfer of calmodulin from brain myosin V to CaMKII, causing its autophosphorylation and subsequent activation. CaMKII would then phosphorylate its most immediate substrates, such as synapsin. This remains an interesting hypothesis to be tested. Thus, the particular identity of a synaptic vesicle-associated myosin and the presynaptic role of myosin V remain obscure.

The localization of synapsin suggests multiple roles in the synaptic vesicle cycle

Using various actin-directed reagents microinjected into the lamprey reticulospinal axons, a dynamic and local actin filament highway was revealed that is necessary for the translocation of newly recycled post-endocytic vesicles from the lateral borders of the active zone to the vesicle cluster. The prevailing hypothesis of interaction between synapsin and actin states that this interaction takes place within the synaptic vesicle cluster and serves to maintain its organization. Contrary to this hypothesis, actin-directed reagents did not alter cluster organization in the absence of stimulation but instead revealed an actin matrix that appeared to participate in the local trafficking of post-endocytic vesicles. Under conditions in which the cluster was dissociated or depleted, evidence of filaments within the cluster was not observed. These observations led to the investigation of synapsin localization after various conditions of synaptic activity. It was shown that synapsin is present at multiple stages of the synaptic vesicle cycle.

After microinjection with anti-synapsin domain E antisera (G304) and low frequency stimulation, clustered synaptic vesicles were dispersed from one another and synaptic vesicles accumulated in the axoplasm lateral to the cluster and overlapping with

the region of post-endocytic transport. This phenotype was dependent on both stimulation frequency and concentration of antibodies, as a more drastic effect on synaptic vesicle clustering was observed following high frequency stimulation and higher concentrations of antibodies, as measured by distance from the injection site (present study and (Pieribone et al., 1995). The analysis of synapses exposed to low levels of synapsin antibodies provided the first morphological evidence of a role for synapsin in recycling as well as in clustering of synaptic vesicles.

Post-embedding immunogold localization of synapsin

In resting synapses, synapsin was found only on synaptic vesicles and primarily on those vesicles within the distal portion of the cluster, as shown previously (Pieribone et al., 1995). With stimulation, there is a two-fold increase in synapsin localization within the first 100 nm from the active zone, in the area typically referred to as the readily-releasable pool of synaptic vesicles. Using extreme stimulation conditions, synaptic vesicle clusters were dramatically reduced, and in some cases limited to only one row of docked vesicles. These vesicles were often labeled for synapsin, further supporting functional studies which suggest that synapsin may play a role in regulating the dynamics of both the releasable and reserve pools of synaptic vesicles. Expanded areas of presynaptic plasma membrane that correlate with vesicle fusion were not significantly labeled for synapsin, indicating that synapsin may dissociate from synaptic vesicles before or during fusion, as expected by previous studies (Torri-Tarelli et al., 1992; Torri-Tarelli et al., 1990).

In active synapses, non-vesicular synapsin was detected in close proximity to the endocytic areas of the plasma membrane. Synapsin was also present on the synaptic vesicles enmeshed in the actin-containing translocation matrix and on the matrix itself. These results demonstrate that in an active nerve terminal, synapsin is not restricted to synaptic vesicles in the distal portion of the nerve terminal but can be localized to other pools within the cluster and to other sites within the synaptic vesicle

cycle. These results have prompted a novel hypothesis of synapsin function, namely that one major interaction between synapsin and actin takes place outside of the vesicle cluster, within the actin-based post-endocytic vesicle translocation pathway. It is thus plausible that additional biochemical interactions of synapsin may also take place outside of the vesicle cluster, an extremely relevant possibility given that many of synapsin's binding partners have identified roles at various stages of the synaptic vesicle cycle.

Binding partners of synapsin

The biochemical identification of several molecular partners of synapsin indicates that overlapping signaling cascades may be relevant to several stages of the synaptic vesicle cycle. The known binding partners of synapsin fall into several categories: cytoskeletal components such as tubulin, spectrin, and actin (Bahler and Greengard, 1987; Okabe and Sobue, 1987), proteins involved in endocytosis (see below) and/or the regulation of actin dynamics such as the non-receptor tyrosine kinase c-Src (McPherson et al., 1994). A physiological relevance for this interaction was recently suggested by a study where increased concentrations of actin were co-immunoprecipitated with both c-Src and synapsin I from hippocampal synaptosomes prepared from animals after they were trained in the water maze model (Zhao et al., 2000).

In the case of *Vaccinia* virus, the tyrosine phosphorylation of the viral protein A36R by c-Src is needed for intracellular movement (Frischknecht et al., 1999b). A36R then associates with the host SH2-SH3 adapter protein, Nck. This adapter protein then recruits several mammalian proteins that interact with the cytoskeleton (Moreau et al., 2000). Tyrosine phosphorylation has also been shown to be important in actin-directed movement of raft-enriched vesicles (Rozelle et al., 2000). Indicating evidence for some common pathways between synapsin and virus-mediated

interactions with actin, the neurotropic rabies virus nucleocapsid is able to inhibit the actin bundling effect of dephospho-synapsin *in vitro* (Ceccaldi et al., 1997).

Synapsins can also bind to other synapsin molecules through homo-and heterodimers (Hosaka and Sudhof, 1999). It can bind to lipid components such as PI3 and PLCγ (Onofri et al., 2000), and signal transduction molecules such as CaMKII (Benfenati et al., 1992b) calmodulin, (Baines et al., 1995; Goold and Baines, 1994; Hayes et al., 1991; Nicol et al., 1997; Nicol et al., 1998), Ca^{2+}, and ATP (Esser et al., 1998; Hosaka and Sudhof, 1998).

The proline-rich domain D of synapsin binds to the SH3 domains of several other proteins implicated in the transport of intracellular cargo in other cellular trafficking systems, including PLCγ, PI3K (Onofri et al., 2000), and Grb2 (McPherson et al., 1994; Vaccaro et al., 1997). Several members of the endocytic protein family of endophilin also bind to synapsin such as SH3/p4 (endophilin) (Onofri et al., 2000), and endophilin 3/SH3p13 (Ringstad et al., 1999; Ringstad et al., 1997), (Marc Flajolet and Paul Greengard, unpublished observations).

Synapsin has also been shown to bind specifically to amphiphysins I and II, (Onofri et al., 2000), which play an established role in synaptic vesicle clathrin-mediated endocytosis (Shupliakov et al., 1997). The binding of amphiphysins to synapsin decreased synapsin's ability to promote actin polymerization (Onofri et al., 2000). Furthermore, synapsin can interact with the actin binding protein profilin (Witke et al., 1998). Most recently, actin binding protein 1 (Abp1, SH3P7/HIP-55) has been found to bind synapsin (Kessels et al., 2001). Abp1 is a protein that binds directly to both dynamin and actin, thus linking the actin cytoskeleton with the endocytic machinery (Kessels et al., 2001). These interactions indicate several avenues by which the biochemical interactions of synapsin could provide a mechanism of coordination

between the endocytic cycle and the activity-dependent formation of the actin-based transport system.

Previously, many such interactions were attributed to synapsin's known participation in synaptogenesis, as the only morphological evidence for synapsin in the adult nerve terminal was within the vesicle cluster. Presently, the distribution of synapsin in a living nerve terminal was determined throughout the synaptic vesicle cycle and provides evidence for the presence of synapsin at several stages of the synaptic vesicle cycle, offering a novel context for many of synapsin's observed biochemical interactions.

Some data already suggests that the actin filament matrix is enhanced in lamprey reticulospinal axons stimulated in the presence of reagents that affect several synapsin binding partners. For example, anti-endophilin antibodies cause an accumulation of filaments (Gad et al., 2000; Ringstad et al., 1999), Figures 3 and 4, and Figure 5A, respectively). Furthermore, stimulation in the presence of the proline-rich synaptojanin peptide caused a massive build-up of this actin matrix (see Figure 2 A, Figure 4, (Gad et al., 2000). Future studies are necessary to determine the sequential influence of biochemical partners on the role(s) of synapsin within the cluster and elsewhere in the nerve terminal. In addition, a role for GTP-dependent processes was recently implicated in regulating the dynamics of the actin translocation matrix. In lamprey reticulospinal axons stimulated in the presence of GTPγS or bacterial toxins affecting the Rho family of GTPases, the accumulation of the actin matrix was strongly promoted (Gustafsson et al., 1999).

Regulation of the synaptic vesicle cycle by phosphorylation

The differential functions of synapsins I and II have remained elusive but may be regulated by phosphorylation. Most of the confirmed phosphorylation sites contained within rat synapsin I are conserved among other vertebrates, such as cow, frog, and lamprey (Figure 37). The effects on synapsin function mediated by

phosphorylation by CaMKII at sites 2 and 3 have been described above. Phosphorylation of synapsin by MAPK also decreases synapsin's abilities to interact with actin (Jovanovic et al., 1996). However, in contrast to the CaMKII sites, synaptosomes maintain a basal level of phosphorylation by MAPK at sites 4/5 and 6 (Jovanovic et al., 2001). Upon 4-AP stimulation and Ca^{2+} entry, sites 4/5 and 6 have a reduced level of phosphorylation. The dephosphorylation appears to be dependent on calcineurin. Calcineurin has been demonstrated to be a key regulator of several proteins involved in the endocytic pathway (Robinson and Dunkley, 1985) such as dynamin, and synaptojanin (Cousin et al., 2001; Lai et al., 1999; Liu et al., 1994; McClure and Robinson, 1996), and possibly amphiphysin (Marks and McMahon, 1998). Proteins that bind to calcineurin and inhibit its activity have been shown to block endocytosis (Lai et al., 2000). This highlights the possibility that several pools of synapsin that are biochemically and therefore functionally distinct may act within the same nerve terminal, at varying stages of the synaptic vesicle cycle. Previous ultrastructural and functional data do not exclude the possibility that intermolecular interactions between synapsins could be responsible for the close association of vesicles within the cluster and that interactions between synapsin and its other binding partners, such as actin, contribute to other stages of the synaptic vesicle cycle.

Dynamin

The GTPase dynamin was among the first members to be identified in a growing variety of proteins that participate in different steps of this clathrin-mediated endocytosis (reviewed in (Brodin et al., 2000). Dynamin has been strongly implicated in the fission process occurring at the neck of the coated pit (reviewed in (Sever et al., 2000). Immunocytochemical studies have, however, localized dynamin not only to the neck of the constricted clathrin-coated pit (Takei et al., 1995a) but also to the clathrin coat itself (Damke et al., 1994; Takei et al., 1996). This observation suggests that dynamin, in addition to its role in fission, may participate in other steps of endocytosis.

Here, it was demonstrated by immunocytochemistry that presynaptic clathrin-coated intermediates are specifically labeled for dynamin and not for synapsin. Unexpectedly, it was observed that dynamin is associated with the earliest detectable stage of clathrin-coated endocytic intermediates. What might then be the role of dynamin at early stages of endocytosis? One possibility is that it participates in the recruitment of the clathrin coat under *in vivo* conditions. In data not shown here, axons injected with the same anti-dynamin antibodies (DG-1) and stimulated at 5 Hz for 20 minutes, exhibited a massive depletion of synaptic vesicles was observed (Gad et al., 2001). The loss of synaptic vesicles at active zones was accompanied by an expansion of the plasma membrane at the sides of the release sites. Via its effect on membrane curvature, dynamin may also participate in the invagination reaction together with endophilin (Ringstad et al., 1999) and possibly amphiphysin (Takei et al., 1999). Alternative or additional explanations for the disruption of coat formation by dynamin antibodies may relate to the proposed role of dynamin in the control of actin dynamics (Qualmann and Kelly, 2000) reviewed in (Qualmann et al., 2000; Sever et al., 2000). By interacting with profilin, and with syndapin that binds N-WASP, dynamin may be critical to preserve the proper function of endocytic sites at the periphery of active zones (Gaidarov et al., 1999). While this thesis was not designed to investigate the role of dynamin in endocytosis, the present results indicate that dynamin takes part in the onset of the formation of clathrin coated pits, in addition to its well-established role in fission.

Figure 37. Alignment of synapsin I sequences reveals conserved phosphorylation sites

Synapsin I from several vertebrate species was aligned using the Clustal computer program. Sequences were obtained from synapsin I. The source for these sequences are shown as Species (Genbank accession number): rat (A30411), cow (AAA30761), lamprey (AAF08805), frog (AAF08809).

The domain structure is indicated by background colors, according to previous figures. The phosphorylation sites are highlighted within the primary amino acid sequence in color.

In the order in which they appear in the sequence: Site 1 for PKA is shown in green. Sites 4 and 5 for MAPK are shown in orange. Site 6 for MAPK is shown in blue. Site 7 for CDK5 is in black. Sites 2 and 3 for CaMKII are shown in pink.

This analysis demonstrates that the sites for potential regulation of synapsin I are conserved across species, indicating the likelihood of a relevant role for all of these sites, possibly in different subsynaptic microdomains.

Alignment of Synapsin I using Clustal and Hand-Alignment of Phosphorylation Sites

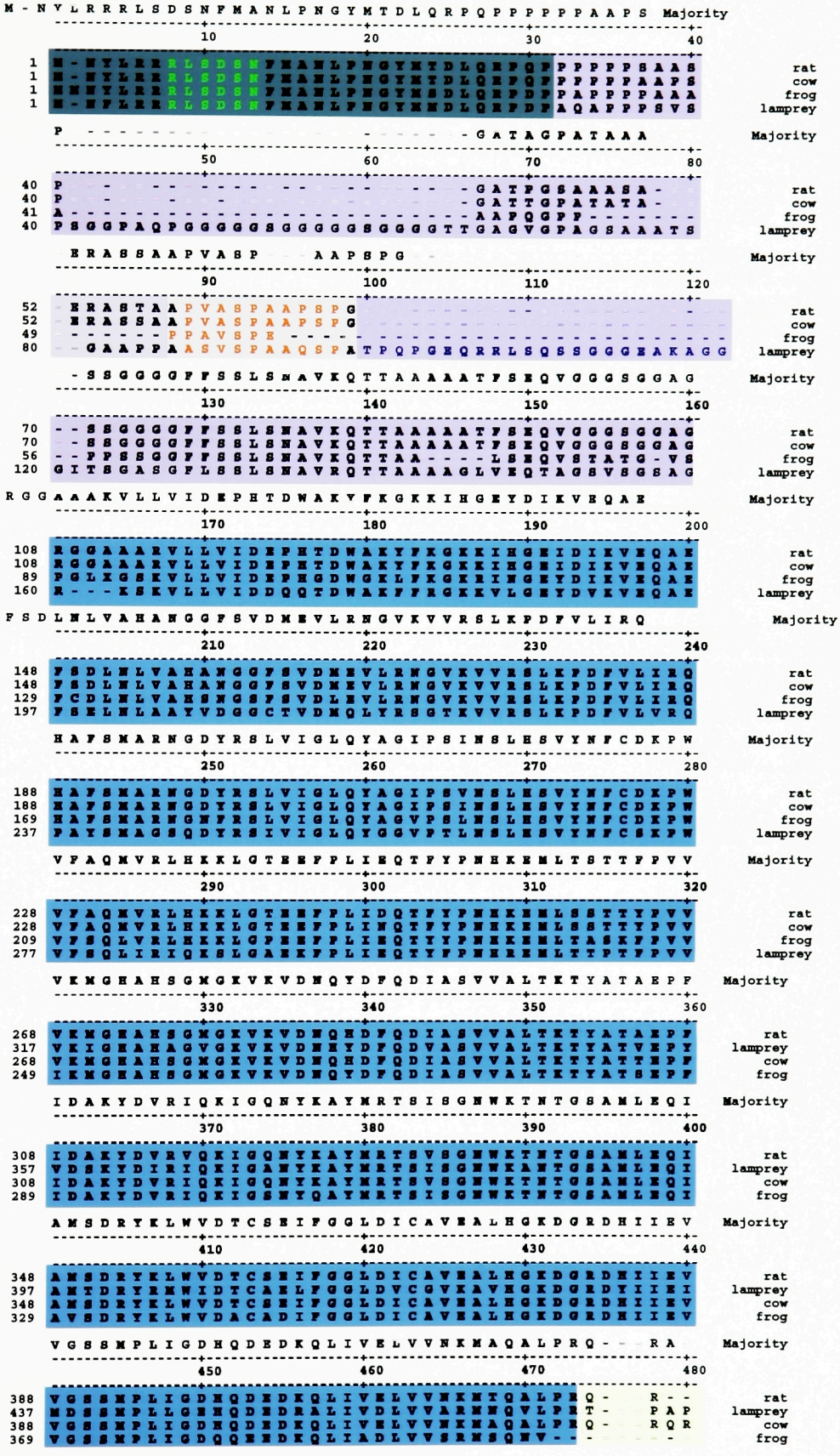

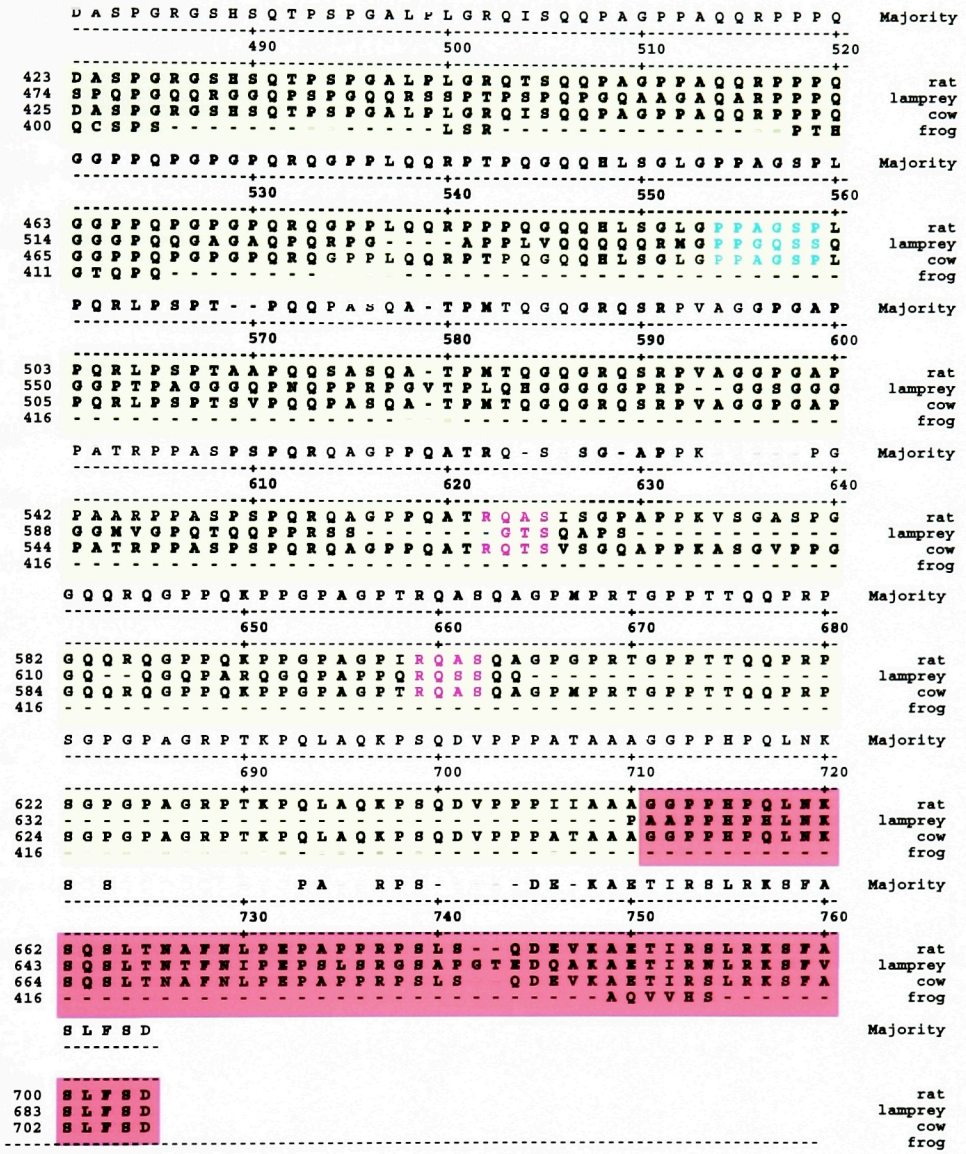
Majority
490
500
510
520
423 D A S P G R G S H S Q T P S P G A L P L G R Q T S Q Q P A G P P A Q Q R P P P Q rat
474 S P Q P G Q Q R G G Q P S P G Q Q R S S P T P S P Q P G Q A A G A Q A R P P P Q lamprey
425 D A S P G R G S H S Q T P S P G A L P L G R Q I S Q Q P A G P P A Q Q R P P P Q cow
400 Q C S P S - - - - - - - - - - - - L S R - - - - - - - - - - - - - - - P T H frog
Majority
530
540
550
560
463 G G P P Q P G P G P Q R Q G P P L Q Q R P P P Q G Q Q H L S G L G P P A G S P L rat
514 G G G P Q Q G A G A Q P Q R P G - - - - A P P L V Q Q Q Q Q R M G P P G Q S S Q lamprey
465 G G P P Q P G P G P Q R Q G P P L Q Q R P T P Q G Q Q H L S G L G P P A G S P L cow
411 G T Q P Q - frog
Majority
570
580
590
600
503 P Q R L P S P T A A P Q Q S A S Q A - T P M T Q G Q G R Q S R P V A G G P G A P rat
550 G G P T P A G G G Q P M Q P P R P G V T P L Q H G G G G G P R P - - G G S G G G lamprey
505 P Q R L P S P T S V P Q Q P A S Q A - T P M T Q G Q G R Q S R P V A G G P G A P cow
416 - frog
Majority
610
620
630
640
542 P A A R P P A S P S P Q R Q A G P P Q A T R Q A S I S G P A P P K V S G A S P G rat
588 G G M V G P Q T Q Q P P R S S - - - - - - - - G T S Q A P S - - - - - - - - - - - lamprey
544 P A T R P P A S P S P Q R Q A G P P Q A T R Q T S V S G Q A P P K A S G V P P G cow
416 - frog
Majority
650
660
670
680
582 G Q Q R Q G P P Q K P P G P A G P I R Q A S Q A G P G P R T G P P T T Q Q P R P rat
610 G Q - - Q G Q P A R Q G Q P A P P Q R Q S S Q Q - - - - - - - - - - - - - - - - lamprey
584 G Q Q R Q G P P Q K P P G P A G P T R Q A S Q A G P M P R T G P P T T Q Q P R P cow
416 - frog
Majority
690
700
710
720
622 S G P G P A G R P T K P Q L A Q K P S Q D V P P P I I A A A G G P P H P Q L N K rat
632 - P A A P P H P H L N K lamprey
624 S G P G P A G R P T K P Q L A Q K P S Q D V P P P A T A A A G G P P H P Q L N K cow
416 - frog
Majority
730
740
750
760
662 S Q S L T N A F N L P E P A P P R P S L S - - Q D E V K A E T I R S L R K S F A rat
643 S Q S L T N T F N I P E P S L S R G S A P G T E D Q A K A E T I R N L R K S F V lamprey
664 S Q S L T N A F N L P E P A P P R P S L S - - Q D E V K A E T I R S L R K S F A cow
416 - A Q V V H S - - - - - - frog
Majority
700 S L F S D rat
683 S L F S D lamprey
702 S L F S D cow
frog

V. CONCLUSIONS

The present studies were designed to test the hypothetical role of actin and synapsin in maintaining the synaptic vesicle cluster. The stimulation of nerve terminals in the presence of actin-directed compounds did not affect cluster organization *per se*, but supports a role for actin in endocytosis of synaptic vesicles. Unexpectedly, these studies visualized the presence of an actin-containing matrix outside of the vesicle cluster that appears to be critical for maintaining the return of synaptic vesicles from the sites of endocytosis to the vesicle cluster.

The exact mechanisms which underlay the specific targeting of this pathway to the synaptic vesicle cluster are presently unknown. Several functional studies have suggested a role for synapsin in mediating both the distal and proximal pools of synaptic vesicles. In the present study, synapsin was demonstrated throughout the vesicle cluster of active nerve terminals, lending morphological support to a functional role for synapsin in both the reserve and releasable pools of synaptic vesicles. In active terminals, non-vesicular synapsin was found to accumulate lateral to the cluster, in the area where the actin-containing matrix was visualized. As synapsin is known to nucleate G-actin, perhaps that activity could be relevant to the activity-dependent formation of the lateral actin matrix. Furthermore, synapsin is associated with the synaptic vesicles enmeshed in the transport network, and the filamentous matrix itself.

In this thesis, a novel mechanism is proposed by which synapsin may perform its key role in maintaining the vesicle population necessary for sustaining neurotransmitter release (summarized in Figure 38). The interaction between synapsin and actin may be physiologically relevant to maintaining the vesicle cluster, not via static interactions within the cluster, but through dynamic interactions outside of the cluster. These dynamic interactions may regulate the movement of recycling synaptic vesicles from the sites of endocytosis along an actin-based translocation network to the vesicle cluster.

Figure 38. Localization of Synapsin Suggests Multiple Roles in the Synaptic Vesicle Cycle

This figure presents an updated model of synapsin in the synaptic vesicle cycle, incorporating the data presented in this thesis. The cartoon uses the color schemes and symbols as shown earlier in this thesis. The known binding partners of synapsin are shown in blue, in association with their proposed function or known presynaptic location. Based on the studies presented in this thesis, synapsin may participate not only in the clustering of synaptic vesicles distal and proximal to the active zone but in several stages of the synaptic vesicle cycle, including the activity-translocation pathway, and in coordination with clathrin-mediated endocytosis.

Localization of Synapsin Suggests Multiple Roles in the Synaptic Vesicle Cycle

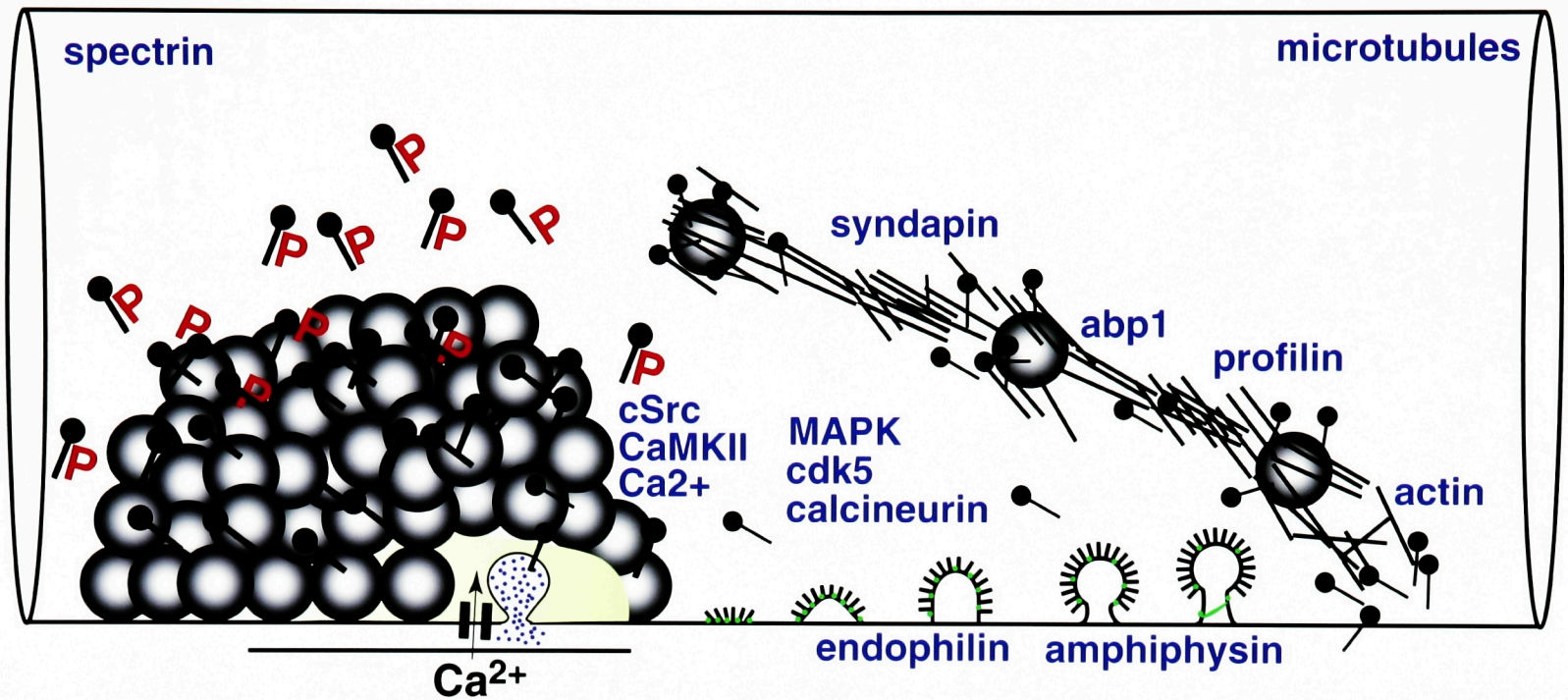

actin

synapsin

neurotransmitter

P phosphosynapsin

clathrin

dynamin

adapted from TINS 1999 Vol. 22:459-464, Annu. Rev Biochem. 2000 Vol. 69: 699-727

VI. REFERENCES

Akert, K., K. Pfenninger, C. Sandri, and H. Moor. 1972. Freeze etching and cytochemistry of vesicles and membrane complexes in synapses of the central nervous system. *In* Structure and Function of Synapses. P.a. Purpura, editor. Raven, New York. 67-86.

Aktories, K. 1997. Bacterial Toxins. Chapman,& Hall.

Aktories, K., P. Sehr, and I. Just. 1997. Actin-ADP-ribosylating Toxins: Cytotoxic Mechanisms of Clostridium botulinum C2 Toxin and Clostridium perfringens lota Toxin. *In* Bacterial Toxins. K. Aktories, editor. Chapman & Hall, Weinheim. 93-101.

Aubert-Foucher, E., and B. Font. 1990. Limited Proteolysis of Synapsin I. Identification of the Region of the Molecule Responsible for its Association with Microtubules. *Biochemistry*. 29:5351-5357.

Bahler, M. 1996. Myosins on the move to signal transduction. *Current Opinion in Cell Biology*. 8:18-22.

Bahler, M., F. Benfenati, F. Valtorta, A.J. Czernik, and P. Greengard. 1989. Characterization of synapsin I fragments produced by cysteine-specific cleavage: a study of their interactions with F-actin. *Journal of Cell Biology*. 108:1841-1849.

Bahler, M., and P. Greengard. 1987. Synapsin I bundles F-actin in a phosphorylation-dependent manner. *Nature*. 326:704-707.

Baines, A.J., and V. Bennett. 1985. Synapsin I is a spectrin-binding protein immunologically related to erythrocyte protein 4.1. *Nature*. 315:410-413.

Baines, A.J., and V. Bennett. 1986. Synapsin I is a microtubule-bundling protein. *Nature*. 319:145-147.

Baines, A.J., K.M. Chan, and R. Goold. 1995. Synapsin I and the cytoskeleton: calmodulin regulation of interactions. *Biochemical Society Transactions*. 23:65-70.

Benedetti, H., S. Raths, F. Crausaz, and H. Riezman. 1994. The END3 gene encodes a protein that is required for the internalization step of endocytosis and for actin cytoskeleton organization in yeast. *Molecular Biology of the Cell*. 5:1023-1037.

Benfenati, F., M. Bahler, R. Jahn, and P. Greengard. 1989a. Interactions of synapsin I with small synaptic vesicles: distinct sites in synapsin I bind to vesicle phospholipids and vesicle proteins. *Journal of Cell Biology*. 108:1863-1872.

Benfenati, F., P. Neyroz, M. Bahler, L. Masotti, and P. Greengard. 1990. Time-resolved fluorescence study of the neuron-specific phosphoprotein synapsin I. Evidence for phosphorylation-dependent conformational changes. *Journal of Biological Chemistry*. 265:12584-12595.

Benfenati, F., F. Valtorta, M. Bahler, and P. Greengard. 1989b. Synapsin I, a neuron-specific phosphoprotein interacting with small synaptic vesicles and F-actin. *Cell Biology International Reports*. 13:1007-1021.

Benfenati, F., F. Valtorta, E. Chieregatti, and P. Greengard. 1992a. Interaction of free and synaptic vesicle-bound synapsin I with F-actin. *Neuron*. 8:377-386.

Benfenati, F., F. Valtorta, M.C. Rossi, F. Onofri, T. Sihra, and P. Greengard. 1993. Interactions of synapsin I with phospholipids: possible role in synaptic vesicle clustering and in the maintenance of bilayer structures. *Journal of Cell Biology*. 123:1845-1855.

Benfenati, F., F. Valtorta, J.L. Rubenstein, F.S. Gorelick, P. Greengard, and A.J. Czernik. 1992b. Synaptic vesicle-associated Ca2+/calmodulin-dependent protein kinase II is a binding protein for synapsin I. *Nature*. 359:417-420.

Bennett, A.F., and A.J. Baines. 1992. Bundling of microtubules by synapsin 1. Characterization of bundling and interaction of distinct sites in synapsin 1 head

and tail domains with different sites in tubulin. *European Journal of Biochemistry*. 206:783-792.
Bennett, A.F., N.V. Hayes, and A.J. Baines. 1991. Site specificity in the interactions of synapsin 1 with tubulin. *Biochemical Journal*. 276:793-799.
Bennett, V., A.J. Baines, and J.Q. Davis. 1985. Ankyrin and synapsin: spectrin-binding proteins associated with brain membranes. *Journal of Cellular Biochemistry*. 29:157-169.
Berl, S., S. Puszkin, and W.J. Nicklas. 1973. Actomyosin-like protein in brain. *Science*. 179:441-446.
Bernstein, B., and J. Bamburg. 1985. Reorganization of Actin in Depolarized Synaptosomes. *The Journal of Neuroscience*. 5:2565-2569.
Bernstein, B., and J. Bamburg. 1989. Cycling of Actin Assembly in Synaptosomes and Neurotransmitter Release. *Neuron*. 3:257-265.
Bernstein, B.W., and J.R. Bamburg. 1987. Depolarization of Brain Synaptosomes Activates Opposing Factors Involved in Regulating Levels of Cytoskeletal Actin. *Biochemical Research*. 12:929-935.
Bernstein, B.W., M. DeWit, and J.R. Bamburg. 1998. Actin disassembles reversibly during electrically induced recycling of synaptic vesicles in cultured neurons. *Molecular Brain Research*. 53:236-250.
Betz, W.J., and A.W. Henkel. 1994. Okadaic acid disrupts clusters of synaptic vesicles in frog motor nerve terminals. *Journal of Cell Biology*. 124:843-854.
Beutner, D., T. Voets, E. Neher, and T. Moser. 2001. Calcium dependence of exocytosis and endocytosis at the cohlear inner hair cell afferent synapse. *Neuron*. 29:681-690.
Bindra, P.S., R. Knowles, and K.M. Buckley. 1993. Conservation of the amino acid sequence of SV2, a transmembrane transporter in synaptic vesicles and endocrine cells. *Genes*. 137:299-302.
Birks, R., H.E. Huxley, and B. Katz. 1960. The fine structure of the neuromuscular junction of the frog. *Journal of Physiology*. 150:134-144.
Blackstad, T.W., T. Karagulle, and O.P. Otterson. 1990. MORFOREL, a computer program for two-dimensional analysis of micrographs of biological specimens, with emphasis on immunogold preparations. *Computations Biological Medicine*. 20:15-34.
Bloom, F.E., T. Ueda, E. Battenberg, and P. Greengard. 1979. Immunocytochemical localization, in synapses, of protein I, an endogenous substrate for protein kinases in mammalian brain. *Proceedings of the National Academy of Sciences*. 76:5982-5986.
Bozzola, J.J., and L.D. Russell. 1992. Electron Microscopy: principles and techniques for biologists. Jones and Bartlett Publishers, Inc., Boston. 542 pp.
Bridgman, P.C. 1999. Myosin Va movements in normal and dilute-lethal axons provide support for a dual filament motor complex. *Journal of Cell Biology*. 146:1045-1060.
Brodin, L., P. Low, and O. Shupliakov. 2000. Sequential steps in clathrin-mediated synaptic vesicle endocytosis. *Current Opinion in Neurobiology*. 10:312-320.
Brown, S., and J.A. Spudich. 1981. Mechansim of Action of Cytochalasin: Evidence That it Binds to Actin Filament Ends. *Journal of Cell Biology*. 88:487-491.
Buckley, K., and R.B. Kelly. 1985. Identification of a Transmembrane Glycoprotein Specific for Secretory Vesicles of Neural and Endocrine Cells. *Journal of Cell Biology*. 100:1284-1294.
Ceccaldi, P., F. Valtorta, S. Braud, R. Hellio, and H. Tsiang. 1997. Alteration of the actin-based cytoskeleton by rabies virus. *Journal of General Virology*. 78:2831-2835.

Ceccaldi, P.E., F. Benfenati, E. Chieregatti, P. Greengard, and F. Valtorta. 1993. Rapid binding of synapsin I to F- and G-actin. A study using fluorescence resonance energy transfer. *FEBS Letters*. 329:301-305.

Ceccarelli, B., R. Fesce, F. Grohovaz, and C. Haimann. 1988. The effect of potassium on exocytosis of transmitter at the frog neuromuscular junction. *Journal of Physiology*. 401:163-183.

Ceccarelli, B., F. Grohovaz, and W.P. Hurlbut. 1979a. Freeze-fracture studies of frog neuromuscular junctions during intense release of neurotransmitter. I. Effects of black widow spider venom and Ca2+-free solutions on the structure of the active zone. *Journal of Cell Biology*. 81:163-177.

Ceccarelli, B., F. Grohovaz, and W.P. Hurlbut. 1979b. Freeze-fracture studies of frog neuromuscular junctions during intense release of neurotransmitter. II. Effects of electrical stimulation and high potassium. *Journal of Cell Biology*. 81:178-192.

Ceccarelli, B., and W.P. Hurlbut. 1975. The effects of prolonged repetitive stimulation in hemicholinium on the frog neuromuscular junction. *Journal of Physiology*. 247:163-188.

Ceccarelli, B., and W.P. Hurlbut. 1980a. Ca2+-dependent recycling of synaptic vesicles at the frog neuromuscular junction. *Journal of Cell Biology*. 87:297-303.

Ceccarelli, B., and W.P. Hurlbut. 1980b. Vesicle hypothesis of the release of quanta of acetylcholine. *Physiological Reviews*. 60:396-441.

Ceccarelli, B., and W.P. Hurlbut. 1990. Ca2+-dependent Recycling of Synaptic Vesicles at Frog Neuromuscular Junction. *Journal of Cell Biology*. 87:297-303.

Ceccarelli, B., W.P. Hurlbut, and A. Mauro. 1972. Depletion of vesicles from frog neuromuscular junctions by prolonged tetanic stimulation. *Journal of Cell Biology*. 54:30-38.

Ceccarelli, B., W.P. Hurlbut, and A. Mauro. 1973. Turnover of transmitter and synaptic vesicles at the frog neuromuscular junction. *Journal of Cell Biology*. 57:499-524.

Cheetham, J.J., S. Hilfiker, F. Benfenati, T. Weber, P. Greengard, and A.J. Czernik. 2001. Identification of synapsin I peptides that insert into lipid membranes. *Biochemical Journal*. 354:57-66.

Cheung, P., and E. Reisler. 1992. Synthetic peptide of the sequence 632-642 on myosin subfragment 1 inhibits actomyosin ATPase activity. *Biochemical & Biophysical Research Communications*. 189:1143-1149.

Chieregatti, E., P.E. Ceccaldi, F. Benfenati, and F. Valtorta. 1996. Effects of synaptic vesicles on actin polymerization. *FEBS Letters*. 398:211-216.

Cole, J.C., R.S. Villa, and R.S. Wilkinson. 2000. Disruption of actin impedes transmitter release in snake motor terminals. *Journal of Physiology*. 525.3:579-586.

Cooper, J.A. 1987. Effects of Cytochalasin and Phalloidin on Actin. *Journal of Cell Biology*. 105:1473-1478.

Costa, M., W. Santoro, E. Espreafico, and R. Larson. 1996. Brain Myosin V binds to calmodulin-dependent protein kinase II and activates its phosphorylating activity. *Annual Meeting of Cell Biology*. Abstract:373a.

Costa, M.C., F. Mani, W. Santoro, Jr., E.M. Espreafico, and R.E. Larson. 1999. Brain myosin-V, a calmodulin-carrying myosin, binds to calmodulin-dependent protein kinase II and activates its kinase activity. *Journal of Biological Chemistry*. 274:15811-15819.

Cousin, M.A., and D.G. Nicholls. 1997. Synaptic vesicle recyling in cultured cerebellar granule cells: role of acidification and refilling. *Journal of Neurochemistry*. 69:1927-1935.

Cousin, M.A., and P.J. Robinson. 1999. Mechansims of Synaptic Vesicle Recycling Illuminated by Fluorescent Dyes. *Journal of Neurochemistry*. 73:2227-2239.

Cousin, M.A., T. Tan, and P.J. Robinson. 2001. Protein phosphorylation is required for endocytosis in nerve terminals: potential role for the dephosphins dynamin I and synaptojanin, but not AP180 or amphiphysins. *Journal of Neurochemistry.* 76:105-116.

Couteaux, R. 1955. Localization of cholinesterases at neuromuscular junctions. *Experimental Cellular Research.* Supplement 5:294-322.

Couteaux, R. 1958. Morhphological and cytochemical observations on post-synaptic membrane at motor end-plates and ganglionic synapses. *Experimental Cell Research.* Suppl. 5:294-322.

Couteaux, R., and M. Pecot-Dechavassine. 1970. Vesicules synaptiques et pches au niveau des zones actives de la jonction neuromusculaire. *C.R. Acad. Sci. Hebd Seances Acad. Sci. D.* 271:2346-2349.

Cremona, O., G. Di Paolo, M.R. Wenk, A. Luthi, W.T. Kim, K. Takei, L. Daniell, Y. Nemoto, S.B. Shears, R.A. Flavell, D.A. McCormick, and P. De Camilli. 1999. Essential role of phosphoinositide metabolism in synaptic vesicle recycling. *Cell.* 99:179-188.

Cudmore, S., P. Cossart, G. Griffiths, and M. Way. 1995. Actin-based motility of vaccinia virus. *Nature.* 378:636-638.

Cudmore, S., I. Reckmann, and M. Way. 1997. Viral maniuplations of the actin cytoskeleton. *Trends in Microbiology.* 5:142-148.

Czernik, A.J., D.T. Pang, and P. Greengard. 1987. Amino acid sequences surrounding the cAMP-dependent and calcium/calmodulin-dependent phosphorylation sites in rat and bovine synapsin I. *Proceedings of the National Academy of Sciences of the United States of America.* 84:7518-7522.

Damke, H., T. Baba, D.E. Warnock, and S.L. Schmid. 1994. Induction of mutant dynamin specifically blocks endocytic coated vesicle formation. *Journal of Cell Biology.* 127:915-934.

Damsky, C., J. Sheffield, G. Tuszynski, and L. Warren. 1977. Is there a role for actin in virus budding? *Journal of Cell Biology.* 75:593-605.

De Camiili, P., T. Ueda, F.E. Bloom, E. Battenberg, and P Greengard. 1979. Widespread distribution of protein I in the central and peripheral nervous systems. *Proceedings of the National Academy of Sciences.* 76:5977-5981.

De Camilli, P., F. Benfenati, F. Valtorta, and P. Greengard. 1990. The synapsins. *Annual Review of Cell Biology.* 6:433-460.

De Camilli, P., R. Cameron, and P Greengard. 1983a. Synapsin I (Protein I), a nerve terminal-specific phosphoprotein. I. Its general distribution in synapses of the central and peripheral nervous system demonstrated by immunofluorescence in frozen and plastic sections. *Journal of Cell Biology.* 96:1337-1354.

De Camilli, P., and P. Greengard. 1986. Synapsin I: a synaptic vesicle-associated neuronal phosphoprotein. *Biochemical Pharmacology.* 35:4349-4357.

De Camilli, P., S.M. Harris, W.B. Huttner, and P. Greengard. 1983b. Synapsin I (Protein I), a nerve terminal-specific phosphoprotein. II. Its specific association with synaptic vesicles demonstrated by immunocytochemistry in agarose-embedded synaptosomes. *Journal of Cell Biology.* 96:1355-1373.

De Robertis, E. 1958a. Submicroscopic morphology and function of the synapse. *Experimental Cell Research.* Suppl. 5:347-369.

De Robertis, E. 1958b. Submicroscopic morphology and function of the synapse. *Proceedings of the Royal Society B.* 146:357-367.

De Robertis, E.D.P., and H.S. Bennett. 1954. Sub-microscopic vesicular components in the synapse. *Federal Proceedings of the American Physiological Society.* 13:35.

De Robertis, E.D.P., and H.S. Bennett. 1955. Some features of the sub-microscopic morphology of synapses in frog and earthworm. *Journal of Biophysics and biochemical cytology.* 1:47-58.

del Castillo, J., and B. Katz. 1954. Quantal components of the end-plate potential. *Journal of Physiology*. 124:560-573.
del Castillo, J., and B. Katz. 1956. Biophysical Aspects of Neuro-Muscular Transmission. *Progress in Biophysics and biophysical chemistry*. 6:121-170.
Delgado, R., C. Maureira, C. Oliva, Y. Kidokoro, and P. Labarca. 2000. Size of Vesicle Pools, Rates of Mobilization, and Recycling at Neuromuscular Synapses of a Drosophila mutant, shibire. *Neuron*. 28:941-953.
Doussau, F., and G.J. Augustine. 2000. The actin cytoskeleton and neurotransmitter release: an overview. *Biochimie*. 82:353-363.
Drenckhahn, D., and H.-W. Kaiser. 1983. Evidence for the concentration of F-actin and myosin in synapses and in the plasmalemmal zone of axons. *European Journal of Cell Biology*. 31:235-240.
Dresbach, T., B. Qualmann, M.M. Kessels, C.C. Garner, and E.D. Gundelfinger. 2001. The presynaptic cytomatrix of brain synapses. *Cellular and Molecular Life Sciences*. 58:94-116.
Dunaevsky, A., and E.A. Connor. 2000. F-Actin Is Concentrated in Nonrelease Domains at Frog Neuromuscular Junctions. *Journal of Neuroscience*. 20:6007-6012.
Durrbach, A., D. Louvard, and E. Coudrier. 1996. Actin filaments facilitate two steps of endocytosis. *Journal of Cell Science*. 109:457-465.
Espreafico, E., R. Cheney, M. Matteoli, A. Nascimento, P. DeCamilli, R. Larson, and M. Mooseker. 1992. Primary structure and cellular localization of chicken brain myosin V (p190), an unconventional myosin with calmodulin light chains. *Journal of Cell Biology*. 119:1541-1557.
Esser, L., C.R. Wang, M. Hosaka, C.S. Smagula, T.C. Sudhof, and J. Deisenhofer. 1998. Synapsin I is structurally similar to ATP-utilizing enzymes. *EMBO Journal*. 17:977-984.
Fath, K.R., and R.J. Lasek. 1988. Two Classes of Actin Microfilaments are Associated with the Inner Axoplasm. *Journal of Cell Biology*. 107:613-621.
Fatt, P. 1954. Biophysics of Junctional Transmission. *Physiological Review*. 34:674-711.
Feng, J., P. Chi, T.A. Blenpied, Y. Xu, A.M. Magarinos, A. Ferreira, R. Takahashi, H.T. Kao, B.S. McEwen, G.J. Augustine, T.A. Ryan, and P. Greengard. 2001. Regulation of neurotransmitter release and axon outgrowth by synapsin III. *Manuscript in preparation*.
Ferreira, A., H.T. Kao, J. Feng, M. Rapoport, and P. Greengard. 2000. Synapsin III: developmental expression, subcellular localization, and role in axon formation. *Journal of Neuroscience*. 20:3736-3744.
Fesce, R. 1999. The kinetics of nerve-evoked quantal secretion. *Philosophical Transactions of the Royal Society of London - Series B*. 354:319-329.
Fesce, R., F. Benfenati, P. Greengard, and F. Valtorta. 1992. Effects of the neuronal phosphoprotein synapsin I on actin polymerization. II. Analytical interpretation of kinetic curves. *Journal of Biological Chemistry*. 267:11289-11299.
Fesce, R., F. Grohovaz, W.P. Hurlbut, and B. Ceccarelli. 1980. Freeze-fracture studies of frog neuromuscular junctions during intense release of neurotransmitter. III. A morphometric analysis of the number and diameter of intramembrane particles. *Journal of Cell Biology*. 85:337-345.
Fifkova, E., and R. Delay. 1982. Cytoplasmic Actin in Neuronal Processes as a Possible Mediator of Synaptic Plasticity. *The Journal of Cell Biology*. 95:345-350.
Fine, R.E., A.L. Blitz, S.E. Hitchcock, and B. Kaminer. 1973. Tropomyosin in brain and growing neurones. *Nat New Biol*. 245:182-186.
Fine, R.E., and D. Bray. 1971. Actin in growing nerve cells. *Nat New Biol*. 234:115-118.

Fiumara, F., F. Onofri, F. Benfenati, P.G. Montarolo, and M. Ghirardi. 2001. Intracellular injection of synapsin I induces neurotransmitter release in C1 neurons of Helix Pomatis contacting a wrong target. *Neuroscience*. 104:271-280.

Foster-Barber, A., and J.M. Bishop. 1998. Src interacts with dynamin and synapsin in neuronal cells. *Proceedings of the National Academy of Sciences of the United States of America*. 95:4673-4677.

Fried, R.C., and M.P. Blaustein. 1976. Synaptic vesicle recycling in synaptosomes in vitro. *Nature*. 261:255-256.

Frischknecht, F., S. Cudmore, V. Moreau, I. Reckmann, S. Rottger, and M. Way. 1999a. Tyrosine phosphorylation is required for actin-based motility of vaccinia but not Listeria or Shigella. *Current Biology*. 9:89-92.

Frischknecht, F., V. Moreau, S. Rottger, S. Gonfloni, I. Reckmann, G. Superti-Furga, and M. Way. 1999b. Actin-based motility of vaccinia virus mimics receptor tyrosine kinase. *Nature*. 401:926-929.

Fujimoto, L.M., R. Roth, J.E. Heuser, and S.L. Schmid. 2000. Actin assembly plays a variable, but not obligatory role in receptor-mediated endocytosis in mammalian cells. *Traffic*. 1:161-171.

Gad, H., O. Bloom, P. Low, V. Slepnev, P. De Camilli, L. Brodin, and O. Shupliakov. 2001. A role for dynamin at early stages of clathrin-mediated endocytosis. *Manuscript*.

Gad, H., P. Low, E. Zotova, L. Brodin, and O. Shupliakov. 1998. Dissociation between Ca2+-triggered synaptic vesicle exocytosis and clathrin-mediated endocytosis at a central synapse. *Neuron*. 21:607-616.

Gad, H., N. Ringstad, P. Low, O. Kjaerulff, J. Gustafsson, M. Wenk, G. Di Paolo, Y. Nemoto, J. Crun, M.H. Ellisman, P. De Camilli, O. Shupliakov, and L. Brodin. 2000. Fission and uncoating of synaptic clathrin-coated vesicles are perturbed by disruption of interactions with the SH3 domain of endophilin. *Neuron*. 27:301-312.

Gaidarov, I., F. Santini, R. Warren, and J. Keen. 1999. Spatial control of coated-pit dynamics in living cells. *Nature Cell Biology*. 1:1-8.

Geli, M.I., R. Lombardi, B. Schmelzl, and H. Reizman. 2000. An intact SH3 domain is required for myosin I-induced actin polymerization. *EMBO Journal*. 19:4281-4291.

Glauert, A.M., and P.R. Lewis. 1998. Biological Specimen Preparation for Transmission Electron Microscopy. Princeton University Press, Princeton.

Gonzales-Gaitan, M., and H. Jackle. 1997. Role of drosophila alpha-adaptin in presynaptic vesicle recycling. *Cell*. 88:767-776.

Goodman, S.R., K.E. Krebs, C.F. Whitfield, B.M. Riederer, and I.S. Zagon. 1988. Spectrin and related molecules. *CRC Critical Reviews in Biochemistry*. 23:171-234.

Goold, R., and A.J. Baines. 1994. Evidence that two non-overlapping high-affinity calmodulin-binding sites are present in the head region of synapsin I. *European Journal of Biochemistry*. 224:229-240.

Gorio, A., and A. Mauro. 1979. Reversibility and Mode of Action of Black Widow Spider Venom on the Vertebrate Neuromuscular Junction. *Journal of General Physiology*. 73:245-263.

Gotow, T., K. Miyaguchi, and P. Hashimoto. 1991. Cytoplasmic architecture of the axon terminal: filamentous strands specifically associated with synaptic vesicles. *Neuroscience*. 40:587-598.

Gottlieb, T.A., I.E. Ivanov, M. Adesnik, and D.D. Sabatini. 1993. Actin microfilaments play a critical role in endocytosis at the apical but not the basolateral surface of polarized epithelial cells. *Journal of Cell Biology*. 120:695-710.

Greengard, P. 1976. Possible role for cyclid nucleotides and phosphorylated membrane protines in post-synaptic actions of neurotransmitter release. *Nature*. 260:101-108.
Greengard, P. 1978. Phosphorylated proteins as physiological effectors. *Science*. 199:146-152.
Greengard, P., F. Benfenati, and F. Valtorta. 1994. Synapsin I, an actin-binding protein regulating synaptic vesicle traffic in the nerve terminal. Raven Press, New York.
Greengard, P., J.F. Kuo, and E. Miyamoto. 1971. Studies on the mechanism of action of cyclic AMP in nervous and other tissues. Pergamon, New York. 113-125 pp.
Greengard, P., F. Valtorta, A.J. Czernik, and F. Benfenati. 1993. Synaptic vesicle phosphoproteins and regulation of synaptic function. *Science*. 259:780-785.
Gustafsson, J., P. Low, L. Brodin, and O. Shupliakov. 1999. Rho GTPases implicated as regulators of actin dynamics at presynaptic endocytic regions. *Society for Neuroscience*. 692.10:1743.
Hackett, J., S. Cochran, J. Greenfield, D. Brosius, and T. Ueda. 1990. Synapsin I injected presynaptically into goldfish mathner axons reduces quantal synaptic transmission. *Journal of Neurophysiology*. 63:701-706.
Hajibagheri, M.A.e. 1999. Electron Microscopy Methods and Protocols, Vol. 117. Humana Press, Totowa, NJ.
Hall, F.L., J.P. Mitchell, and P.R. Vulliet. 1990. Phosphorylation of synpasin I at a novel site by proline-directed kinase protein kinase. *Journal of Biological Chemistry*. 265:6944-6948.
Hayat, M.A. 1975. Positive staining for electron microscopy. Van Nostrand Reinhold Company, New York. 361 pp.
Hayes, N.V., A.F. Bennett, and A.J. Baines. 1991. Selective Ca2(+)-dependent interaction of calmodulin with the head domain of synapsin 1. *Biochemical Journal*. 275:93-97.
Heuser, J. 1989. The role of coated vesicles in recycling of synaptic vesicle membrane. *Cell Biology International Reports*. 13:1063-1077.
Heuser, J., and T.S. Reese. 1972. Stimulation induced uptake and release of peroxidase from synaptic vesicles in frog neuromuscular junctions. *Anatomical Record*. 172:329-330.
Heuser, J.E., and M.W. Kirschner. 1980. Filament organization revealed in platinum replicas of freeze-dried cytoskeletons. *Journal of Cell Biology*. 86:212-234.
Heuser, J.E., and T.S. Reese. 1973. Evidence for recycling of synaptic vesicle membrane during transmitter release at the frog neuromuscular junction. *Journal of Cell Biology*. 57:315-344.
Heuser, J.E., T.S. Reese, M.J. Dennis, Y. Jan, L. Jan, and L. Evans. 1979. Synaptic vesicle exocytosis captured by quick freezing and correlated with quantal transmitter release. *Journal of Cell Biology*. 81:275-300.
Heuser, J.E., T.S. Reese, and D.M. Landis. 1974. Functional changes in frog neuromuscular junctions studied with freeze-fracture. *Journal of Neurocytology*. 3:109-131.
Heuser, J.E., T.S. Reese, and D.M. Landis. 1976. Preservation of synaptic structure by rapid freezing. *Cold Spring Harbor Symposia on Quantitative Biology*. 40:17-24.
Hilfiker, S., V.A. Pieribone, A.J. Czernik, H.T. Kao, G.J. Augustine, and P. Greengard. 1999. Synapsins as regulators of neurotransmitter release. *Philosophical Transactions of the Royal Society of London - Series B: Biological Sciences*. 354:269-279.
Hilfiker, S., F.E. Schweizer, H.T. Kao, A.J. Czernik, P. Greengard, and G.J. Augustine. 1998. Two sites of action for synapsin domain E in regulating

neurotransmitter release [published erratum appears in Nat Neurosci 1998 Aug;1(4):329]. *Nature Neuroscience*. 1:29-35.
Hirokawa, N. 1989. The arrangement of actin filaments in the postsynaptic cytoplasm of the cerebellar cortex revealed by quick-freeze deep-etch electron microscopy. *Neuroscience Research*. 6:269-275.
Hirokawa, N., K. Sobue, K. Kanda, A. Harada, and H. Yorifuji. 1989. The cytoskeletal architecture of the presynaptic terminal and molecular structure of synapsin 1. *Journal of Cell Biology*. 108:111-126.
Ho, M.F., M. Bahler, A.J. Czernik, W. Schiebler, F.J. Kezdy, E.T. Kaiser, and P. Greengard. 1991. Synapsin I is a highly surface-active molecule. *Journal of Biological Chemistry*. 266:5600-5607.
Holm, P.K., S.H. Hansen, K. Sandvig, and B. van Deurs. 1993. Endocytosis of desmosomal plaques depends on intact actin filaments and leads to a nondegradative compartment. *European Journal of Cell Biology*. 62:362-371.
Hosaka, M., R.E. Hammer, and T.C. Sudhof. 1999. A phospho-switch controls the dynamic association of synapsins with synaptic vesicles. *Neuron*. 24:377-387.
Hosaka, M., and T.C. Sudhof. 1998. Synapsins I and II are ATP-binding proteins with differential Ca2+ regulation. *Journal of Biological Chemistry*. 273:1425-1429.
Hosaka, M., and T.C. Sudhof. 1999. Homo- and heterodimerization of synapsins. *Journal of Biological Chemistry*. 274:16747-16753.
Humeau, Y., F. Dousseau, D. Vitiello, P. Greengard, F. Benfenati, and B. Poulain. 2001. Synapsin controls both reserve and releasable synaptic vesicle pools during neuronal activity and short-term plasticity in Aplysia. *Journal of Neuroscience*. 21:4195-4206.
Hurlbut, W.P., and B. Ceccarelli. 1974. Transmitter release and recycling of synaptic vesicle membrane at the neuromuscular junction. *Advances in Cytopharmacology*. 2:141-154.
Huttner, W.B., L.J. DeGennaro, and P. Greengard. 1981. Differential phosphorylation of multiple sites in purified protein I by cyclic AMP-dependent and calcium-dependent protein kinases. *Journal of Biological Chemistry*. 256:1482-1488.
Huttner, W.B., and P. Greengard. 1979. Multiple phosphorylation sites in protein I and their differential regulation by cyclic AMP and calcium. *Proceedings of the National Academy of Sciences of the United States of America*. 76:5402-5406.
Huttner, W.B., W. Schiebler, P. Greengard, and P. De Camilli. 1983. Synapsin I (protein I), a nerve terminal-specific phosphoprotein. III. Its association with synaptic vesicles studied in a highly purified synaptic vesicle preparation. *Journal of Cell Biology*. 96:1374-1388.
Inestrosa, N.C., H.L. Fernandez, and J. Garrido. 1976. Actin-like filaments in synaptosomes detected by heavy mearomyosin binding. *Neuroscience Letters*. 2:217-221.
Job, C., and L. Lagnado. 1998. Calcium and protein kinase C regulate the actin cytoskeleton in the synaptic terminal of retinal bipolar cells. *Journal of Cell Biology*. 143:1661-1672.
Jorgensen, E.M., E. Hartwieg, K. Schuske, M.L. Nonet, Y. Jin, and H.R. Horvitz. 1995. Defective recycling of synaptic vesicles in synaptotagmin mutants of Caenorhabditis elegans. *Nature*. 378:196-199.
Jovanovic, J., T.S. Sihra, A.C. Nairn, H.C. Hemmings, Jr., P. Greengard, and A.J. Czernik. 2001. Bi-directional changes in synapsin I phosphorylation during voltage-dependent Ca2+ entry and neurotransmitter release in isolated nerve terminals (synaptosomes). *Manuscript in preparation*.
Jovanovic, J.N., F. Benfenati, Y.L. Siow, T.S. Sihra, J.S. Sanghera, S.L. Pelech, P. Greengard, and A.J. Czernik. 1996. Neurotrophins stimulate phosphorylation of

synapsin I by MAP kinase and regulate synapsin I-actin interactions. *Proceedings of the National Academy of Sciences of the United States of America*. 93:3679-3683.

Kanseki, T., and K. Kadota. 1969. The "Vesicle in a Basket": A morphological study of coated vesicle isolated frmo the nerve endings of the guinea pig brain, with special reference to the mechanism of membrane movements. *Journal of Cell Biology*. 42:202-220.

Kao, H.T., B. Porton, A.J. Czernik, J. Feng, G. Yiu, M. Haring, F. Benfenati, and P. Greengard. 1998. A third member of the synapsin gene family. *Proceedings of the National Academy of Sciences of the United States of America*. 95:4667-4672.

Kao, H.T., B. Porton, S. Hilfiker, G. Stefani, V.A. Pieribone, R. DeSalle, and P Greengard. 1999. Molecular evolution of the synapsin gene family. *Journal of Experimental Zoology*. 285:360-377.

Katz, B. 1971. Quantal mechanism of neural transmitter release. *Science*. 173:123-126.

Kennedy, M.B., and P. Greengard. 1981. Two calcium/calmodulin-dependent protein kinases, which are highly concentrated in brain, phosphorylate protein I at distinct sites. *Proceedings of the National Academy of Sciences of the United States of America*. 78:1293-1297.

Kennedy, M.B., T. McGuinness, and P. Greengard. 1983. A calcium/calmodulin-dependent protein kinase from mammalian brain that phosphorylates Synapsin I: partial purification and characterization. *Journal of Neuroscience*. 3:818-831.

Kessels, M.M., A.E. Engqvist-Goldstein, D.G. Drubin, and B. Qualmann. 2001. Mammalian Abp1, a signal-responsive F-actin-binding protein, links the actin cytoskeleton to endocytosis via the GTPase dynamin. *Journal of Cell Biology*. 153:351-366.

Kim, C.H., and J.E. Lisman. 1999. A role of actin filament in synaptic transmission and long-term potentiation. *Journal of Neuroscience*. 19:4314-4324.

Klingauf, J., E.T. Kavalali, and R.W. Tsien. 1998. Kinetics and regulation of fast endocytosis at hippocampal synapses. *Nature*. 394:581-585.

Koenig, J.H., and K. Ikeda. 1983. Evidence for a presynaptic blockage of transmission in a temperature-sensitive mutant of Drosophila. *Journal of Neurobiology*. 14:411-419.

Kubler, E., and H. Riezman. 1993. Actin and fimbrin are required for the internalization step of endocytosis in yeast. *EMBO Journal*. 12:2855-2862.

Kuczmarksi, E., and J. Rosenblum. 1979. Studies on the organization and localization of actin and myosin in neurons. *Journal of Cell Biology*. 80:356-371.

Kuczmarkski, E.R., and J.L. Rosenbaum. 1979. Chick brain actin and myosin. Isolation and characterization. *Journal of Cell Biology*. 80:341-355.

Kuromi, H., and Y. Kidokoro. 1998. Two Distinct Pools of Synaptic Vesicles in Single Presynaptic Boutons in a Temperature-Sensitive Drosophila Mutant, Shibere. *Neuron*. 20:917-925.

Kuznetsov, S.A., G.M. Langford, and D.G. Weiss. 1992. Actin-dependent organelle movement in squid axoplasm. *Nature*. 356:722-725.

LaFountain, J.R., Jr., C.R. Zobel, H.R. Thomas, and C. Galbreath. 1977. Fixation and staining of F-actin and microfilaments using tannic acid. *Journal of Ultrastructure Research*. 58:78-86.

Lai, M., J. Hong, A. Ruggiero, P. Burnett, V. Slepnev, P. De Camilli, and S. Snyder. 1999. The calcineurin-dynamin I complex as a calcium sensor for synaptic vesicle endocytosis. *Journal of Biological Chemistry*. 274:25963-25966.

Lai, M., H. Luo, P. Burnett, J. Hong, and S. Snyder. 2000. The calcineurin-binding protein cain is a negative regulator of synaptic vesicle endocytosis. *Journal of Biological Chemistry*. 275:34017-34020.

Lamaze, C., T.H. Chuang, L.J. Terkecky, G.M. Bokoch, and S.L. Schmid. 1996. Regulation of receptor-mediated endocytosis by Rho and Rac. *Nature*. 382:177-179.

Lamaze, C., L. Fujimoto, H. Yin, and S. Schmid. 1997. The Actin Cytoskeleton is Required for Receptor-mediated Endocytosis in Mammalian Cells. *The Journal of Biological Chemistry*. 272:20332-20335.

Landis, D.M., A.K. Hall, L.A. Weinstein, and T.S. Reese. 1988. The organization of cytoplasm at the presynaptic active zone of a central nervous system synapse. *Neuron*. 1:201-209.

Langford, G.M. 1995. Actin- and microtubule-dependent organelle motors: interrelationships between the two motility systems. *Current Opinion in Cell Biology*. 7:82-88.

Langford, G.M. 1999. ER transport on actin filaments in squid giant axon: implications for signal transduction at synapse. *FASEB Journal*. 13:S248-250.

Lengsfeld, A.M., I. Low, T. Wieland, P. Dancker, and W. Hasselback. 1974. Interaction of Phalloidin with Actin. *Proceedings of the National Academy of Sciences*. 71:2803-2807.

Li, L., L.S. Chin, O. Shupliakov, L. Brodin, T.S. Sihra, O. Hvalby, V. Jensen, D. Zheng, J.O. McNamara, P. Greengard, and et al. 1995. Impairment of synaptic vesicle clustering and of synaptic transmission, and increased seizure propensity, in synapsin I-deficient mice. *Proceedings of the National Academy of Sciences of the United States of America*. 92:9235-9239.

Lin, C.H., E.M. Espreafico, M.S. Mooseker, and P. Forscher. 1996. Myosin drives retrograde D-actin flow in neuronal growth cones. *Neuron*. 16:769-782.

Lin, J.W., M. Sugimori, R.R. Llinas, T.L. McGuinness, and P. Greengard. 1990. Effects of synapsin I and calcium/calmodulin-dependent protein kinase II on spontaneous neurotransmitter release in the squid giant synapse. *Proceedings of the National Academy of Sciences of the United States of America*. 87:8257-8261.

Liu, J.P., A.T.R. Sim, and P.J. Robinson. 1994. Calcineurin inhibition of dynamin I GTPase activity coupled to nerve terminal depolarization. *Science*. 265:970-973.

Llinas, R., J.A. Gruner, M. Sugimori, T.L. McGuinness, and P. Greengard. 1991. Regulation by synapsin I and Ca(2+)-calmodulin-dependent protein kinase II of the transmitter release in squid giant synapse. *Journal of Physiology*. 436:257-282.

Llinas, R., T.L. McGuinness, C.S. Leonard, M. Sugimori, and P. Greengard. 1985. Intraterminal injection of synapsin I or calcium/calmodulin-dependent protein kinase II alters neurotransmitter release at the squid giant synapse. *Proceedings of the National Academy of Sciences of the United States of America*. 82:3035-3039.

Llinas, R., M. Sugimori, and R.B. Silver. 1992. Microdomains of high calcium concentration in a presynaptic terminal. *Science*. 256:677-679.

Longenecker, H.E., W.P. Hurlbut, A. Mauro, and A.W. Clark. 1970. Effects of Black Widow Spider Venom on the Frog Neuromuscular Junction. *Nature*. 225:701-703.

Machesky, L.M., and K.L. Gould. 1999. The Arp2/3 complex: a multifunctional actin organizer. *Current Opinion in Cell Biology*. 11:117-121.

Machesky, L.M., R.D. Mullins, H.N. Higgs, D.A. Kaiser, L. Blanchoin, R.C. May, M.E. Hall, and T.D. Pollard. 1999. Scar, a WASp-related protein, activates nucleation of actin filaments by the Arp2/3 complex. *Proceedings of the National Academy of Sciences of the United States of America*. 96:3739-3744.

Maeno, H., E.M. Johnson, and P. Greengard. 1971. Subcellular distribution of adenosine 3',5'-monophosphate dependent protein kinase in rat brain. *Journal of Biological Chemistry*. 246:134-142.

Mandell, J.W., E. Townes-Anderson, A.J. Czernik, R. Cameron, P. Greengard, and P. De Camilli. 1990. Synapsins in the vertebrate retina: absence from ribbon synapses and heterogeneous distribution among conventional synapses. *Neuron.* 5:19-33.

Maples, C.J., W.G. Ruiz, and G. Apodaca. 1997. Both microtubules and actin filaments are required for efficient postendocytotic traffic of the polymeric immunoglobulin receptor in polarized Madin-Darby canine kidney cells. *Journal of Biological Chemistry.* 272:6741-6751.

Marks, B., and H. McMahon. 1998. Calcium triggers calcineurin-dependent synaptic vesicle recycling in mammalian nerve terminals. *Current Biology.* 8:740-749.

Matsubara, M., M. Kusubata, K. Ishiguro, T. Uchida, K. Titani, and H. Taniguchi. 1996. Site-specific phosphorylation of synpasin I by mitogen-activated protein kinase and Cdk5 and its effects on physiological functions. *Journal of Biological Chemistry.* 271:21108-21113.

Matter, K., F. Dreyer, and K. Aktories. 1989. Actin Involvement in Exocytosis from PC12 Cells: Studies on the Influence of Botulinum C2 Toxin on Stimulated Noradrenaline Release. *Journal of Neurochemistry.* 52:370-376.

Maupin, P., and T.D. Pollard. 1983. Improved preservation and staining of HeLa cell actin filaments, clathrin-coated membranes, and other cytoplasmic structures by tannic acid-glutaraldehyde-saponin fixation. *Journal of Cell Biology.* 96:51-62.

Maupin-Szamier, P., and T.D. Pollard. 1978. Actin filament destruction by osmium tetroxide. *Journal of Cell Biology.* 77:837-852.

McClure, S.J., and P.J. Robinson. 1996. Dynamin, endocytosis, and intracellular signalling. *Molecular Membrane Biology.* 13:189-215.

McGuinness, T.L., S.T. Brady, J.A. Gruner, M. Sugimori, R. Llinas, and P. Greengard. 1989. Phosphorylation-dependent inhibition by synapsin I of organelle movement in squid axoplasm. *Journal of Neuroscience.* 9:4138-4149.

McGuinness, T.L., Y. Lai, P. Greengard, J.R. Woodgett, and P. Cohen. 1983. A multifunctional calmodulin-dependent protein kinase. Similarities between skeletal muscle glycogen synthase kinase and a brain synapsin I kinase. *FEBS Letters.* 163:329-334.

McPherson, P.S., A.J. Czernik, T.J. Chilcote, F. Onofri, F. Benfenati, P. Greengard, J. Schlessinger, and P. De Camilli. 1994. Interaction of Grb2 via its Src homology 3 domains with synaptic proteins including synapsin I. *Proceedings of the National Academy of Sciences of the United States of America.* 91:6486-6490.

Meeusen, R.L., and W.Z. Cande. 1979. N-ethylmaleimide-modified Heavy Meromyosin. *Journal of Cell Biology.* 82:57-65.

Mellman, I. 1996. Endocytosis and molecular sorting. *Annual Review of Cell & Developmental Biology.* 12:575-625.

Merrifield, C.J., S.E. Moss, C. Ballestrem, B.A. Imhof, G. Giese, I. Wunderlich, and W. Almers. 1999. Endocytic vesicles move at the tips of actin tails in cultured mast cells. *Nature Cell Biology.* 1:72-74.

Miller, M., E. Bower, P. Levitt, D. Li, and P. Chantler. 1992. Myosin II Distribution in Neurons Is Consistent with a Role in Growth Cone Motility but Not Synaptic Vesicle Mobilization. *Neuron.* 8:25-44.

Miller, T.M., and J.E. Heuser. 1984. Endocytosis of synaptic vesicle membrane at the frog neuromuscular junction. *Journal of Cell Biology.* 98:685-698.

Miyamoto, E., J.F. Kuo, and P. Greengard. 1969. Cyclic nucleotide dependent protein kinases. III. Purification and properties of adenosine 3':5'-monophosphate-dependent protein kinase from bovine brain. *Journal of Biological Chemistry.* 244:6395-6402.

Mochida, S. 1995. Role of myosin in neurotransmitter release: functional studies at synapses formed in culture. *Journal of Physiology, Paris.* 89:83-94.

Mochida, S., H. Kobayashi, Y. Matsuda, Y. Yuda, K. Muramoto, and Y. Nonomura. 1994. Myosin II is involved in transmitter release at synapses formed between rat sympathetic neurons in culture. *Neuron*. 13:1131-1142.
Morales, M., M. Colicos, and Y. Goda. 2000. Actin-Dependent Regulation of Neurotransmitter Release at Central Synapses. *Neuron*. 27:539-550.
Moreau, V., F. Frischknecht, I. Reckmann, R. Vincentelli, G. Rabut, D. Stewart, and M. Way. 2000. A complex of N-WASP and WIP integrates signalling cascades that lead to actin polymerization. *Nature Cell Biology*. 2:441-448.
Morris, J.R., and R.J. Lasek. 1984. Monomer-Polymer Equilibria in the Axon:Direct Measurement of Tubulin and Actin as Polymer and Monomer in Axoplasm. *Journal of Cell Biology*. 98:2064-2076.
Munn, A.L., B.J. Stevenson, M.I. Geli, and H. Riezman. 1995. end5, end6, and end7: mutations that cause actin delocalization and block the internalization step of endocytosis in Saccharomyces cerevisiae. *Molecular Biology of the Cell*. 6:1721-1742.
Murthy, V.N., and C.F. Stevens. 1998. Synaptic vesicles retain their identity through the endocytic cycle. *Nature*. 392:497-501.
Navone, F., P. Greengard, and P. De Camilli. 1984. Synapsin I in nerve terminals: selective association with small synaptic vesicles. *Science*. 226:1209-1211.
Neher, E. 1998. Vesicle Pools and Ca2+ Microdomains: New Tools for Understanding Their Roles in Neurotransmitter Release. *Neuron*. 20:389-399.
Nestler, E.J., and P.G. Greengard. 1984. Protein phosphorylation in the nervous system. John Wiley & Sons, Inc., New York.
Nicklas, W.J., and S. Berl. 1974. Effects of cytochalasin B on uptake and release of putative transmitters by synaptosomes and on brain actomyosin-like protein. *Nature*. 247:471-473.
Nicol, S., D. Rahman, and A.J. Baines. 1997. Ca2+-dependent interaction with calmodulin is conserved in the synapsin family: identification of a high-affinity site. *Biochemistry*. 36:11487-11495.
Nicol, S., D. Rahman, and A.J. Baines. 1998. Interaction of synapsin IIb with calmodulin: identification of a high affinity site. *Biochemical Society Transactions*. 26:S109.
Nonet, M.L., A.M. Holgado, F. Brewer, C.J. Serpe, B.A. Norbeck, J. Holleran, L. Wei, E. Hartwieg, E.M. Jorgensen, and A. Alfonso. 1999. UNC-11, a Caenorhabditis elegans AP180 homologue, regulates the size and protein composition of synaptic vesicles. *Molecular Biology of the Cell*. 10:2343-2360.
Okabe, T., and K. Sobue. 1987. Identification of a new 84/82 kDa calmodulin-binding protein, which also interacts with actin filaments, tubulin and spectrin, as synapsin I. *FEBS Letters*. 213:184-188.
Onofri, F., S. Giovedi, H.T. Kao, F. Valtorta, L.B. Borbone, P. De Camilli, P. Greengard, and F. Benfenati. 2000. Specificity of the binding of synapsin I to Src homology 3 domains. *Journal of Biological Chemistry*. 275:29857-29867.
Onofri, F., S. Giovedi, P. Vaccaro, A.J. Czernik, F. Valtorta, P. De Camilli, P. Greengard, and F. Benfenati. 1997. Synapsin I interacts with c-Src and stimulates its tyrosine kinase activity. *Proceedings of the National Academy of Sciences of the United States of America*. 94:12168-12173.
Palade, G. 1954. Electron microscope observations of interneuronal and neuromuscular synapses. *The Anatomical Record*. 118:335-336.
Palade, G.E., and R.R. Bruns. 1968. Structural modulations of plasmalemmal vesicles. *Journal of Cell Biology*. 37:633-649.
Palay, S. 1954. Electron microscope study of the cytoplasm of neurons. *The Anatmoical Record*. 118:336.
Palay, S.L. 1956. Synapses in the Central Nervous System. *Journal of Biophysical and Biochemical Cytology*. 2:193-207.

Palay, S.L. 1958. The morphology of synapses in the central nervous system. *Experimental Cell Research.* Suppl. 5:275-293.
Palay, S.L., and G.E. Palade. 1955. The Fine Structure of Neurons. *Journal of Biophysical and Biochemical Cytology.* 1:69-88, plus 26 plates.
Pearse, B.M. 1976. Clathrin: a unique protein associated with intracellular transfer of membrane by coated vesicles. *Proceedings of the National Academy of Sciences of the United States of America.* 73:1255-1259.
Pfenninger, K.H., and C.M. Rovainen. 1974. Stimulation- and calcium-dependence of vesicle attachment sites in the presynaptic membrane; a freeze-cleave study on the lamprey spinal cord. *Brain Research.* 72:1-23.
Pieribone, V., O. Shupliakov, L. Brodin, S. Hilfiker-Rosenfluh, A. Czernik, and P. Greengard. 1995. Distinct Pools of synaptic vesicles in neurotransmitter release. *Nature.* 375:493-497.
Polak, and Varnell. 1984. Immunolabelling for Electron Microscopy. Elsevier Science Publishers, Amsterdam.
Porter, K., A. Claude, and E. Fullam. 1944. A study of tissue culture cells by electron microscopy. *Journal of Experimental Medicine.* 81:233-246.
Prekeris, R., and D. Terrian. 1997. Brain Myosin V Is a Synaptic Vesicle-associated Motor Protein: Evidence for a Ca2+-dependent Interaction with the Synaptobrevin-Synaptophysin Complex. *The Journal of Cell Biology.* 137:1589-1601.
Pumplin, D.W., T.S. Reese, and R. Llinas. 1981. Are the presynaptic membrane particles the calcium channels? *Proceedings of the National Academy of Sciences.* 78:7210-7213.
Puszkin, S., and S. Berl. 1970. Actin-like properties of colchicine binding protein isolated from brain. *Nature.* 225:558-559.
Puszkin, S., and S. Berl. 1972. Actomyosin-like protein from brain. Separation and characterization of the actin-like component. *Biochimica et Biophysica Acta.* 256:695-709.
Puszkin, S., S. Berl, E. Puszkin, and D.D. Clarke. 1968. Actomyosin-like protein isolated from mammalian brain. *Science.* 161:170-171.
Puszkin, S., and S. Kochwa. 1974. Regulation of neurotransmitter release by a complex of actin with relaxing protein isolated from rat brain synaptosomes. *Journal of Biological Chemistry.* 249:7711-7714.
Puszkin, S., M. Lisanti, K. Haver, E.L. Hua, N. Moskowitz, W.S. Bloom, and W.J. Schook. 1982. Brain clathrin complex: II. Immunofluorescent correlation and biochemical affinity for actin. *Journal of Histochemistry & Cytochemistry.* 30:497-503.
Puszkin, S., W.J. Nicklas, and S. Berl. 1972. Actomyosin-like protein in brain: subcellular distribution. *Journal of Neurochemistry.* 19:1319-1333.
Pyle, R., A. Schivell, H. Hidaka, and S. Bajjalieh. 2000. Phosphorylation of synaptic vesicle protein 2 modulates binding to synaptotagmin. *Journal of Biological Chemistry.* 275:17195-17200.
Qualmann, B., and R.B. Kelly. 2000. Syndapin isoforms participate in receptor-mediated endocytosis and actin organization. *Journal of Cell Biology.* 148:1047-1062.
Qualmann, B., M.M. Kessels, and R.B. Kelly. 2000. Molecular links between endocytosis and the actin-cytoskeleton. *Journal of Cell Biology.* 150:F111-F116.
Qualmann, B., J. Roos, P.J. DiGregorio, and R.B. Kelly. 1999. Syndapin I, a synaptic dynamin-binding protein that associates with the neural Wiskott-Aldrich syndrome protein. *Molecular Biology of the Cell.* 10:501-513.
Ramon y Cajal, S. 1894. New Ideas on the Structure of the Nervous System in Man and Vertebrates. MIT Press, Cambridge. page 160 pp.

Raths, S., J. Rohrer, F. Crausaz, and H. Riezman. 1993. end3 and end4: two mutants defective in receptor-mediated and fluid-phase endocytosis in Saccharomyces cerevisiae. *Journal of Cell Biology*. 120:55-65.

Ringstad, N., H. Gad, P. Low, G. Di Paolo, L. Brodin, O. Shupliakov, and P. De Camilli. 1999. Endophilin/SH3p4 is required for the transition from early to late stages in clathrin-mediated synaptic vesicle endocytosis [see comments]. *Neuron*. 24:143-154.

Ringstad, N., Y. Nemoto, and P. De Camilli. 1997. The SH3p4/Sh3p8/SH3p13 protein family: binding partners for synaptojanin and dynamin via a Grb2-like Src homology 3 domain. *Proceedings of the National Academy of Sciences of the United States of America*. 94:8569-8574.

Robertson, J.D. 1954. Electron microscope study of an invertebrate synapse. *The Anatomical Record*. 118:346.

Robertson, J.D. 1955. Recent Electron Microscope Observations on the Ultrastructure of the Crayfish Median-to-Motor Giant Synapse. *Experimental Cell Research*. 8:226-229.

Robinson, P.J., and P.R. Dunkley. 1985. Depolarisation-dependent protein phosphorylation and dephosphorylation in rat cortical synaptosomes is modulated by calcium. *Journal of Neurochemistry*. 44:338-348.

Rosahl, T.W., M. Geppert, D. Spillane, J. Herz, R.E. Hammer, R.C. Malenka, and T.C. Sudhof. 1993. Short-term synaptic plasticity is altered in mice lacking synapsin I. *Cell*. 75:661-670.

Rosahl, T.W., D. Spillane, M. Missler, J. Herz, D.K. Selig, J.R. Wolff, R.E. Hammer, R.C. Malenka, and T.C. Sudhof. 1995. Essential functions of synapsins I and II in synaptic vesicle regulation. *Nature*. 375:488-493.

Roth, T.F., and K.R. Porter. 1964. Yolk protein uptake in the oocyte of the mosquito Aedes Aegypti. L. *Journal of Cell Biology*. 20:313-332.

Rovainen, C.M. 1967. Physiological and anatomical studies on large neurons of central nervous system of the sea lamprey (Petromyzon marinus). *Journal of Neurophysiology*. 30:1000-1023.

Rovainen, C.M. 1976. Regeneration of Muller and Mauthner Axons after Spinal Cord Transsection in Larval Lampreys. *Journal of Comparative Neurology*. 168:545-554.

Rovainen, C.M. 1979. Neurobiology of Lampreys. *Physiological Reviews*. 59:1008-1077.

Rozelle, A.L., L.M. Machesky, M. Yamamoto, M.H. Driessens, R.H. Insall, M.G. Roth, K. Luby-Phelps, G. Marriott, A. Hall, and H.L. Yin. 2000. Phosphatidylinositol 4,5-bisphosphate induces actin-based movement of raft-enriched vesicles through WASP-Arp2/3. *Current Biology*. 10:311-320.

Rubin, L.L., A. Gorio, and A. Mauro. 1976. Effect of cytochalasin B on neuromuscular transmission in tissue culture. *Brain Research*. 104:171-175.

Ryan, T.A. 1999. Inhibitors of myosin light chain kinase block synaptic vesicle pool mobilization during action potential firing. *Journal of Neuroscience*. 19:1317-1323.

Ryan, T.A., L. Li, L.S. Chin, P. Greengard, and S.J. Smith. 1996a. Synaptic vesicle recycling in synapsin I knock-out mice. *Journal of Cell Biology*. 134:1219-1227.

Ryan, T.A., H. Reuter, B. Wendland, F.E. Schweizer, R.W. Tsien, and S.J. Smith. 1993. The kinetics of synaptic vesicle recycling measured at single presynaptic boutons. *Neuron*. 11:713-724.

Ryan, T.A., N.E. Ziv, and S.J. Smith. 1996b. Potentiation of evoked vesicle turnover at individually resolved synaptic boutons. *Neuron*. 17:125-134.

Sabatini, D.D., K. Bensch, and R.J. Barrnett. 1963. Cytochemistry and electron microscopy: The Preservation of Cellular Ultrastructure and Enzymatic Activity by Aldehyde Fixation. *Journal of Cell Biology*. 17:19-58.

Sanders, G., B. Licthe, H. Meyer, and M. Kilimann. 1992. cDNA encoding the chicken ortholog of the mouse dilute gene product. *FEBS Letters*. 311:295-298.
Sandvig, K., and B. van Deurs. 1990. Selective modulation of the endocytic uptake of ricin and fluid phase markers without alteration in transferrin endocytosis. *Journal of Biological Chemistry*. 265:6382-6388.
Schiavo, G., M. Matteoli, and C. Montecucco. 2000. Neurotoxins Affecting Neuroexocytosis. *Physiological Reviews*. 80:717-766.
Schneggenburger, R., and E. Neher. 2000. Intracellular calcium dependence of transmitter release rates at a fast central synapse. *Nature*. 406:889-893.
Schook, W., S. Puszkin, W. Bloom, C. Ores, and S. Kochwa. 1979. Mechanochemical properties of brain clathrin: Interactions with actin and alpha-actinin and polymerization into basketlike structures or filaments. *Proceedings of the National Academy of Sciences*. 76:116-120.
Sever, S., H. Damke, and S.L. Schmid. 2000. Garrotes, springs, ratchets and whips: putting dynamin models to the test. *Traffic*. 1:385-392.
Shupliakov, O., and L. Brodin. 2000. A model glutamate synapse: the lamprey giant reticulospinal axon. *In* Handbook of Chemical Neuroanatomy: Glutamate. O.P. Ottersen and J.S. Mathisen, editors. Elsevier, Amsterdam.
Shupliakov, O., P. Low, D. Grabs, H. Gad, H. Chen, C. David, K. Takei, P. De Camilli, and L. Brodin. 1997. Synaptic vesicle endocytosis impaired by disruption of dynamin-SH3 domain interactions. *Science*. 276:259-263.
Simon, S., and R. Llinas. 1985. Compartmentallzation of the submembrane calcium activity during calcium influx and its signficance in transmitter release. *Biophysical Journal*. 48:485-498.
Sjostrand, F.S. 1953a. The ultrastructure of the innersegments of the retinal rods of the guinea pig eye as revealed by electron microscopy. *Journal of Cellular and Comparative Physiology*. 42:45-70.
Sjostrand, F.S. 1953b. The ultrastructure of the outer segments of rods and cones of the eye as revealed by the electron microscope. *Journal of Cellular and Comparative Physiology*. 42:15-44.
Stefani, G., F. Onofri, F. Valtorta, P. Vaccaro, P. Greengard, and F. Benfenati. 1997. Kinetic analysis of the phosphorylation-dependent interactions of synapsin I with rat brain synaptic vesicles. *Journal of Physiology*. 504:501-515.
Sudhof, T.C., A.J. Czernik, H.T. Kao, K. Takei, P.A. Johnston, A. Horiuchi, S.D. Kanazir, M.A. Wagner, M.S. Perin, and P. De Camilli. 1989. Synapsins: mosaics of shared and individual domains in a family of synaptic vesicle phosphoproteins. *Science*. 245:1474-1480.
Sugita, S., W. Han, S. Butz, X. Liu, R. Fernandez-Chacon, Y. Lao, and T.C. Sudhof. 2001. Synaptotagmin VII as a Plasma Membrane Ca2+ Sensor in Exocytosis. *Neuron*. 30:459-473.
Takei, K., P.S. McPherson, S.L. Schmid, and P. De Camilli. 1995a. Tubular membrane invaginations coated by dynamin rings are induced by GTP-gamma S in nerve terminals [see comments]. *Nature*. 374:186-190.
Takei, K., O. Mundigl, L. Daniell, and P. De Camilli. 1996. The synaptic vesicle cycle: a single vesicle budding step involving clathrin and dynamin. *Journal of Cell Biology*. 133:1237-1250.
Takei, K., V.I. Slepnev, V. Haucke, and P. De Camilli. 1999. Functional partnership between amphiphysin and dynamin in clathrin-mediated endocytosis. *Nature Cell Biology*. 1:E8-E9.
Takei, Y., A. Harada, S. Takeda, K. Kobayashi, S. Terada, T. Noda, T. Takahashi, and N. Hirokawa. 1995b. Synapsin I deficiency results in the structural change in the presynaptic terminals in the murine nervous system. *Journal of Cell Biology*. 131:1789-1800.

Tansey, E.M. 1997. Not Comitting Barbarisms: Sherrington and the Synapse, 1897. *Brain Research Bulletin.* 44:211-212.

Tashiro, T., and H. Stadler. 1978. Chemical Composition of Cholinergic Synaptic Vesicles from Torpedo marmorata Based on Improved Purification. *European Journal of Biochemistry.* 90:479-487.

Terada, S., T. Tsujimoto, Y. Takei, T. Takahashi, and N. Hirokawa. 1999. Impairment of inhibitory synaptic transmission in mice lacking synapsin I. *Journal of Cell Biology.* 145:1039-1048.

Thoa, N.B., G.F. Wooten, J. Axelrod, and I.J. Kopin. 1972. Inhibition of release of dopamine- -hydroxylase and norepinephrine from sympathetic nerves by colchicine, vinblastine, or cytochalasin-B (hypogastric nerve stimulation-exocytosis-microtubules-microfilaments-guinea pig). *Proceedings of the National Academy of Sciences of the United States of America.* 69:520-522.

Toh, B.H., H.A. Gallichio, P.L. Jeffrey, B.G. Livett, H.K. Muller, M.N. Cauchi, and F.M. Clarke. 1976. Anti-actin stains synapses. *Nature.* 264:648-650.

Torri-Tarelli, F., M. Bossi, R. Fesce, P. Greengard, and F. Valtorta. 1992. Synapsin I partially dissociates from synaptic vesicles during exocytosis induced by electrical stimulation. *Neuron.* 9:1143-1153.

Torri-Tarelli, F., A. Villa, F. Valtorta, P. De Camilli, P. Greengard, and B. Ceccarelli. 1990. Redistribution of synaptophysin and synapsin I during alpha-latrotoxin-induced release of neurotransmitter at the neuromuscular junction. *Journal of Cell Biology.* 110:449-459.

Turner, K.M., R.D. Burgoyne, and A. Morgan. 1999. Protein phosphorylation and the regulation of synaptic membrane traffic. *Trends in Neurosciences.* 22:459-464.

Ueda, T., P. Greengard, K. Berzins, R.S. Cohen, F. Blomberg, D.J. Grab, and P. Siekevitz. 1979. Subcellular distribution in cerebral cortex of two proteins phosphorylated by a cAMP-dependent protein kinase. *Journal of Cell Biology.* 83:308-319.

Vaccaro, P., L. Dente, F. Onofri, A. Zucconi, S. Martinelli, F Valtorta, P. Greengard, G. Cesareni, and F. Benfenati. 1997. Anti-synapsin monoclonal antibodies: epitope mapping and inhibitory effects on phosphorylation and Grb2 binding. *Brain Research. Molecular Brain Research.* 52:1-16.

Valtorta, F., A. Villa, R. Jahn, P. De Camilli, P. Greengard, and B. Ceccarelli. 1988. Localization of synapsin I at the frog neuromuscular junction. *Neuroscience.* 24:593-603.

von Gersdorff, H., and G. Matthews. 1994. Dynamics of synaptic vesicle fusion and membrane retrieval in synaptic terminals [see comments]. *Nature.* 367:735-739.

von Gersdorff, H., and G. Matthews. 1999. Electrophysiology of synaptic vesicle cycling. *Annual Review of Physiology.* 61:725-752.

Walker, J.H., C.M. Boustead, and V. Witzemann. 1985. Cytoskeletal proteins at the cholinergic synapse: distribution of desmin, actin, fodrin, neurofilaments, and tubulin in Torpedo electric organ. *European Journal of Cell Biology.* 38:123-133.

Wang, X.H., J.Q. Zheng, and M.M. Poo. 1996. Effects of cytochalasin treatment on short-term synaptic plasticity at developing neuromuscular junctions in frogs. *Journal of Physiology.* 491:187-195.

Wickelgren, W., J. Leonard, M. Grimes, and R. Clark. 1985. Ultrastructural Correlates of Transmitter Release in Presynaptic Areas of Lamprey Reticulospinal Axons. *The Journal of Neuroscience.* 5:1188-1201.

Witke, W., A.V. Podtelejnikov, A. Di Nardo, J.D. Sutherland, C.B. Gurniak, C. Dotti, and M. Mann. 1998. In mouse brain profilin I and profilin II associate with regulators of the endocytic pathway and actin assembly. *EMBO Journal.* 17:967-976.

Wulf, E., A. Deboben, F.A. Bautz, H. Faulstich, and T. Wieland. 1979. Fluorescent phallotoxin, a tool for the visualization of cellular actin. *Proceedings of the National Academy of Sciences*. 76:4498-4502.

Zhang, J.Z., B.A. Davletov, T.C. Sudhof, and R.G. Anderson. 1994. Synaptotagmin I is a high affinity receptor for clathrin AP-2: implications for membrane recycling. *Cell*. 78:751-760.

Zhao, W., S. Cavallaro, P. Gusev, and D.L. Alkon. 2000. Nonreceptor tyrosine protein kinase pp60c-src in spatial learning: synapse-specific changes in its gene expression, tyrosine phosphorylation, and protein-protein interactions. *Proceedings of the National Academy of Sciences of the United States of America*. 97:8098-8103.

Zimmerman, H., and H. Denston. 1977. Recycling of Synaptic Vesicles in the Cholinergic Synapes of the Torpedo Electric Organ During Induced Transmitter Release. *Neuroscience*. 2:695-714.